HWANG, JENN-SHYONG

DYNAMIC LIGHT SCATTERING STUDIES OF COLLAGEN-GELATIN AND GEL

City University of New York PH.D. 1980

DYNAMIC LIGHT SCATTERING STUDIES OF COLLAGEN-GELATIN AND GEL

by

JENN-SHYONG HWANG

A dissertation submitted to the Graduate Faculty in Physics in partial fulfillment of the requirements for the degree of Doctor of Philosophy, The City University of New York.

1980

This manuscript has been read and accepted for the Graduate Faculty in Physics in satisfaction of the dissertation requirement for the degree of Doctor of Philosophy.

5/15/80 — date — Chairman of Examining Committee

6/17/80 — date — Executive Officer

Supervisory Committee

Abstract

DYNAMIC LIGHT SCATTERING STUDIES OF
COLLAGEN-GELATIN AND GEL

by

Jenn-Shyong Hwang

Adviser: Professor Herman Z. Cummins

The technique of intensity correlation spectroscopy using a digital autocorrelator was employed to investigate the collagen-gelatin and gel systems. Various hydrodynamic properties were derived from the autocorrelation functions of different samples. In this thesis a general review of the previous studies and physico-chemical properties of these systems are given first, followed by a brief outline of the theory of intensity fluctuation spectroscopy and a description of the apparatus and experimental technique used in this study. The research work and results are then discussed in three separate parts, each dealing with one topic -- the gelatin solutions, gelatin gels and collagen solutions.

For the extremely polydisperse gelatin solution the concentration dependence of the diffusion coefficient was investigated and a relation $N \propto C^5$ for the polymerization index of the aggregates and the concentration was obtained. Moderately polydisperse solutions obtained by the

centrifugation of the gelatin solutions however show that the gelatin particles execute free diffusion at low concentrations and form a polymer network at high concentrations. The z-average free diffusion coefficient is independent of concentration and is proportional to q^2. The hydrodynamic radii and polydispersities of the gelatin molecules at different salt concentrations and temperatures were also studied. The results lead to the conclusion that most of the aggregates are covalently linked and the hydrogen bonded and collagen-folded aggregates do not make significant contributions at 20°C or higher temperatures.

Single exponential autocorrelation functions were obtained for gelatin gels with and without crosslinking agent. The elastic continuum model was found to describe all the observed properties better than the bounded diffusion model. As the concentration increases the cooperative diffusion coefficient decreases in the solution state but increases in the gel state. For gels without a crosslinking agent the decay rate of the correlation function was found to remain constant after it reached a terminal value several hours after its temperature was changed to 20°C. However, for gels with a crosslinking agent the decay rate continuously increased in time and the spatial correlation length became shorter with age.

Very monodisperse collagen samples were obtained through the purification of density gradient separation. Autocorrelation functions were measured at 31.8° and 90° scattering angles. The translational and rotational diffusion coefficients were calculated from the directly measured correlation functions of non-zero degree scattering. A length of 2715 ± 100Å was obtained for the tropocollagen molecules and is in agreement with previous literature values.

ACKNOWLEDGEMENTS

I would like to thank Professor Herman Z. Cummins for his support and patient guidance during the course of this work. I would also like to thank Professor Harry L. Swinney for his help while he was at City College.

To Dr. Randolph Fenstermacher, I am deeply indebted for the useful discussions in various computer techniques, physical topics and in the preparation of this thesis.

Thanks should also go to Dr. P. I. Rose of the Eastman Kodak Research Laboratory and Dr. Jack Coffey of the Hoffmann La Roche Laboratory for providing the gelatin and collagen stocks respectively.

I would also like to thank Dr. Fang-Chung Chen for the useful discussions especially the suggestion of using the density gradient technique. To Drs. James Frost and Dennis Wonica, I would also like to express my special thanks.

To Professors H. H. Schulz, T. Heinse and S. Cosloy I am grateful for their kindness in letting me use their equipment.

The moral support from all of the other members of the light scattering group especially Mr. J. Wicksted is also deeply appreciated. I also thank Mrs. Frances Tritt for typing this thesis.

Finally, I express deep appreciation to my parents and my sister, Pi-Zong for their encouragement and all kinds of support throughout these years. Without their support I would never have completed this work. I would like to take this opportunity to apologize to my son, Ying-Long for the fact that this work has taken so much of my time away from him. The failure in providing him a complete family is the deepest regret of my life.

TABLE OF CONTENTS

LIST OF FIGURES

LIST OF TABLES

CHAPTER I

INTRODUCTION

Collagen is the most abundant protein in the animal world and is the main constituent of connective tissue. It accounts for a third of the protein content in the human body.[1,2] Gelatin, which is the denatured product of collagen, is a basic component of glue, photographic emulsions, and food. When a gelatin solution with concentration high enough is cooled to a certain temperature, the gel point, it forms gelatin gel. The collagen-gelatin and gel systems represent an important area of study both because of the biological and medical importance of collagen and because of the great commercial interest in gelatin and gels.

The collagen-gelatin system has been studied widely by a variety of techniques. The high viscosity and the tendency of the molecules to aggregate make the collagen-gelatin system difficult to study. Light scattering measurements which have played a critical role, however, are particularly suited for the examination of the nature and extent of agregate formation in collagen and dilute gelatin solutions. Conventional light scattering techniques have been used to determine the dimensions, shapes, and molecular weights of macromolecules in solutions.[3] The most widely used method was to measure the scattered light as a function of concentration and angle, and combine the data into a "Zimm plot".[4] From the plot, the molecular weight, radius of gyration and the second virial coefficient have been calculated. These applications however, assumed that the light was scattered elastically and neglected the broadening effect in the scattered light spectrum

due to Doppler effects from Brownian motion of the macromolecules.

Two difficulties in measuring the spectrum of the scattered light from the solution of macromolecules were due to: (i) the lack of light sources which were sufficiently monochromatic and simultaneously of high intensity, and (ii) the extremely high resolution required to measure the small amount of broadening in the scattered light spectrum. These difficulties were removed with the advent of lasers and the introduction of the new technique of IFS (Intensity Fluctuation Spectroscopy) or Light Beating Spectroscopy or Optical Mixing Spectroscopy. This new technique has been used to study solutions of macromolecules and has been proven to be a powerful approach.

The primary subject of this study is therefore to apply the IFS technique to the study of the collagen-gelatin system and to the gel dynamics which represent a broad field of study in polymer science and in industry. An in depth analysis of Intensity Fluctuation Spectroscopy is given by Cummins and Swinney[5] and also by many other authors.[6-9] In the next chapter we will give an overview of the theory and applications of this technique. We will first briefly discuss the previous studies of the collagen-gelatin and gel systems and then outline their biological and physico-chemical properties.

1.1 PREVIOUS STUDIES OF PHYSICO-CHEMICAL PROPERTIES

A. Collagen Solution and Denaturation

Microscopic, x-ray and electron microscopic techniques have been used to study collagen fibers since 1927. Investigations of collagen in solution by biological techniques were started 20 years thereafter by Bresler, et al,[10] who obtained molecular weights of about 70,000

for a soluble skin collagen. The first report of light scattering measurements was given by Mathews, et al,[11] who found a number average molecular weight of 74,000 from osmatic pressure measurements and a weight average molecular weight of 10^7 from light scattering measurements for a similar material to that studied by Bresler, et al. The presence of large aggregates was claimed to account for the difference in the measured molecular weights. Veis, et al (1955)[12] obtained a molecular weight of several millions for the soluble skin collagen extracted at 60°C. Another light scattering investigation of soluble collagen by M'Ewen and Pratt (1953)[13] yielded a molecular weight of about 7 million for skin collagen and 10 to 25 million for tendon collagen. The discrepancies in these observed high molecular weights indicated the presence of both light and heavy macromolecular particles.

In 1953 Gallop[14] obtained very pure citrate extracted collagen, ichthyocal, from the tunic of carp swim bladders. Sedimentation, viscosity and light scattering studies led him to interpret these soluble collagens as long and thread-like with a molecular weight of 1.7×10^6 and a length of 13,000 A. Gallop also found that collagen solutions underwent a dramatic, irreversible change when heated to 40°C at pH 3.7. The product, called parent gelatin, was shown to have a molecular weight of 70,000. This procedure, called denaturation, seemed to account for the huge difference in the molecular weight results in the previous studies. However, one contradiction which still remained was that the intrinsic viscosities of the samples had stayed nearly constant even while denaturation was being carried out.

Schmitt, Cross and Highberger (1953, 1954),[15-16] from the studies of the electron micrographs of collagen fibers, concluded that the upper limit for the fundamental unit which formed the collagen fiber did not exceed 3000 A. Boedtker and Doty (1956),[17] from the results of osmotic pressure, intrinsic viscosity and molar weight, sedimentation and viscosity, flow birefringence and viscosity, and light scattering studies on the ichthyocal and its denatured state concluded that collagen molecules from the carp swim bladder had rod-like shape with a length of 3000 A, a diameter of 13.6 A and a molecular weight of 345,000 and are composed of three mutually arranged polypeptide chains running lengthwise. Hall and Doty (1958)[18] obtained a weight average length of 2820 A and a diameter of 15 A for collagen molecules and Hodge and Schmitt (1960)[19] obtained a value of 2850 A for the molecular length. Gallop, et al (1957),[20] Von Hippel, et al (1960)[21] and French, et al (1971)[22] studied ichthyocal in neutral and salt solutions and found that acid extracted collagens have a lesser tendency to aggregate and were thus more monodispersive.

The most recent light scattering studies on the physico-chemical properties of collagens were carried out by using either dynamic light scattering or electric birefringence measurements. The dynamic light scattering technique measured the power spectrum or the autocorrelation function of the scattered light and then calculated the rotational and/or translational diffusion coefficients. The birefringence measurements gave the rotational diffusion coefficient from its growth or decay rates.

French, et al (1971)[22] have carried out some preliminary dynamic light scattering studies of rat tail collagen. From the half-width of the intensity spectrum of Rayleigh scattering, they obtained the translational diffusion coefficient and compared their results with that calculated from hydrodynamic theory for the tropocollagen rod. Obrink (1972)[23] studied lathynitic collagen at pH 7.4 in a phosphate buffer by performing some brief dynamic light scattering measurements and obtained a translational diffusion coefficient of 7.8×10^{-8} cm^2/sec for the collagen monomeric molecules. It was in agreement with the result that was calculated from hydrodynamic theory for a rod molecule of 3000 A in length and 14 A in diameter. Ananthanarayanan and Veis (1972)[24] obtained 2790 A for the length of collagen molecules from birefringence measurements and 2850 A from electron micrograph studies. Bernengo, et al (1974)[25] investigated, by electric birefringence measurements, the monomeric nature of skin acid-soluble collagen in 100 mM acetic solution and obtained a monomer length of 2700±100 A. In 1976, they studied the aggregative properties of acid-soluble skin collagen (native or treated) and pepsin-extracted collagen from bovine articular cartilage via birefringence and low shear rate viscosity. They found unique types of aggregates, about 7000 A long for native skin collagen, 5300 A for pepsin treated collagen, and 4400 A for pronase treated collagen. The number of aggregates increased with collagen concentration, as was expected for electrostatic interactions. The pepsin-extracted cartilage collagen was found to have aggregates of 5300 A long which was very close to those found in pepsin treated skin collagen.

However, the number of aggregates which formed in a covalent nature was independent of collagen concentration.

Herbage, et al (1976)[26] from electrical birefringence measurements found that, in addition to the tropocollagen, molecules with length slightly less than twice that of tropocollagen (2800 A) also appeared in the calf skin and cartilage collagen solutions. They pointed out that these molecules could be dimers composed of two monomers linked by intermolecular head-to-tail bonds whose theoretical length (5300 A), according to the quarter-stagger theory, was in good agreement with their measured values (5100 - 5300 A).

Fletcher (1976)[27] studied native collagen extracted from rat tail tendons using intensity measurements. He found that the translational diffusion coefficient depended on the concentration of collagen, and that intensity fluctuations due to the molecular rotational diffusion did not make a contribution to the scattered light at a scattering angle of 45°. Thomas and Fletcher (1979)[28] studied the depolarized forward-scattered light from solutions of rat tail collagen by autocorrelation spectroscopy. From the autocorrelation functions, they obtained a rotational diffusion coefficient of 1082±30 sec^{-1} corresponding to a molecular length of 2530±70 A.

B. Gelatin Solution

Gelatin systems have been extensively investigated by osmotic pressure and sedimentation measurements. Pouradier and Venet (1950)[29-30] measured the osmotic pressure of an alkali-precursor calf skin gelatin in aqueous solutions containing various reagents. They found that the number average molecular weight varied from 60,800 in distilled

water to 66,600 in 4.0 M urea solvent and the gelatin was molecularly dispersed in each of the solvent systems.

A number of light scattering studies have been made on gelatin but only a few of these, dealing with the characterization of molecularly dispersed gelatins will be mentioned here. The remaining studies have been discussed in the book by Veis.[1] The most common characters obtained from light scattering studies are the weight average molcular weight M_w and the radius of gyration of the molecule (R_G). Boedtker and Doty (1954)[17] used light scattering techniques to study properties of an ossein gelatin and its gel. They found the gelatin molecule to have a random coil-like shape with mean configuration comparable to those of typical synthetic polymers and weight average molecular weight of 96,000 in 2M KCNS solvent. They also found that at all temperatures below the equilibrium melting temperature, the aggregates of gelatin molecules were readily discernible, even in extremely dilute solutions that were incapable of gelation. The aggregate size, however, was related to the temperature and the thermal path by which the gelatin solution was brought to the measurement temperature. Williams, et al (1954)[31] from sedimentation analysis obtained the weight average end-to-end chain extension of 258 A by assuming a random coil model.

Gallop (1955)[14] carried out the denaturation of the ichthyocal he obtained and made a variety of physical chemistry measurements on sedimentation coefficients, diffusion coefficients, particle specific volume, and intrinsic viscosity of the parent gelatin in pH 3.7 sodium citrate buffer. He also obtained weight average molecular

weight of 1.7 x 10^6 and 70,000 for collagen and gelatin respectively, using light scattering measurements. Boedtker and Doty (1956)[32] repeated Gallop's study and obtained number average molcular weights 310,000 and 125,000 and weight average molecular weights 345,000 and 138,000 for collagens and gelatins respectively. They concluded that three molecules with substantially different molecular weights were formed from each collagen molecule upon denaturation. Extensive studies of sedimentation and ultracentrifuge measurements were later made to clarify different components in the parent gelatin from collagen. A single coherent picture can now be drawn to account for varied observations and will be presented in the next section.

Courts and Stainsby[33] studied the gelatin from ox hide limed collagen and found the molecular weights ranged from 320,000 to 64,000 depending on the solvent system and gelatin concentrations. They also studied a series of acid-processed ox bone gelatin fractions and found the weight average molecular weight ranged from 1.94 x 10^5 to 0.25 x 10^5. Veis, et al (1955, 1956, 1957, 1958, 1960)[34-38] studied gelatins from unlimed purified steer hide corium collagen by a variety of short neutral or acid extractions. Molecular weights were found to range from 8.3 x 10^6 to 0.2 x 10^6 in various fractions.

The results from the light scattering studies indicated that although gelatins are molecularly dispersed in aqueous solutions, gelatins are extremely heterogeneous with molecular weight varying in a fairly wide range up to values larger than 10^6 and a single configuration model is unable to represent all gelatins.

C. Gelatin Gels

Ferry (1948)[39] pointed out the similarity of the gelation of gelatin to the gelation of celluloses and many synthetic linear polymers. Under appropriate conditions, these polymers form an infinite three-dimensional insoluble polymer network. Boedtker and Doty (1954)[17] measured the intensity of the scattered light as a function of concentration, scattering angle, and age of the gel. The intensity of the scattered light from the gelatin gel was found to be substantially greater than in the corresponding solutions at 40°C. However, the scattering intensity decreased while the gel concentration increased. They made a comparison of this gelatin concentration dependence of scattering intensity of gels with that predicted for a hard sphere fluid and concluded that the scattering centers in the gels were density fluctuations similar in weight and volume to the aggregates in gelatin solutions. They claimed that the decrease in scattering intensity did not necessarily indicate smaller scattering centers and attributed the gelation of gelatin to the simultaneous growth and interlocking of aggregates arising from crystallite formation. The decrease in scattering with increase in gel concentration arose from an increasing ordering of the scattering centers rather than a decrease in the aggregate size.

Eldridge and Ferry (1954)[40] studied the relationship between the melting temperature T_g of gel and its concentration and molecular weight in some well characterized fractionated gelatin systems. They found that T_g was a pronounced function of both molecular weight and concentration and interpreted the relations in terms of the cross-

links. They noted that all the cross-links did not have equivalent stabilities and that tempering or slow gel formation allows more stable cross-links to be established at the expense of the weaker bonds. Rapid chilling causes a more haphazard formation of weaker or less well-organized, cross-linked regions. The average crystallite size of the gelatin network was less in a quenched gel formed at high concentration than an equally rapid quenched gel formed at lower concentration and thus the experimental results of decreasing scattered light intensity with increasing concentration may be a result of a decrease in the average crystallite size.

Studies on the effect of pH values and salt concentration of the gelatin gel stability have also been done and were discussed in detail in the book by Veis.[1] Viscoelastic properties of gels are traditionally investigated by mechanical means. Measurements of shear modulus,[41-42] compression or extension moduli,[43-45] birefringence[46-47] have been made by static and dynamic methods. The existence of phase separation of gelatin gels having methanol-water mixtures as the gel fluid was found by T. Tanaka et al, (1979).[48] Measurements of the spectrum and the autocorrelation function of the scattered light intensity from gels giving the information of the collective mode of the polymer network were also performed. These results and their relationship to mechanical measurements will be discussed later.

1.2 PHYSICAL STRUCTURE OF COLLAGEN-GELATIN AND GEL SYSTEMS

A. Collagen

Collagen is unique among proteins because of its amino acid composition. Analyses of collagen of varying origins show different

compositions. Slight differences in composition also exist for collagen of the same source. It is extraordinarily rich in glycine and proline. Eastoe,[49-51] however, made the point that except for the amide group and arginine residue contents, the amino acid compositions of collagen were quite similar. On the other hand, all collagens have the same overall physical structure despite a fairly wide range of compositions. Besides amino acids, collagen also contains very small amounts of glucose[52] and galactose[53] which are covalently attached to its hydroxylpine residues.

Fig. 1 [54] shows the seven steps of the formation of collagen into connective tissue. The basic unit of collagen is tropocollagen consisting of three left-handed helical polypeptide chains, called α chains wrapped around each other to form a right-handed superhelix. The extruded tropocollagen, which is a long rigid rod with approximately 3000 A in length and 14 A in diameter, self-assembles into fibers of overlapping molecules (with 700 A periodicity). These fibers are then organized to form complex tissue.

The three polypeptide chains which are hydrogen-bonded to each other have the same size. Two of the chains, called $\alpha 1$, are identical, whereas the third chain, called $\alpha 2$, is similar in structure but slightly different in composition. Each chain has about a thousand amino residues. The amino acid sequence of collagen is remarkably regular: nearly every third residue is glycine and the sequence of glycine-proline-hydroxyproline occurs frequently. The rise per residue in the single-chain coiled helix is 2.86 A and the number per turn is nearly 3.3.

12

Fig. 1. The formation of collagen tissues. (From ref. 54)

FREE AMINO ACIDS

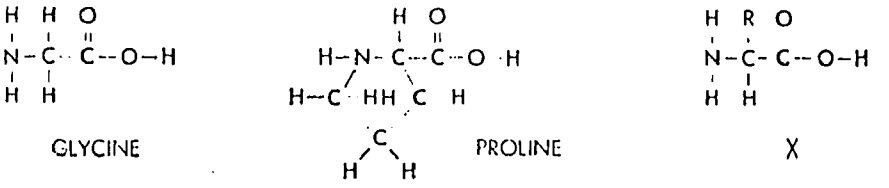

MOLECULAR CHAIN

SINGLE-CHAIN MOLECULAR HELIX

MAGNIFICATION 17,500,000

SINGLE-CHAIN COILED HELIX

MAGNIFICATION 17,500,000

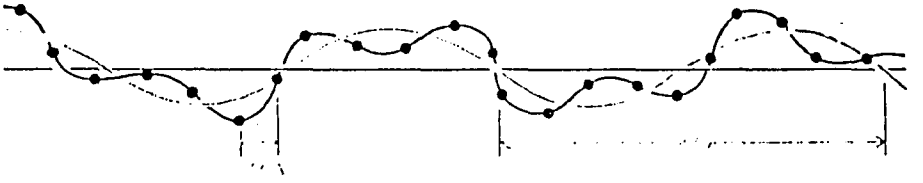

THREE-CHAIN COILED HELIX

MAGNIFICATION 17,500,000

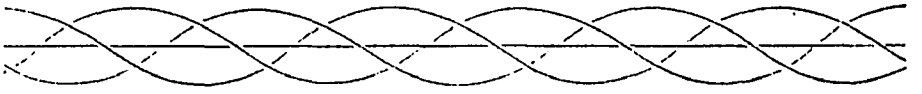

TROPOCOLLAGEN MOLECULE

MAGNIFICATION 350,000

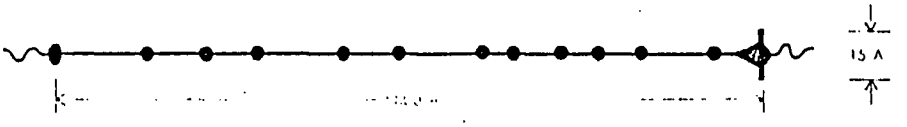

COLLAGEN FIBRIL

MAGNIFICATION 120,000

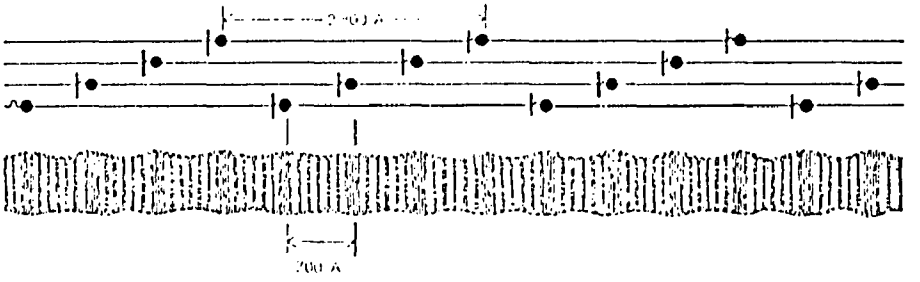

MAGNIFICATION 50,000

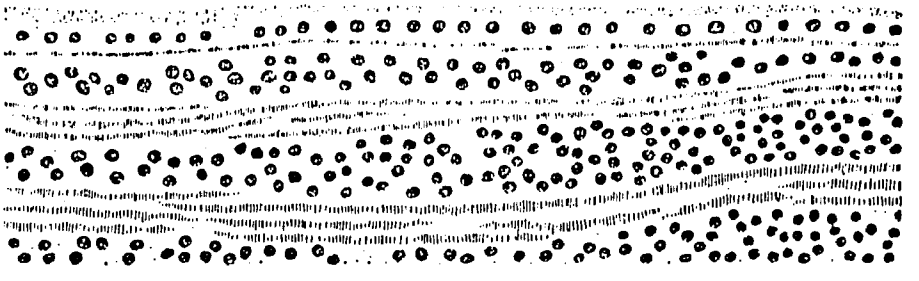

Most collagens develop covalent, non-peptide bonds between chains known as covalent cross-links. Two kinds of covalent cross-links are formed in the collagen fibers: intramolecular (within a tropocollagen unit) and intermolecular (between different tropocollagen units). The extent and type of cross-linking varies with the physiological function and age of the tissue. Only a small weight fraction of mature mammalian collagenous tissue can be put into solution in the form of acid or salt soluble tropocollagen. The major portion of the collagen is extensively cross-linked and insoluble.

B. Gelatin - The Denatured State of Collagen

The ordered hydrogen-bonded configuration of the collagen monomer molecule, tropocollagen, can be melted out readily by heating monodisperse collagen solutions in acid to about 40°C. This collagen to gelatin conversion called denaturation, is sharp and completed within a few minutes over a small temperature interval. The disordered molecule falls apart in one of the three ways shown in Fig. 2[1]. If there are no additional restraining bonds between chains (Path 1) three randomly coiled single-strand peptide chains, each with sedimentation constants $S^{\circ}_{20,w}$ = 3.0S, are created. In those cases (Path 2) where two chains are covalently cross-linked denaturation leads to two particles; one α chain, the other a two-strand molecule with $S^{\circ}_{20,w}$ = 4.5S called the β component. In the final case (Path 3) it can be imagined that at least two covalent cross-links hold the three chains together. This three-chain structure is called the γ component.

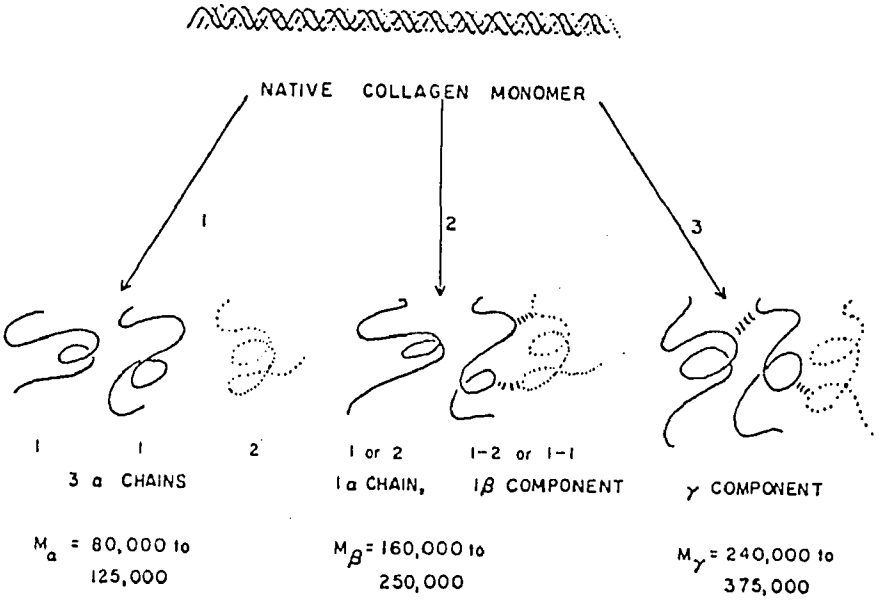

Fig. 2. A schematic diagram of the modes of conversion of monomeric tropocollagen to various types of gelatins, assuming no rupture of peptide bonds. (From ref. 1).

The denatured solution of extensively cross-linked collagen contains molecules with a very wide molecular weight distribution. Each particle may contain from one to more than ten covalent cross-linked α chains.

Most of the work on the preparation of gelatin has been carried out in the laboratories of the glue and gelatin manufacturers. Their aim is to maximize the amount of soluble protein with minimum degradation of the extracted gelatin. The main problem for these manufacturers is to identify and obtain a reproducible and well-defined starting material. It is also essential in the photography industry to get fine and homogeneous photographic emulsions. The IFS technique provides a very powerful approach to monitoring new procedures designed to improve these products.

C. Gelatin Gel

The gelation of a gelatin system can be delineated by three essential events. When the system is cooled down, particles form aggregates through the collagen-fold formation or hydrogen bond contacts. These aggregates, identified as the "crystallites" can then form the basis of the network junction points joined together by flexible, unstructured individual particle chains. Tempering or aging of the gel system, a reorganization process, progressively alters the average aggregate size in the network and increases the ordering and stability of the gel.

The structure of a network gel is determined by the mode of gel formation. If the network formation is brought about rapidly or at high concentration, random chain contacts and polymer chain entanglements lead to the formation of fine network structures. On the other

hand, slow formation of interchain contacts in dilute polymer solution permits a greater ordering of interacting segments, leading to the development of large crystallites in which chains are aligned for relatively long distances, and the formation of coarse networks. A gel formed as a fine network will gradually rearrange itself to a more ordered structure and become a more coarse network. Coarse network gels have higher and sharper melting temperatures T_g, than gels of fine networks since T_g depends on the relative number of bonds involved in each set of interacting chain segments, increasing as the number of bonds per segment increases. The sharpness of T_g is due to the fact that the disruption of an interacting pair of chain segments is a cooperative phenomenon involving the simultaneous rupture of several bonds. A coarse network gel scatters more light than a fine network gel since it has bigger crystallite sizes.

CHAPTER 2

INTENSITY FLUCTUATION SPECTROSCOPY

2.1 INTRODUCTION

Among the various techniques for the study of biopolymer and other macromolecular and colloidal systems, dynamic light scattering is of great current interest. It is both supplementary and complementary to other physical methods of investigating the properties of these systems. Particularly since the introduction of digital autocorrelation technique it is now possible to determine the diffusion coefficient and then size, weight and activity coefficient of macromolecules in solution accurately and rapidly. For fragile preparations that are prone to suffer an undesirable fate at the slightest change in solution condition, this technique may be the perfect technique. It is nondestructive, relatively rapid, and requires only modest amounts of material.

Intensity fluctuation spectroscopy is the main approach of the dynamic light scattering technique and will be employed in the experiments discussed in this thesis. Since the applications of dynamic light scattering have been widely discussed in literature we will only discuss briefly in this chapter.

2.2 RAYLEIGH SCATTERING FROM A SOLUTION

Consider a scattering volume V which contains N identical particles in a medium with dielectric constant ε and refractive index $n_o = \sqrt{\varepsilon}$. The volume is illuminated with a monochromatic plane wave of frequency ω_o, wave vector $\vec{K}_o$, amplitude $\vec{A}_o$ and is polarized perpendicular to the scattering plane, as shown in Fig. 3.

The electric field of the incident light in the medium can be written as:

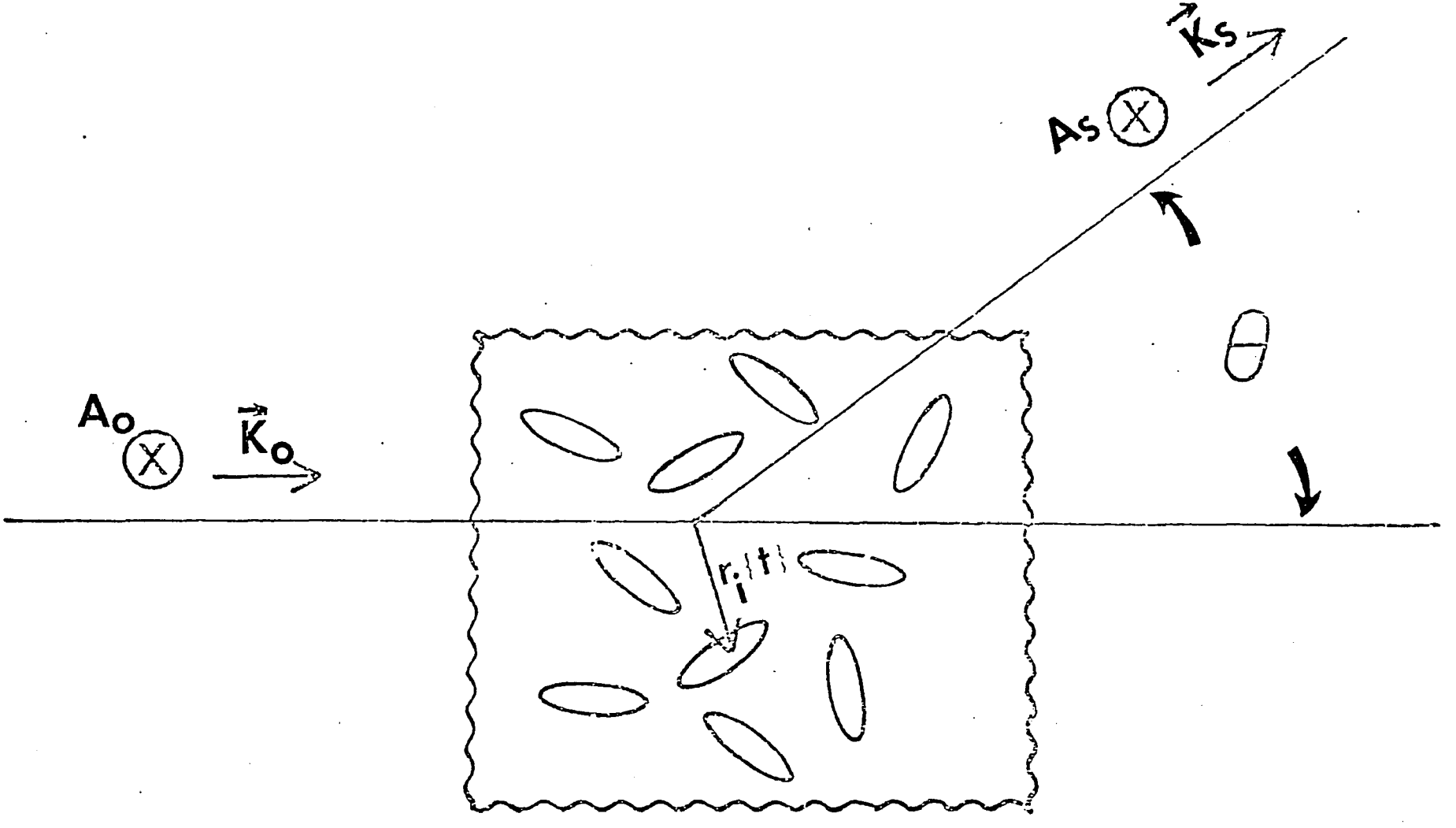

Fig. 3. Scattering geometry for intensity correlation spectroscopic measurements.

$$\vec{E}_o(\vec{r},t) = \vec{A}_o \exp(i\vec{k}_o \cdot \vec{r} - i\omega_o t) \ldots\ldots \quad (1)$$

The scattered electric field at a large distance $\vec{R}_o$ and scattering angle θ due to the j^{th} scatterer will be

$$\vec{E}_j(t) = \vec{A}_j(t)\, e^{i\vec{k}_s \cdot \vec{R}_o}\, e^{i(\vec{q}\cdot\vec{r}_j - \omega_o t)} \ldots\ldots \quad (2)$$

with scattering vectors

$$\begin{aligned} |\vec{q}| \equiv |\vec{k}_s - \vec{k}_o| &\simeq \frac{4\pi n_o}{\lambda_o} \sin^2\frac{\theta}{2} \\ |\vec{k}_s| &\cong |\vec{k}_o| \qquad \ldots\ldots \end{aligned} \quad (3)$$

where λ_o is the wavelength of the light in vacuum, $\vec{k}_s$ is the wave vector of the scattered field in the solution, $\vec{r}_j$ is the position of the j^{th} particle and the amplitude $\vec{A}_j$ may depend on the orientation of the j^{th} scatterer. In case the multiple scattering can be neglected, the scattered field at $\vec{R}_o$ due to all the scatterers is then[5,55]

$$\vec{E}_s(t) = \sum_{j=1}^{N} \vec{E}_j(t) = e^{i\vec{k}_s\cdot\vec{R}_o}\left[\sum_{j=1}^{N} \vec{A}_j(t) \exp i(\vec{q}\cdot\vec{r}_j(t) - \omega_o t)\right] \quad (4)$$

The average total scattered intensity is given as

$$I_s = \langle |E_s(t)|^2 \rangle_{time}$$

and by the Wiener-Khintchine theorem the optical spectrum is given [5,7,55,59] as

$$\begin{aligned} I_s(\omega) &= \frac{1}{2\pi} \int_{-\infty}^{\infty} e^{i\omega\tau} \langle \vec{E}_s^*(t)\ \vec{E}_s(t+\tau) \rangle\, d\tau \\ &= \frac{1}{2\pi} \int_{-\infty}^{\infty} e^{i\omega\tau}\ G^{(1)}(\tau)\, d\tau \end{aligned} \quad (5)$$

where the angular brackets denote an ensemble average and $G^{(1)}(\tau)$ is the electric field autocorrelation function defined as

$$G^{(1)}(\tau) = \langle E_s^*(t)\, E_s(t+\tau) \rangle = \langle |E_s|^2 \rangle\ g^{(1)}(\tau) \quad (6)$$

Similarly we define the intensity autocorrelation function $G^{(2)}(\tau)$ as

$$G^{(2)}(\tau) = \langle I_s^*(t)\, I_s(t+\tau)\rangle = \langle |I_s|^2\rangle\; g^{(2)}(\tau) \qquad (7)$$

where $g^{(1)}(\tau)$, $g^{(2)}(\tau)$ are the normalized autocorrelation functions of scattered field and intensity respectively.

For a random gaussian field, the second-order correlation function $g^{(2)}(\tau)$ is related to $g^{(1)}(\tau)$ by the Siegert relation[5,55-57],

$$g^{(2)}(\tau) = 1 + |g^{(1)}(\tau)|^2 \qquad (8)$$

2.3 LIGHT BEATING SPECTROSCOPY

There are two complementary methods of performing an analysis of the time dependence of randomly fluctuating light beams. One measures the frequency spectrum of fluctuations in the detector photocurrent. The other measures the time autocorrelation function of detected photons and thereby determine the range in time over which the intensity fluctuations are correlated.

The photo-electric effect provides a method of detecting the optical field. The probability $W^{(1)}(t)$ per unit time of photoelectron emission from a photocathode is proportional to the energy of the incident radiation field, which is proportional to the square of the amplitude of the electric field.

$$W^{(1)}(t) = \sigma E^*(t)E(t) = \sigma I(t)$$

$$i(t) = eW^{(1)}(t)$$

$$\langle i(t)\rangle = e\,\langle W^{(1)}(t)\rangle = e\sigma\,\langle E^*_{(t)}E_{(t)}\rangle = e\sigma\langle I\rangle$$

$$\langle i(t)\; i(t+\tau)\rangle = e^2\sigma^2\langle E^*_{(t)}E_{(t)}\; E_{(t+\tau)}E_{(t+\tau)}\rangle = e^2\sigma^2\langle I^2\rangle\; g^{(2)}(\tau) \qquad (9)$$

It is seen that the photocurrent output i(t) contains information on the intensity power spectrum and the autocorrelation function of the optical field. The power spectrum of the photocurrent $P_i(\omega)$ and the auto-

correlation function of the photocurrent also form a Fourier transform pair according to the Wiener-Khintchine theorem:

$$P_i(\omega) = \frac{1}{2\pi} \int_{-\infty}^{\infty} e^{i\omega\tau} \langle i(t)\ i(t+\tau)\rangle\ d\tau$$

2.4 AUTOCORRELATION FUNCTION

By substituting eq. (4) into eq. (6), we have the general equation for the correlation function of the field scattered from the solution assuming that multiple scattering can be neglected. It is

$$G^{(1)}(\tau) = \langle e^{-i\omega_o\tau} \sum_{i=1}^{N} A_i^*(t)\ A_j(t+\tau) \exp\ [-i\vec{q}\cdot\{\vec{r}_i(t)-\vec{r}_j(t+\tau)\}]\rangle \quad (10)$$

A. Dilute Solutions

When the solution is dilute, the particles are statistically independent and their positions and orientations are uncorrelated. Eq. (10) then reduces to

$$G^{(1)}(\tau) = e^{-i\omega_o\tau} \sum_{j=1}^{N} \langle A_j^*(t)\ A_j(t+\tau)\rangle \langle \exp\ [-i\vec{q}\cdot\{\vec{r}_i(t)-\vec{r}_j(t+\tau)\}]\rangle \quad (11)$$

(1) Monodisperse Systems

Assume that all the particles are identical, so that each particle has the same autocorrelation function. Thus

$$G^{(1)}(\tau) = Ne^{-i\omega_o\tau}\langle A^*(t)\ A(t+\tau)\rangle\langle \exp\ -i\vec{q}\cdot\{\vec{r}(t)-\vec{r}(t+\tau)\}]\rangle \ldots. \quad (12)$$

(a) Free translational diffusion. If the particles are spherical and/or small compared to the reciprocal of scattering vector, i.e. $q\ell<<1$, A(t) is independent of time. Then

$$G^{(1)}(\tau) = NA^2e^{-i\omega_o\tau}\langle \exp -i\vec{q}\cdot[\vec{r}(t)-\vec{r}(t+\tau)]\rangle \quad (13)$$

For particles undergoing Brownian motion, eq (13) becomes[5,7,55,66]

$$G^{(1)}(\tau) = NA^2e^{-i\omega_o\tau}e^{-D_Tq^2\tau} \quad (14)$$

where D_T is the translational diffusion constant of the particle and is

related to the friction coefficient f through the Einstein equation

$$D_T = kT/f \tag{15}$$

where k is Boltzmann's constant and T is the absolute temperature.

The friction coefficient f is given by Stoke's equation:

$$f = 6\pi\eta R_h \tag{16}$$

where η is viscosity of the solvent and R_h is the hydrodynamic radius of the particle. For spherical particles, R_h equals the radius of the particle R.

(b) Rotational Diffusion. When the particles are not spherical and do not meet the Rayleigh criterion ($qL<<1$), $A_i(t)$ will fluctuate as the particle rotates. For particles undergoing independent rotational and translational Brownian motions, it can be shown from Eq (12) that $|g^{(1)}(\tau)|$ consists of an infinite sum of exponential terms involving both D_T and the rotational diffusion coefficient D_R.[55,60,61,62] For rigid rod-shaped particles of length L,

$$g^{(1)}(\tau) = N|A|^2 e^{-i\omega_o\tau}\, e^{-D_T q^2 \tau} \sum_{\substack{\ell=0 \\ \text{even}}}^{\infty} B_\ell \exp[-\ell(\ell+1)\, D_R\tau] \tag{17}$$

It is assumed that the Rayleigh-Gans criterion

$$2K_oL(n-n_o)<<1$$

is satisfied above, where n is the refractive index of the particle.

Pecora[61] and also Cummins et al[62] have calculated the values of B_ℓ and found $B_o(qL)\to 1$ and $B_2(qL)$, $B_4(qL)$ etc $\to 0$ as $qL \to 0$. We can thus determine D_T from $g^{(1)}(\tau)$ at the scattering angle in which B_2 (qL), $B_4(qL)$ etc. are zero and then calculate D_R from $g^{(1)}(\tau)$ at large scattering angle where B_2 (but not B_4, B_6, etc.), is considerably different from zero.

The translational and rotational diffusion constants can be calculated through the Broersma theory[63,64] for cylindrical rod-shaped particles with length L and diameter d. The Broersma equations are

$$D_T = (kT/3\pi\eta L)\ [\delta - \tfrac{1}{2}(r_{\parallel} + r_{\perp})] \tag{18}$$

$$D_R = (3kT/\pi\eta L^3)\ (\delta - \xi) \tag{19}$$

where $\delta = \mathrm{Ln}(2L/d)$, $\xi = 1.57 - 7(\frac{1}{\delta} - 0.28)^2$

$r_{\parallel} = 1.3 - 8(\frac{1}{\delta} - 0.3)^2$ and $r_{\perp} = 0.35 - 4(\frac{1}{\delta} - 0.43)^2$

Alternatively, one can determine the shape and size of the particles in terms of D_T and D_R.

(2) Polydisperse Solution

For particles with different sizes and/or shapes, the diffusion coefficients are also different. The autocorrelation function of a solution containing non-interacting, non-identical particles in the far field approximation, is given by [55,65,66]

$$G^{(1)}(\tau) = \sum_{j=1}^{N} |A_j|^2\ e^{-i\omega_o\tau}\ e^{-D_j q^2 \tau} \tag{20}$$

where D_j is the translational diffusion constant of particle j. Eq. (20) can be rewritten in terms of species of scatterer.

$$G^{(1)}(\tau) = \sum_{j=1}^{N} N_j\ |A_j|^2\ e^{-i\omega_o\tau}\ e^{-\Gamma_j \tau} \tag{21}$$

where N_j is the number of scatterers of species j with diffusion constant D_j and $\Gamma_j = D_j q^2$. Note that

$$|g^{(1)}(\tau)| = \sum_j N_j\ |A_j|^2\ e^{-\Gamma_j \tau} \Big/ \sum_j N_j\ |A_j|^2 \tag{22}$$

For a solution with the particle's molecular weight distribution characterized by a continuous function f(M), we have

$$|g^{(1)}(\tau)| = \int \left[\frac{f(M)\ A(M)}{\int f(M)|A(M)|^2 dM}\right] e^{-D(M)\ q^2 \tau} dM \tag{23}$$

or

$$|g^{(1)}(\tau)| = \int F_{(\Gamma)}\ e^{-\Gamma\tau} d\Gamma \tag{24}$$

where f(M)dM is the weight fraction of molecules with molecular weights

in the range M to M + dM and $F(\Gamma)d\Gamma$ is the fraction of scattered intensity due to particles with decay rate $\Gamma = Dq^2$ between Γ and $\Gamma + d\Gamma$

Different methods have been used to analyze the photon correlation data for polydisperse solutions. However, the most common method of analysis is the method of moments or cumulants described by Koppel.[63] Following Koppel[65] and Cummins et al,[55,56] Eq. (24) is expanded as

$$Ln|g^{(1)}(\tau)| = -\langle\Gamma\rangle\tau + \tfrac{1}{2}\mu_2\tau^2 - \tfrac{1}{3}\mu_3\tau^3 + \tfrac{1}{4}[\mu_4 - 3\mu_2^2]\tau^4 + \ldots = \sum_{m=1}^{\infty} K(\Gamma)(-\tau)^m \frac{1}{m!} \qquad (25)$$

where

$\langle\Gamma\rangle = \int\Gamma F(\Gamma)d\Gamma$ is the mean decay rate,

$\mu_n = \int F(\Gamma)(\Gamma - \langle\Gamma\rangle)^n d\Gamma$ is the n^{th} moment of $F(\Gamma)$ about mean,

and K_m is the m^{th} cumulant of $F(\Gamma)$

Note that $K_1 = \langle\Gamma\rangle = \mu_1$

$K_2 = \mu_2$

$K_3 = \mu_3$

$K_4 = \mu_4 - 3(\mu_2)^2$

the first cumulant is directly proportional to the z-average diffusion coefficients $\langle D_z\rangle$,[65] the second cumulant K_2 which is equal to the second order moment, is a good measure of the relative width of the distribution i.e., the polydispersity. Frequently, polydispersity is estimated from K_2/K_1^2.

Pusey has given an approximate expression which is valid in the limit of low polydispersity:[67]

$$\frac{M_w}{M_N} \simeq 1 + \mu_2/\alpha^2\langle\Gamma\rangle^2 \qquad (26)$$

where α is about 1/2 for Gaussian random coils and 1/3 for spheres.

B. Semi-dilute Solution

When the concentration of a solution is low, the particles are far enough apart that the effect of interactions between particles is small, and each particle executes its individual Brownian motion characterized by the free diffusion coefficient D_o which is independent of the solution concentration. As the solution concentration is increased, the particles start to interact with each other through the long-range repulsive coulombic force, the hydrodynamic interaction, and the excluded volume effect. The diffusion constant then depends on concentration.

A hydrodynamic model,[68-72] based on scaling law theories has been proposed, describing static and dynamic properties of both dilute and semi-dilute solutions of chain particles. The semi-dilute solution is considered as an entangled network with a finite lifetime T_r. The average distance between two crosslinks is given by the screening length ξ according to the scaling law by Daoud et al.[70]

$$\xi \alpha C^{-0.75} \tag{27}$$

The cooperative diffusion constant of the chains of the network is thus given by [72]

$$D_{(c)} = \frac{kT}{6\pi\eta\xi} \quad \alpha \quad C^{0.75} \tag{28}$$

The cross-over concentration between dilute and semi-dilute regions for a solution of macromolecules of molecular weight M is given by[72]

$$C^* = \frac{3M}{4\pi N_A R_G^3} \tag{29}$$

where N_A is the Avogadro number, R_G the radius of gyration of the chain molecule.

Beside the collective excitation of the polymer network described above, the polymer chains in semi-dilute solutions also execute individual motion described by introducing the "reptation" concept by DeGennes[73] : To renew its configuration, the chain has to slip in a tube of diameter ξ defined by its neighbors. The diffusion coefficient along the tube is[74]

$$D_{tube} = kT/6\pi\eta(\frac{N}{g})\xi \qquad (30)$$

where $g = n\xi^3$, n is the monomer concentration proportional to the mass concentration C in gram per cubic centimeter, N is the polymerization index.

The self-diffusion coefficient D_{self} measured in a macroscopic experiment corresponds to a three-dimensional random walk. It is shown theoretically and experimentally[74] that

$$D_{self} \cong N^{-2}C^{-1.75} \qquad (31)$$

The concentration dependence of a diffusion coefficient also depends on the solvent. From the relationships between the diffusion coefficient, chemical potential and friction coefficient, the diffusion coefficient can be expressed by[55,75]

$$D(c) = D_o(1+K_D c + ...) \qquad (32)$$

with $K_D = 2A_2M - K_f - \bar{\nu}$

where A_2 is the second osmotic pressure virial coefficient, K_f is the first order concentration dependence of the friction (or sedimentation) coefficient and $\bar{\nu}$ is the partial volume of the polymer.

The contribution from $2A_2M$ term can make a dramatic difference to K_D in theta and nontheta solvents and thus make the concentration dependence different.

The electric field correlation function of the semi-dilute solution

can be written as[72]

$$g^{(1)}(\tau) = e^{-D(c)q^2\tau} \tag{33}$$

where $D_{(c)}$, which depends on solution concentration, is the cooperative diffusion coefficient of the polymer network in ordinary Rayleigh scattering and is the self diffusion coefficient of the individual chain motion in forced Rayleigh scattering.

The normalized autocorrelation function of intensity will be discussed in the next section and is[72]

$$g^{(2)}(\tau) = 1 + A \exp(-D_c q^2 \tau) \tag{34}$$

where A is a constant determined by the experimental configuration.

C. Gels

When a macromolecular solution forms a gel, molecules form interchain contacts to form a polymer network with solvent contained inside the network. The molecule is no longer free to diffuse but is confined to a region of the network compatible with the number of effective cross-links. Two theoretical models of gel dynamics have been proposed, the elastic continuum model of Tanaka, Hacker and Benedek (THB),[45] and the bounded diffusion model of Carlson and Fraser (CF).[76,77]

(1) Bounded Diffusion Model

The CF model assumes that each molecule undergoes Brownian motion within a volume restricted by the surrounding network to which it is harmonically bound. This model predicts

$$g^{(1)}(\tau) = e^{-Dq^2(1-e^{-2\gamma\tau})/2\gamma} \tag{35}$$

and

$$g^{(2)}(\tau) = 1-\exp(-2Dq^2/\gamma)+\exp[(-2Dq^2/\gamma)\cdot(1-e^{-\gamma\tau})] \tag{36}$$

where $\gamma = k/f$, k is the spring constant with which the molecule is bound in place, f is the friction constant opposing its motion and D

is the free diffusion coefficient of the individual particles.

(2) Elastic Continuum Model

The THB model considers the polymer network and the solvent, which constitute the gel structure, as two interpenetrating isotropic elastic continua. The light scattered from a gel arises from longitudinal deformation modes of the network. The deformation of the swollen network has been shown to obey a diffusion equation and the correlation function of the polarized scattered light is given as

$$G^{(1)}(\tau) = I \exp(-D_c q^2 \tau) \tag{37}$$

where $D_c = c_{11}/f$ is the cooperative diffusion constant of the chains of the network, c_{11} (dyne/cm^2) is the longitudinal compressional modulus and f (dyne sec/cm^4) the frictional force per unit volume of the network as it moves with unit velocity relative to the surrounding liquid. Note that the correlation function has the form of a single exponential decay.

When we take account of the static scattering due to spatial non-randomness of the crosslinking, the static scattered component works as local heterodyne source, we have:[72]

$$g^{(2)}(\tau) = \frac{\langle I(t)I(t+\tau)\rangle}{|I|^2} = 1 + \frac{2I_o I_S}{(I_o+I_S)^2} \exp(-D_c q^2 \tau) + \frac{I_S^2}{(I_o+I_S)^2} \exp(-2D_c q^2 \tau) \tag{38}$$

where I_S is the intensity of the static component, I_o the intensity scattered from longitudinal fluctuations.

In case $I_S >> I_o$ Eq (38) reduces to

$$g^{(2)}(\tau) = 1 + 2\frac{I_o}{I_S} \exp(-D_c q^2 \tau) \tag{39}$$

Munch et al[72] have obtained the following relation for the cooperative diffusion constant

$$D_c \cong \frac{kT}{6\pi\eta R_h} = D_T \qquad (40)$$

where D_T is the translational diffusion constant for a dilute solution of free macromolecules having hydrodynamic radius R_h equivalent to that of one polymer chain between two interchain contacts of the gel network, η is the viscosity of the swelling liquid.

2.5 CURRENT STUDIES

The broadening of the scattered light spectrum due to Doppler effects from Brownian motion of macromolecules was first observed in 1964 in a dilute solution of polystyrene latex spheres.[62] It was in good quantitative agreement with the theory. Since then the light beating spectroscopy technique has been employed increasingly to study the hydrodynamic properties of systems of macromolecules. Some of these studies related to our measurements will be discussed briefly in the following.

A. Dilute Solutions of Rodlike Macromolecules

In 1967 Dubin et al.[78] measured the Rayleigh linewidths of a series of biological macromolecules by fitting their light scattering spectra to single Lorentzian functions. They found serious discrepancies for tobacco mosaic virus (TMV), the most anisotropic molecule they studied. In 1969 Cummins et al.[62] measured the spectrum of laser light scattered from dilute aqueous solution of TMV using homodyne and heterodyne light beating techniques. From the spectra they inferred the translational and rotational diffusion coefficients using Pecora's theoretical treatment. For the similarly rodlike shaped macromolecular-collagen, studies using the light beating technique were not performed until 1971 by French et al.[22] as mentioned in 1.1A where studies on collagen solutions

using techniques of dynamic light scattering were described.[22-28] Measurements of the intensity autocorrelation function of light scattered from collagen solutions at non-zero scattering angles were not reported before the current studies.

B. Dilute and Semi-dilute Solutions

Keller et al.[79] measured the diffusion coefficients of hemoglobin and serum albumin over a broad range of concentration by both tracer and mutual diffusion techniques. Some of their results are shown in Fig. 4a. King et al.[75] studied the concentration dependence of the translational diffusion coefficient of polystyrene in cyclohexane and 2-butanone solvents by performing the scattered laser light linewidth measurements. Their results were well fitted by eq.(32) and are shown in Fig. 4b. M Daoud et al.[70] performed small angle neutron scattering studies on polystyrene in a good solvent (carbon disulfide) in the semidilute regime where the molecular chains overlap strongly. They found that R_G^2 was proportional to C^{-X} where R_G was the radius of gyration, χ a constant ($\chi = 0.25 \pm 0.02$) and the screening length $\xi(C)$ giving the range of the $<C(\vec{\gamma})C(\vec{\gamma}')>$correlations was proportional to C^{-Z} with $z = 0.72 \pm 0.06$ compared with 0.75 mentioned in section 2.4B.

Photon correlation spectroscopy was used by R. Frost et al.[80] to measure the diffusion coefficient of polystyrene in a mixture of benzene and 2-propanal with benzene volume fraction $\phi = 0.64$. They found that D varied linearly with C, $D = D_o (1 + K_D C)$, and D_o, the translational diffusion coefficient in the limit of $C = 0$, varied as M^{-b} where K_D was defined before, M was the molecular weight and b was a

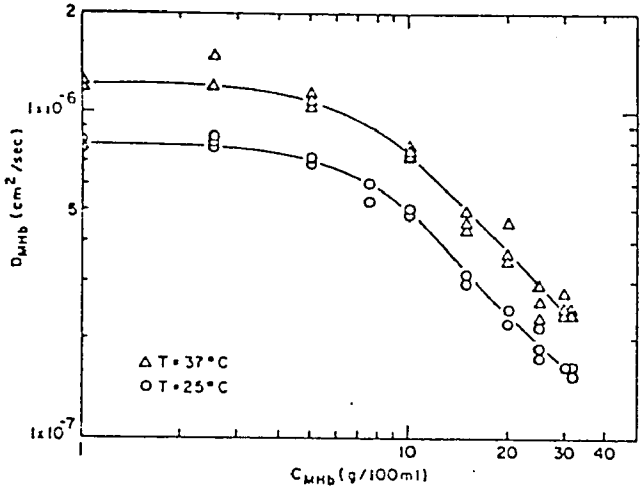

a. Hemoglobin diffusion coefficient measurements at 25° and 37° obtained by interdiffusion of methemoglobin and cyanomethemoglobin. (From ref. 79)

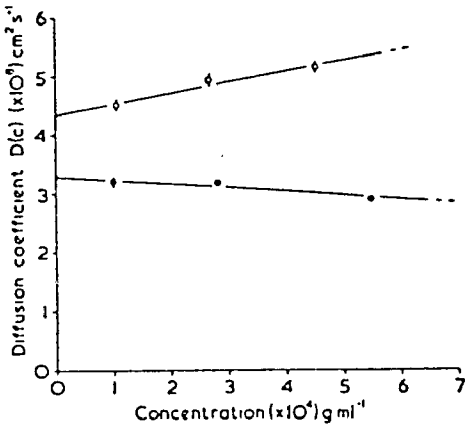

b. Concentration dependence of the diffusion coefficient of polystyrene ($\bar{M}_w = 17 \times 10^6$) in cyclohexane at 35°C (●); and 2-butanone at 25°C (○). (From ref. 75)

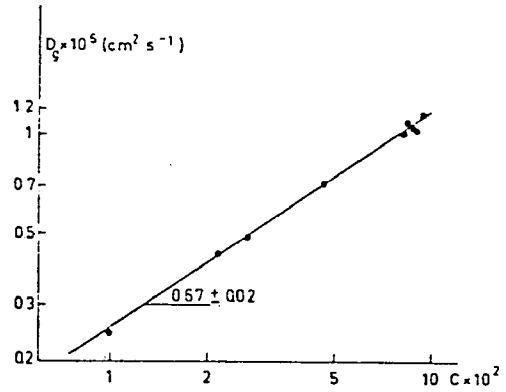

Diffusion in the pseudogel domain as a function of the concentration (log–log scale). (From ref.71)

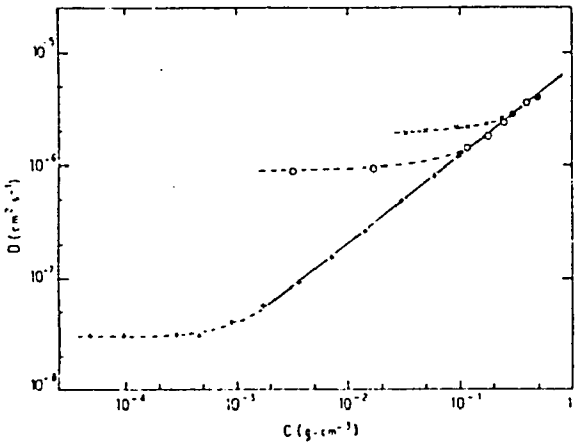

d. — Semi-dilute solutions of linear PDMS samples in toluene. + $M_w = 6 \times 10^6$; ○ $M_n = 17\,100$; × $M_n = 4\,500$.

(From ref. 72)

Fig. 4. The concentration dependence of the diffusion coefficients

constant. Adam et al.[71] also used the technique of intensity fluctuation spectroscopy to study the dynamic behavior of polymer (polystyrene) solutions in good solvents at different concentration regimes. In dilute solutions, the hydrodynamic radius R_h of the polymer increased with the molecular weight as M^{χ} where $\chi = 0.55 \pm 0.02$ and the effective diffusion coefficient $D_{(C,M)}$ followed the relation:

$$D_{(C,M)} = D_{o(M)}(1 + \phi_{(M)}C)$$

where $D_o(M) \propto M^{-\chi}$, was the translational diffusion coefficient of those particles with molecular weight M in the limit of C = 0. In the semidilute region where the polymer chains overlap strongly, they found that the solutions behaved like gels of finite lifetime. The cooperative diffusion coefficient depended on concentration only and increased with concentration as C^B where $B = 0.67 \pm 0.02$ compared with 0.75 from the deGennes' calculation. Some of their results are shown in Fig. 4c.

Munch et al.[72] using intensity fluctuation spectroscopy studied the solutions of polydimethylsiloxane in toluene in different concentration regimes. They found that the translational diffusion coeffcient was independent of concentration in the dilute regime, while the cooperative diffusion coefficient increased with polymer concentration as $C^{0.77 \pm 0.03}$ in the semi-dilute regime. These results were in agreement with deGennes' predictions and are shown in Fig. 4d.

The self-diffusion coefficient D_{self} which was defined in section 4.4B was measured by Hervet et al.[74] recently using the forced Rayleigh scattering technique. In the semidilute regime they found that D_{self} decreased with the concentration as $C^{-1.7 \pm 0.1}$.

C. Gels

Tanaka et al.[45] in 1973 first measured the correlation functions of the scattered light intensity from 5% and 2.5% polyacrylamide gels and interpreted their results in terms of the elastic continuum model they proposed. As predicted by their model, the correlation functions were well fitted by a single exponential function $e^{-\Gamma\tau}$ and the decay rate Γ which should be $(C_{11}/f)q^2$ or $D_c q^2$ was proportional to q^2. They also measured, using macroscopic methods, C_{11} and f and compared the numerical predictions of the model with the experimental measurements of the correlation function. Both results were in good agreement.

Carlson and Fraser[76] measured the autocorrelation functions of the scattered light intensity from solutions of F-actin and F-actin complexed with myosin sulifragments. They found that the initial amplitude of the normalized intensity autocorrelation function was drastically reduced going from the "sol" to the "gel" state. The behavior was interpreted by the harmonically bound particle model they proposed. This model predicted that the initial amplitude was correlated with the constraint imposed on the motion of the macromolecules in its "gel" state. Further study on polyacrylamide gels was made by Wun and Carlson.[77] They measured the correlation function and deduced physical properties in terms of the bound particle model and then compared the results derived from unilateral compression and Rayleigh ratio measurements. In addition, they found that the autocorrelation function for the gels were not single exponential in form.

Munch et al.[81b] measured, using light beating spectroscopy, the spectra of polarized light intensity scattered from model networks of polystyrene swollen by benzene. They investigated various series of networks of dif-

ferent functionalities and different lengths of the elastic chain elements. The photocurrent spectra of different gels were fitted well to single Lorentzian curves. The compression moduli of gels were also measured and these results along with the data of light scattering measurements were used to determine the elastic and frictional coefficients. Later, a gel of a mixture (1/1) in weight of two "living" polystyrenes of molecular weights 17,000 and 73,000 respectively was studied by Munch et al.[82] Single exponential correlation functions were obtained and the ratio Γ/q^2 was independent of q^2. The hydrodynamic theory based on a cooperative diffusion process of network deformation was used to interpret this behavior. Munch et al.[72] also measured the autocorrelation functions of scattered light from polydimethyl-siloxane-toluene gels formed by swelling permanent networks or by dissolving linear macromolecules at semi-dilute regime. In both cases, the cooperative diffusion coefficient varies with concentration according to a power law.

Studies on the critical behavior of density fluctuations of gels, collapse of gels and the critical endpoint, phase separation and gelation in gelatin gels were carried out recently by Tanaka et al.[43,83,84] Macroscopic measurements[85] were employed.

CHAPTER 3

APPARATUS AND EXPERIMENTAL TECHNIQUES

A schematic diagram of the apparatus used for the photon correlation spectroscopy experiments is shown in Fig. 5. In order to minimize the stray light, the entire spectrometer was enclosed in a light-tight blackened box. The whole system including the laser was mounted on a Modern Optics pneumatic vibration isolation table upon which all the experiments were performed. Various parts of the apparatus are briefly described below:

3.1 LASER AND OPTICAL DESIGN

An Argon ion laser (Spectra Physics 165) operating at 4880 Å was used as the light source in all light scattering measurements. The signal-to-background ratios $G\binom{2}{0}/G\binom{2}{\infty}$ were improved by operating the laser in a single longitudinal mode by the use of an air spaced etalon (Spectra Physics No. 589) in the laser cavity. To obtain the best intensity stability of the laser output during experiments, the laser was operated in the light mode which maintains constant intensity by means of a light feedback loop. The intensity has been found to be stable to about ±0.1% for many hours.

A monochromatic incident laser beam was polarized perpendicular to the scattering plane by a Glan-Thomas prism. The intensity of the laser beam on the sample was adjusted by rotating the half-wave plate (a mica sheet) which rotated the plane of polarization of the light incident on the prism. The laser beam was then focused onto the center of the sample cell by a lens. The sample cell was mounted in the center of a thermostated bath which was mounted on an x-y translational

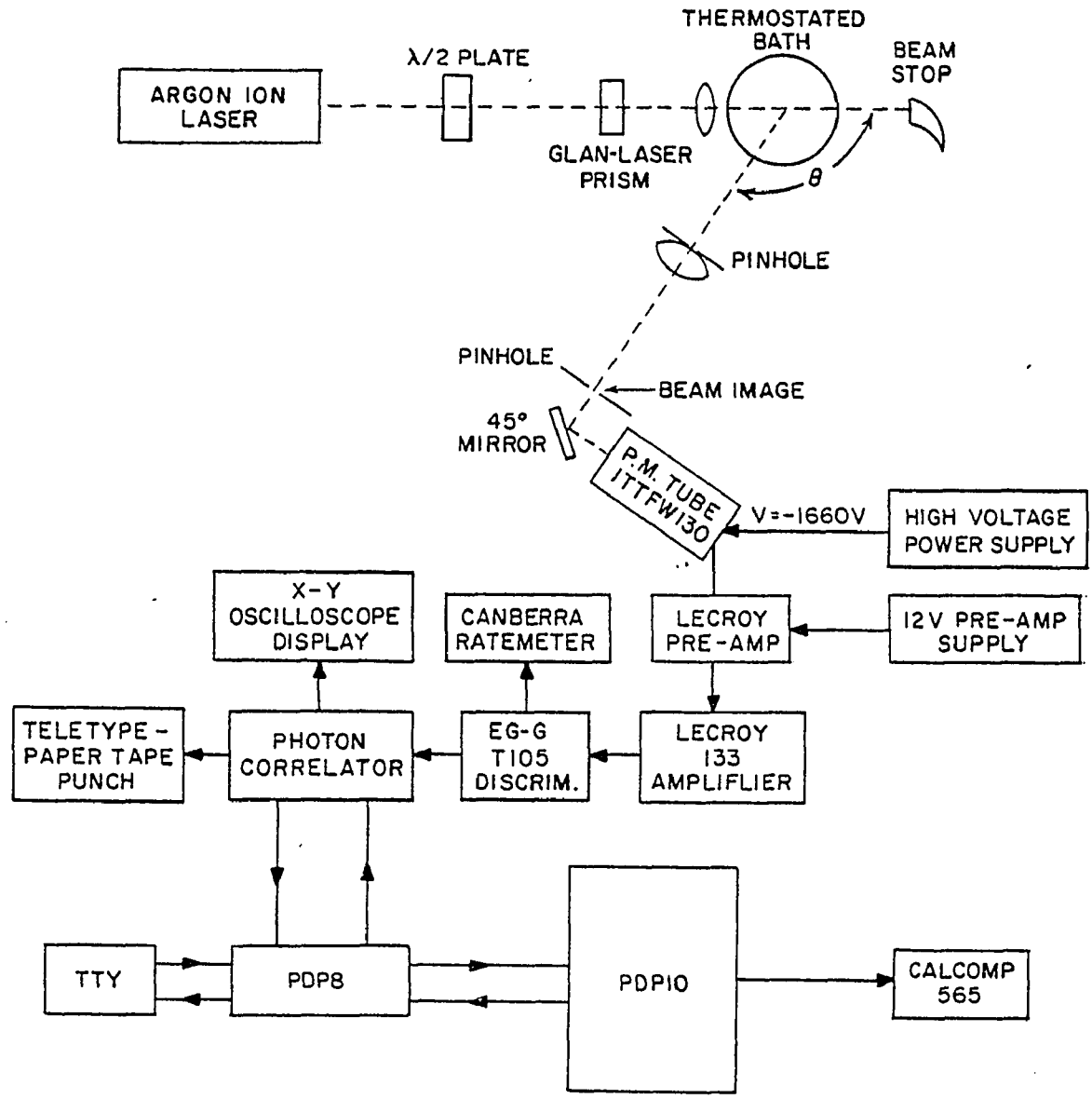

Fig. 5. Block diagram of the apparatus used for the photon correlation spectroscopic measurements. Top view of the optics except that the phototube was actually mounted vertically above the 45° mirror.

stage at the center of a goniometer. All detector components were mounted on a tunable counterbalanced arm with the pivot point at the center of the goniometer. The detector optical system consisted of a PM tube (ITT FW 130) and two pinholes which defined the effective volume and the angular aperture of the scattering region. A lens was placed directly behind the first pinhole to image the scattering column onto the second pinhole. The light passing through the second pinhole was reflected by a 45° mirror onto the photocathode of the vertically mounted photomultiplier tube.

3.2 COHERENCE AREA CONSIDERATIONS

To obtain the best signal-to-background ratio, the detector area was kept in the neighborhood of one coherence area. A useful estimate of the coherence area A_{coh} for a typical light scattering experiment is given by

$$A_{coh} = \frac{\lambda^2}{\Omega} = \frac{r^2\lambda^2}{A_s}$$

where λ is the wavelength of the laser light, Ω is the solid angle subtended by the source at the detector, r is the optical distance from the source to the detector and A_s is the area of the source seen by the detector. In our optical system, the two detector pinholes have diameters d_1 and d_2 spaced at a distance r apart. The scattering column is magnified by the lense immediately behind the first pinhole by a factor of M. Then we have

$$A_{coh} = \frac{r^2\lambda^2}{\pi\left(\frac{d_2}{2}\right)^2/M}$$

The number of coherence areas within the area of the second pinhole is

$$N_{coh} = \frac{A_1}{A_{coh}} = \frac{\pi^2 d_1^2 d_2^2}{16 r^2 \lambda^2 M}$$

For our geometry r = 13 cm, λ = 4880 Å, M = 1.9

we need

$$d_1 d_2 \leq \frac{4r\lambda}{\pi} \sqrt{M}$$

to have the best signal-to-background ratio. Thus, we selected pin holes with sizes such that the above equation is satisfied. Since the sizes of pin holes also affected the count rate, the optimum choice of sizes does not correspond to the largest signal-to-background ratio. In the experiment, one of the following combinations of pin holes was chosen for different samples according to their light scattering ability

	d_1 (Å)	d_2 (Å)
1	1000	100
2	500	100
3	500	250

3.3 ELECTRONICS

The output signal from the PM tube was preamplified by a factor of 10 using a LeCroy Model A1007 preamplifier mounted directly on the phototube housing. The amplified signal was then sent through a shielded 50Ω coaxial cable to a LeCroy 2-stage linear amplifier (Model 133B) with total gain set at 12. Low level noise was eliminated by a discriminator (EG&G T105/N Model) with the threshold voltage set at 55 mV. The discriminated signal was then fed to the input of a digital autocorrelator for correlation measurements.

The output pulses from the PM tube had relatively broad widths and tailed off very slowly. If a pulse was followed immediately by another pulse as in the case of high scattered intensity, the second pulse might not be counted. This caused a droop in the very first few channels of the correlation function. To prevent this undesirable effect, a 50 cm coaxial cable was attached parallel to the end of the 50Ω cable. Pulses traveling down to the end of the 50Ω cable were then reflected by the attached 50 cm cable. The reflected pulses then interfered with the original pulses and the result consisted of a relatively sharp peak of positive amplitude immediately followed by a sharp peak of negative amplitude which would then ready the discriminator for another count. By attaching the 50 cm cable, amplitudes of the resultant pulses were only half of the original pulses. The total gain of the amplifier was thus increased from 12 to 24 to bring the amplitudes back to the original values. However, this also increased the amplitude of the noise. The threshold voltage of the discriminator therefore was readjusted to 90 mV to cut off the increased noise.

3.4 DIGITAL AUTOCORRELATOR AND COMPUTER FACILITIES

A 60 channel digital autocorrelator designed by A. Fraser and built at Johns Hopkins Applied Physics Laboratories was used. It can be operated in single clipping, double clipping, fast clipping, prescaling and multiscaling functions. A detailed discussion has been given previously[86] (Newman 1975). The functions of the correlator have been discussed by many authors.[87-89]

The correlator was interfaced with a PDP 8 minicomputer, which was then interfaced with a PDP 10 main computer. The contents of the

60 channel memory of the correlator can be displayed locally on an oscilloscope and plotter by the PDP 8 or sent to the main PDP 10 computer which permitted very rapid on-line data acquisition, analysis and curve plotting on a Cal Comp precision plotter. The experiment was controlled from the console terminal of the PDP 8 computer. From one to twelve consecutive experiments are carried out and data accumulated in the PDP 8 automatically. The analysis programs in the PDP 10 utilized this multiple-record capability to reduce the variance of statistical estimators.

3.5 TEMPERATURE CONTROL

The sample cell was mounted immersed in water inside a thermostated bath which consisted of a precision machined brass cylinder clamped between two plates with O-ring seals. The brass cylinder contained a series of high quality optical windows centered at scattering angles of 0°, 11.82°, 21.92°, 31.82°, 45.03°, 69.83°, 90°, 122.63°. Each window was seated in a hole on the bath with its normal along a radial direction of the goniometer's arc. The temperature was controlled to ±0.05°C by a Brinkmann Lauda temperature controller (Model K2-R). The circulated water was filtered through a millipore filter with 142 mm diameter and 0.45μ pore sizes.

3.6 PREPARATION OF SOLUTIONS

The most common difficulty in autocorrelation measurements is caused by the presence of dust, inhomogeneities, or other contaminants in the solutions. In order to minimize the amount of dust, extensive effort was devoted to cleaning the glassware and the cuvettes - the sample cells. All the glassware was ultra-sonicated in a detergent

solution, distilled water, and then rinsed with millipore filtered deionized distilled water.

The cuvettes (Hellma special optical glass cells type 111-OS) were first immersed in warm detergent solution, washed repeatedly with water, immersed in chromic acid cleaning solution for 5 to 10 minutes and then rinsed with deionized distilled water. The final step was to rinse the cuvettes with freshly distilled warm acetone in a specially designed cuvette cleaner[90] for at least an hour.

High speed centrifugation was used extensively in order to remove dust in water, solvents and solutions. Millipore filters were also used. However, high speed centrifugation was preferred since the millipore filters contain some residual surfactants.

3.7 CALIBRATIONS AND ADJUSTMENTS

The optical system was realigned periodically. Before any measurements on samples were taken, a monodisperse solution of polystyrene latex spheres with known particle size was used to check the entire apparatus. Autocorrelation measurements were not started until one-half hour after the samples were loaded into the thermostated bath to allow thermal equilibration.

For the greatest accuracy, many short experiments, each one normalized independently against its own background, were preferable to a single long experiment. To obtain the optimum operating condition for digital photon correlation, the detector area was maintained around one coherence area and the clipping level was set equal to the average number of photocounts per bin. The single clipped mode was employed in studies of collagen and gelatin solutions when the

scattered light is Gaussian. For the gels, however, which produce non-Gaussian scattered fields, prescaling was used rather than clipping.

CHAPTER 4

GELATIN SOLUTIONS

4.1 SAMPLE PREPARATION AND EXPERIMENTAL PROCEDURE

The gelatin solutions were prepared, as required, from Kodak limed ossein gelatin, batch No. 102-125 provided by Dr. P.I. Rose. Gelatin solids were added to the solvents and kept at 4°C at least overnight. Then the solutions were rapidly heated to 40°C and kept at that temperature for an hour, stirred for several minutes and then diluted to a series of different concentrations. For semi-dilute solutions, samples were obtained simply by loading these solutions into cuvettes. For dilute gelatin solutions, the series of diluted solutions were loaded into centrifuge tubes and centrifuged using an RC2 Sorvall centrifuge at a speed of 48,000 g at a temperature near but less than 30°C for three hours. Samples were obtained by transferring the supernatants of the centrifuged solutions into well cleaned cuvettes using a syringe and tygon tubing.

All the solvents were prepared from deionized distilled water from the same source and filtered with a millipore filter of 0.2μ pore size. In Table I we list all the solvents used in preparing gelatin solutions along with their pH values and viscosities. The only solvent used in preparing semi-dilute solutions is solvent A which consists of 0.15M NaCl and 0.05M Tris.

Light scattering measurements were performed either on the same day as the samples were prepared and/or after the samples had been in a 4°C refrigerator overnight to several days. Samples removed from the refrigerator were allowed to sit at room temperature at least three hours before any measurements were taken. Samples not measured on the day of preparation could be stored at 4°C for as long as several days without degradation.

TABLE I

SOLVENTS USED FOR GELATIN SOLUTIONS

Solvents	Ingredients	pH Values	Viscosities			
			20°C		35°C	
			η/η_ω *	η cp	η/η_ω *	η cp
A	0.05M NaCl, .05M Tris	9.03	1.005	1.0070	1.005	0.7244
B	.15M NaCl, .05M Tris	9.70	1.0123	1.0143	1.0148	0.7315
C	1M NaCl, .05M Tris	9.75	1.0873	1.0895	1.1049	0.7964
D	3M NaCl, .05M Tris	9.75	1.3325	1.3352	1.3572	0.9783
E	1M CaCl , 0.05M Tris	9.00	1.3155	1.3181	1.3263	0.9560

* $\eta_\omega^{35^\circ}$ = 0.7208 cp

η_ω^{20} = 1.0020 cp

From CRC Handbook of Chemistry and Physics, 60th edition (1979-1980)

For each sample, correlation spectra at four or five different delay times τ were measured so that the total delay times spanned approximately from 0.2 to 2 correlation times. At each delay time four experiments were performed and the experimental durations were chosen so that the total counts of detected photopulses were higher than 10^6. When the delay times per channel were set longer than 1 usec, the single clip mode of the correlator was used. When it was 1 usec or shorter, the fast mode which is equivalent to double clipped at zero level was preferred. Data were analyzed using a single exponential fit and the method of moments immediately after all measurements for each sample were completed. Curves of moments vs. τ_{max} were plotted by the Cal Comp plotter and the results of the first and second order cumulants were obtained within 10 minutes.

4.2 DATA ANALYSIS

A. DILUTE SOLUTIONS

Since the solutions were highly polydispersive, we employed the method of moments or cumulants to analyze our data. Correlation data obtained at a scattering angle $\theta = 90°$ from a 2.0 mg/ml gelatin solution in 0.15M NaCl and 0.05M Tris at 35°C are shown in Fig. 6 along with their best fits to different order of multiexponential functions.

The logarithms of the normalized data Ln $[\frac{C(\tau_i)-B}{B}]$ were first least square fitted to a linear function of τ for preliminary check and then to different order polynomials in powers of τ as in Eq.25. The background level B due to random correlations of photopulses was first independently calculated from the Eq.:

$$B = \frac{NNc}{(T/\Delta T)}$$

where N is the total counts of photopulses, N_c is the total clipped counts, T is the experimental duration and ΔT is the delay time per channel. Since the scattered field from gelatin solutions is a Gaussian field, the Siegert relation (Eq. 8) can be applied and the parameters K1, K2, K3,$\cdots$ in Eq. 25 were determined by minimizing the quantity:[66]

$$\sum_{i=2}^{M} [1/2 \, \mathrm{Ln} \, (\frac{C(\tau_i)-B}{B} - \sum_{m=0}^{M} \frac{Km}{m!} (-\tau_i)^m]^2 \, W(\tau_i) \qquad (41)$$

where the $C(\tau_i)$ are the raw data, the sum is over a set of channel times $\tau_i = i\Delta T$ with i ranging from 2 to M_2 where M_2 is the channel up to which the correlation data were analyzed and M corresponds to the order of polynomials to be least squares fitted. Note that for a single exponential fit, M equals 1. The proper weighting function was discussed by Koppel[65] and was shown to be

$$W(\tau) = \frac{\exp(4\tau/\tau_c)}{1+\exp(-2\tau/\tau_c)} \qquad (42)$$

where τ_c is the correlation time and is equivalent to the reciprocal of the decay rate of the correlation function. An estimated value for τ_c which was used in Eq.42 was obtained by analyzing the data with $W(\tau_i)=1$; then the data were reanalyzed with the correct weighting. The values of the parameters K1, K2 obtained from these fittings were then plotted as a function of τ_{max} which was the total delay time up to which the spectra were fitted to the polynomials and was equal to the bin time ΔT times M_2 defined in Eq. 41. Each moment was then extracted from the common intercept at $\tau_{max} = 0$ of the different polynomial fit trajectories which is the procedure proposed by Koppel. Fig. 7 and Fig. 8 show such plots for values of K1 and K2 respectively, using the correlation data obtained from a 2.0 mg/ml gelatin solution, a portion of which was shown in Fig. 6.

FIGURE 6

Normalized correlation data for a 2.0 mg/ml gelatin solution in 0.15 M NaCl and 0.05M tris.

(NOTE: 128 bin delay after bin 44)

$T = 35°C, \quad \theta = 90°$

Theoretical fits to $G^{(2)}(\tau) = B(1 + \frac{A}{B}|g^{(1)}(\tau)|^2)$

- τ = 1 usec/bin

  Dark line: single exponential fit, $\frac{A}{B} = 0.392$

  $|g^{(1)}(\tau)| = \exp(-1.955 \times 10^4\tau)$

  Light line: quadratic fit, $\frac{A}{B} = 0.404$

  $|g^{(1)}(\tau)| = \exp(-2.801 \times 10^4\tau + \frac{1}{2!}\ 1.372 \times 10^9\tau^2 - \frac{1}{3!}$

  $1.226 \times 10^{14}\tau^3 + \frac{1}{4!}\ 6.352 \times 10^{18}\tau^4)$

- ▲ τ = 2 usec/bin

  Dark line: single exponential fit, $\frac{A}{B} = 0.389$

  $|g^{(1)}(\tau)| = \exp(-1.713 \times 10^4\tau)$

  Light line: quadratic fit, $\frac{A}{B} = 0.404$

  $|g^{(1)}(\tau)| = \exp(02.048 \times 10^4\tau + \frac{1}{2!}\ 7.185 \times 10^7\tau^2 + \frac{1}{3!}$

  $1.227 \times 10^{12}\tau^3 - \frac{1}{4!}\ 3.453 \times 10^{16}\tau^4)$

- ■ τ = 5 usec/bin

  Dark line: single exponential fit, $\frac{A}{B} = 0.3477$

  $|g^{(1)}(\tau)| = \exp(-1.438 \times 10^4\tau)$

  Light line: quadratic fit, $\frac{A}{B} = 0.3477$

  $|g^{(1)}(\tau)| = \exp(-1.925 \times 10^4\tau + \frac{1}{2!}\ 4.828 \times 10^7\tau^2 + \frac{1}{3!}$

  $7.154 \times 10^{11}\tau^3 - \frac{1}{4!}\ 1.151 \times 10^{16}\tau^4)$

H = number of correlation time spanned by 44 bins

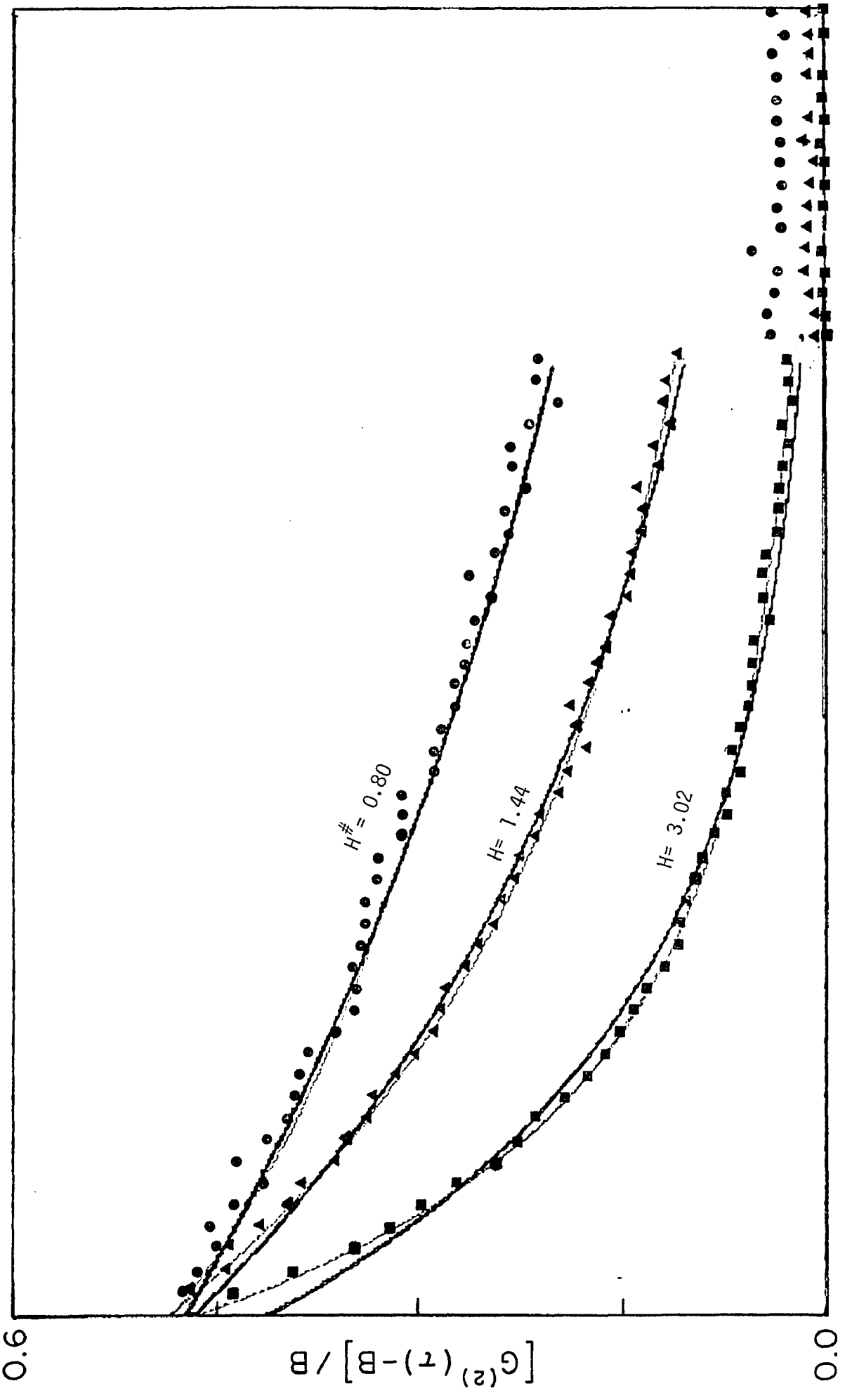
9.0
0.0
$[G^{(2)}(\tau)-B]/B$
$H^{\#}$= 0.80
H= 1.44
H= 3.02

Fig. 7. Estimates of the first order cumulant from linear, quadratic and cubic polynomial fits to gelatin correlation data. The extrapolation procedure of Koppel gives $\langle 2K1 \rangle = 2.12 \times 10^4$ or $\langle \Gamma \rangle = 1.06 \times 10^4$.

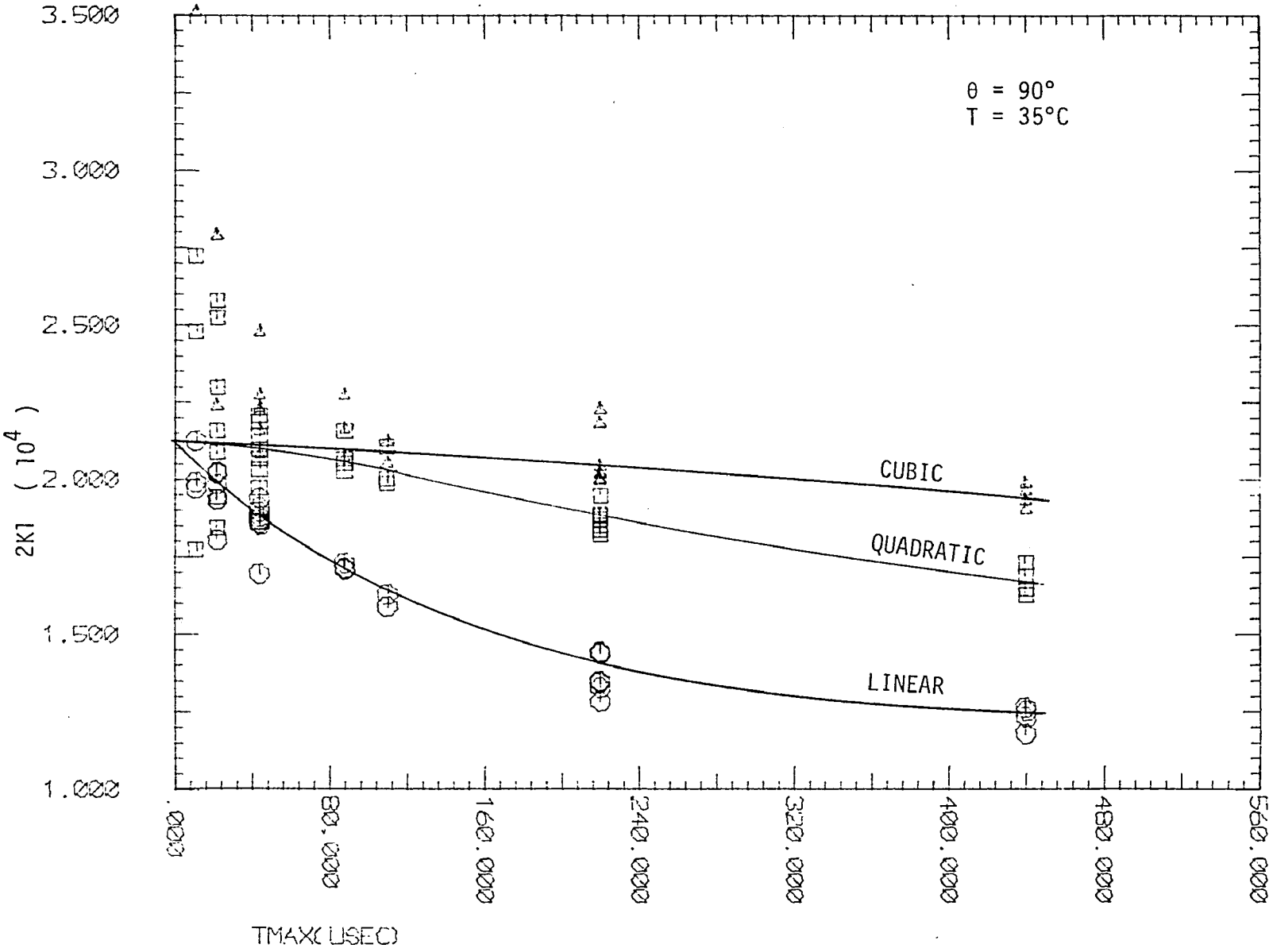
θ = 90°
T = 35°C
CUBIC
QUADRATIC
LINEAR
2K1 (10^4)
3.500
3.000
2.500
2.000
1.500
1.000
.000
80.000
160.000
240.000
320.000
400.000
480.000
560.000
TMAX(USEC)

Fig. 8. Estimates of the second order cumulant from quadratic and cubic polynomial fits to gelatin correlation data. Extrapolation procedure of Koppel gives $\langle 2K2 \rangle = 1.28 \times 10^8$ or $\mu_2 = 0.64 \times 10^8$.

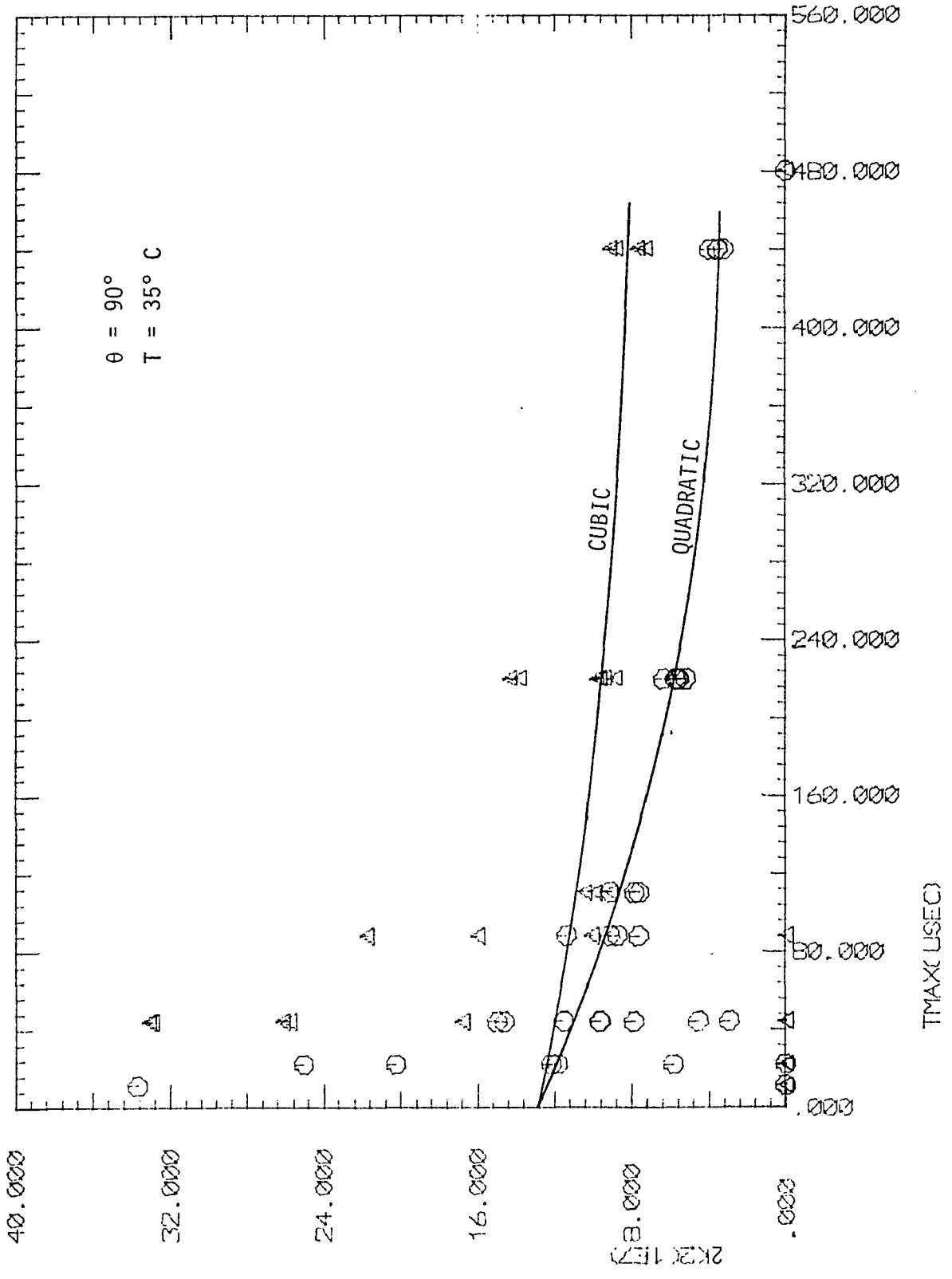
θ = 90°
T = 35° C
CUBIC
QUADRATIC
560.000
480.000
400.000
320.000
240.000
160.000
80.000
.000
TMAX(USEC)
40.000
32.000
24.000
16.000
8.000
.000
2K2(1E7)

The random and systematic errors make it difficult to extract moments higher than second order so that the result of a moment analysis normally only consists of the z-average decay rate $\langle\Gamma\rangle_z$ and the quantity $\mu_2/\langle\Gamma\rangle^2$ which is an useful index of the polydispersity of the solution.

B. SEMI-DILUTE SOLUTIONS

The correlation function of a solution of polymer network proposed by DeGennes is

$$G^{(2)}(\tau) = B + A \exp(-D_c q^2 \tau) \qquad (43)$$

where D_c is the cooperative diffusion coefficient of the chains of the network, B is the background level and A is a parameter which depends on the number of coherence areas viewed, the clipping level and the dead time effect. In Eq. 43 we have assumed that the scattered intensity of the static components I_s (including dust trapped in the network) is much larger than that from longitudinal fluctuations I_o. Thus the prescaling function of the correlator should be used to measure the correlation functions. However, itwas not clear whether the uncentrifuged gelatin solutions form a polymer network and the clipping function was used in the experiments. The correlation spectra were least squares fitted to Eq.

$$G^{(2)}(\tau) = B + A \exp(-2Dq^2\tau) \ldots\ldots \qquad (44)$$

The parameters B, A, and D were determined by the method discussed in the last section. We also analyzed the data using the method of cumulants discussed before.

4.3 EXPERIMENTAL RESULTS

A. DILUTE SOLUTIONS

Each point on the curves shown in Figs. 9 to 16 represents a

result extrapolated from an analysis of a complete set of data. The concentration dependence of the z-average diffusion coefficient D_z and the polydispersity $\mu_2/\langle\Gamma\rangle^2$ of gelatin solutions of 0.15M NaCl and 0.05M Tris at different temperatures are shown in Figs 9 and 10 respectively. These curves show that D_z has an upward trend at concentrations higher than the crossover concentration 1.8 mg/ml. However, the polydispersity remains approximately the same at 52%. The z-average free diffusion coefficients D_z^f of gelatin solutions of different solvents are listed in Table II. Similar results for solutions of 1M$CaCl_2$ and 0.05M Tris are shown in Fig. 11, Fig. 12 and Table II.

Fig. 13 shows the dependence of D_z on the ionic strength of the solvents. Note that D_z is inversely proportional to the ionic strength of NaCl. Since D_z depends on the viscosity of the solvent, we calculate the hydrodynamic radii from Einstein's relation and Stokes' law using the proper viscosity listed in Table I. The hydrodynamic radii and the polydispersity of gelatin solutions of different ionic strength are shown in Figs. 14 and 15 respectively. Note that in the solvent of sodium chloride the hydrodynamic radius at 35°C increases slightly as the ionic strength increases more than 30 times and only a very small increase is observed when the temperature is lowered to 20°C. The hydrodynamic radius in the solution of $CaCl_2$ solvent is smaller than it is in the solution of NaCl solvent of the same ionic strength. Fig. 16 shows the q^2 dependence of D_z^f. We have the z-average free diffusion coefficient directly proportional to q^2. In Table III we list the values of the first two cumulants ($\bar{\Gamma}$, μ_2) and D_z for a gelatin solution with 1.25 mg/ml concentration at 35°C measured at different angles.

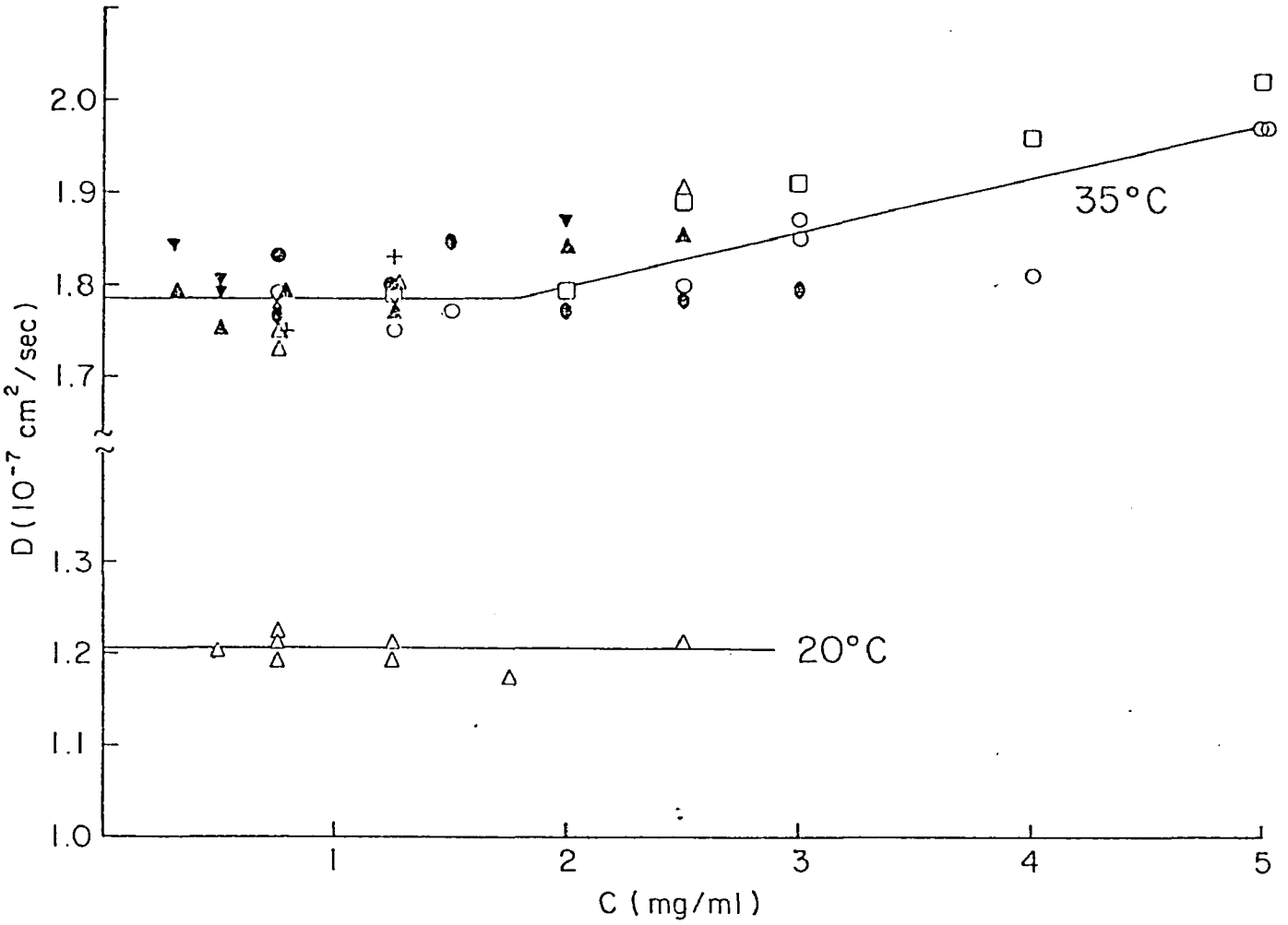

Fig. 9. The concentration and temperature dependence of the z-average diffusion coeficient (Note points with the same symbol represent results of the samples prepared at the same time).

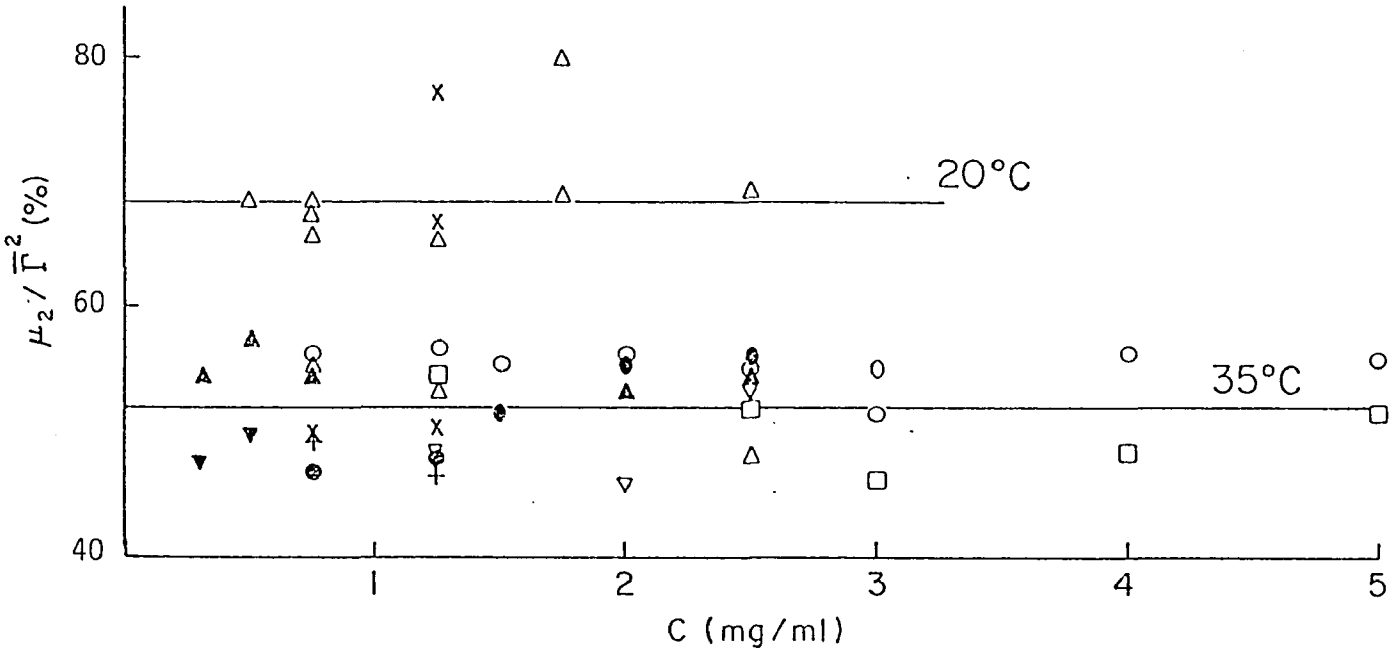

Fig. 10. The concentration dependence of the polydispersity of gelatin solutions in 0.15M NaCl and 0.05M tris. $\theta = 90°$

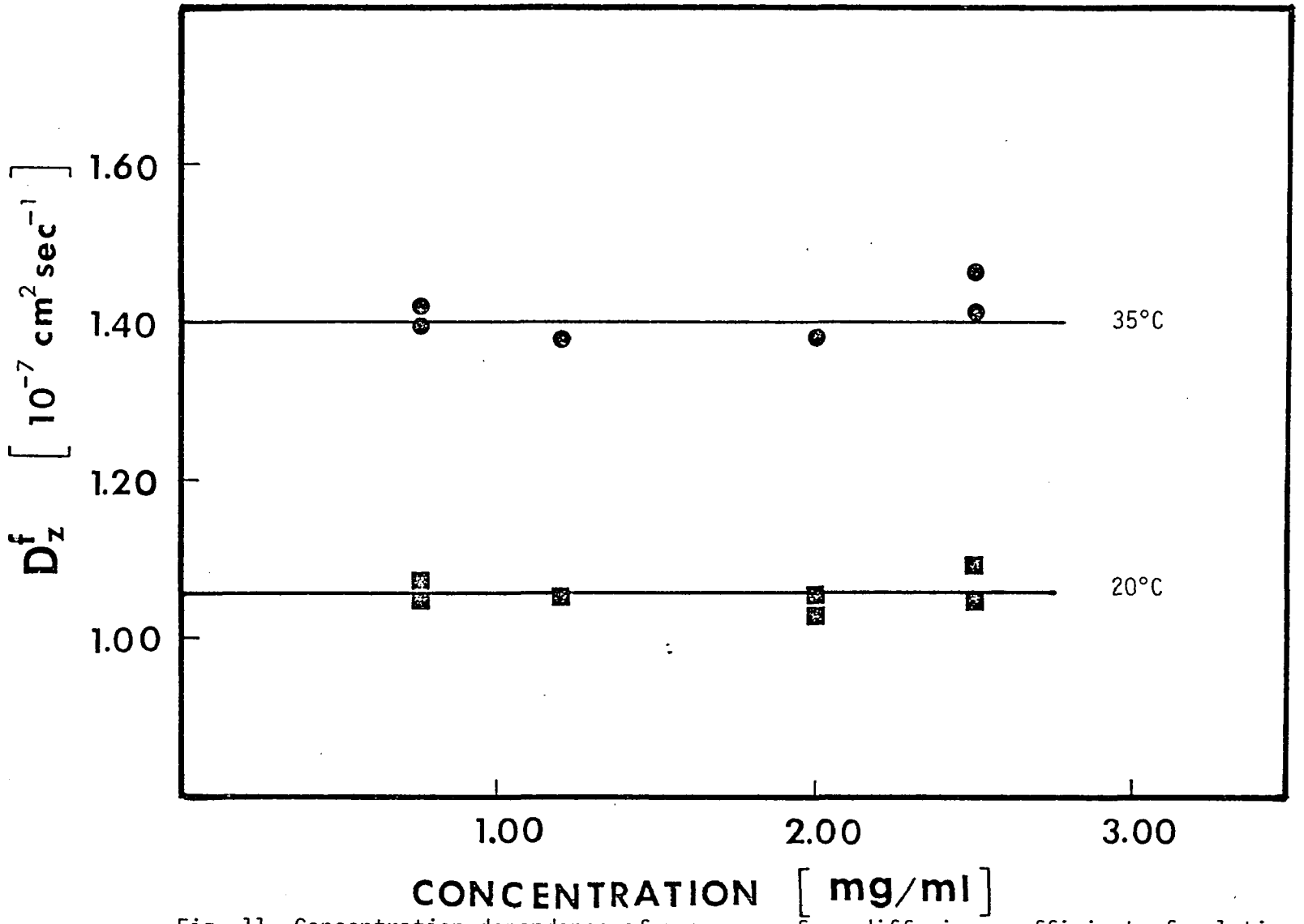

Fig. 11. Concentration dependence of z-average free diffusion coefficient of gelatin solutions in 1M $CaCl_2$ and 0.05M tris. ($\theta = 90°$)

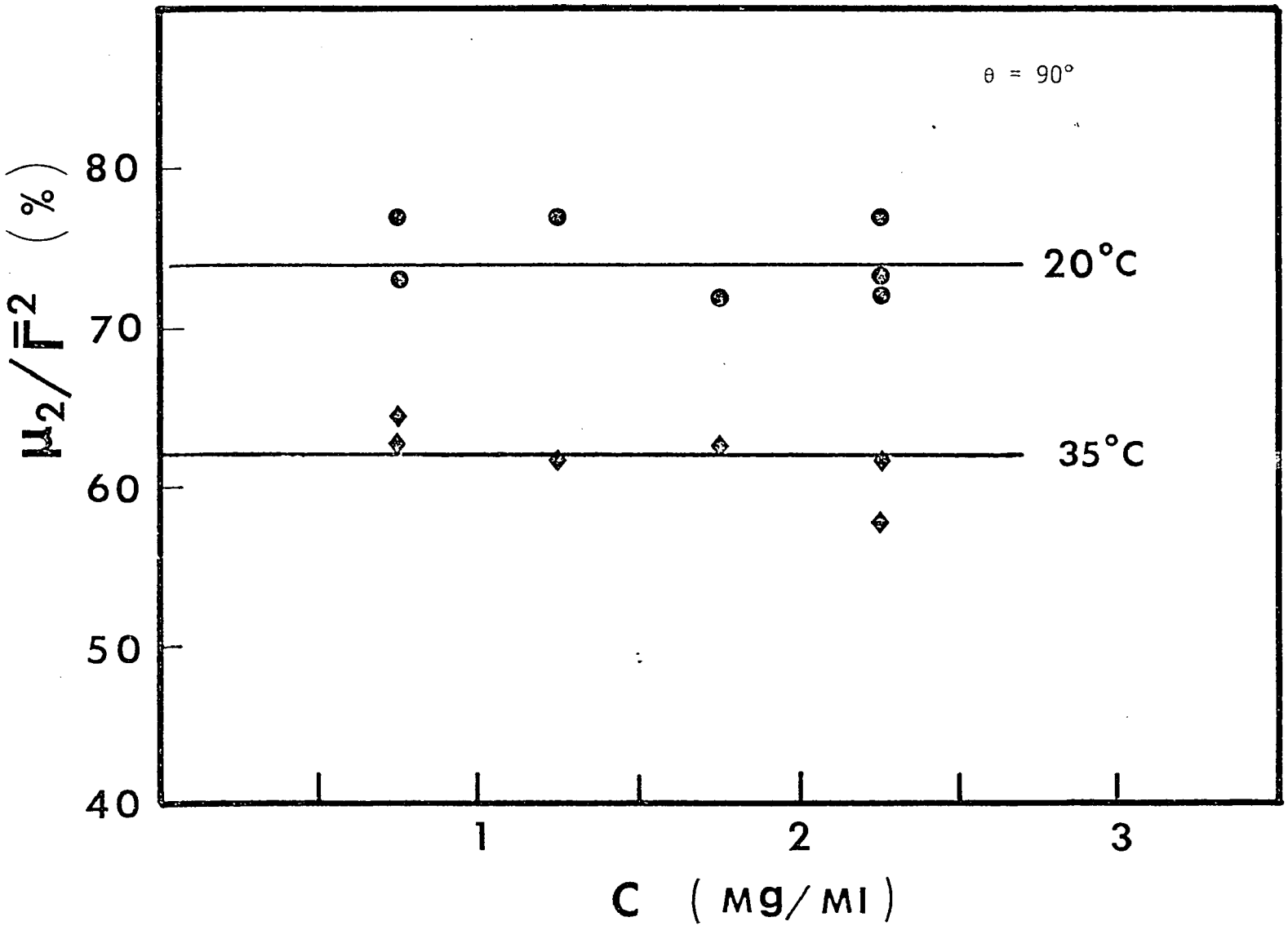

Fig. 12. The concentration dependence of the polydispersity of gelatin solutions in 1M $CaCl_2$ and 0.05M tris.

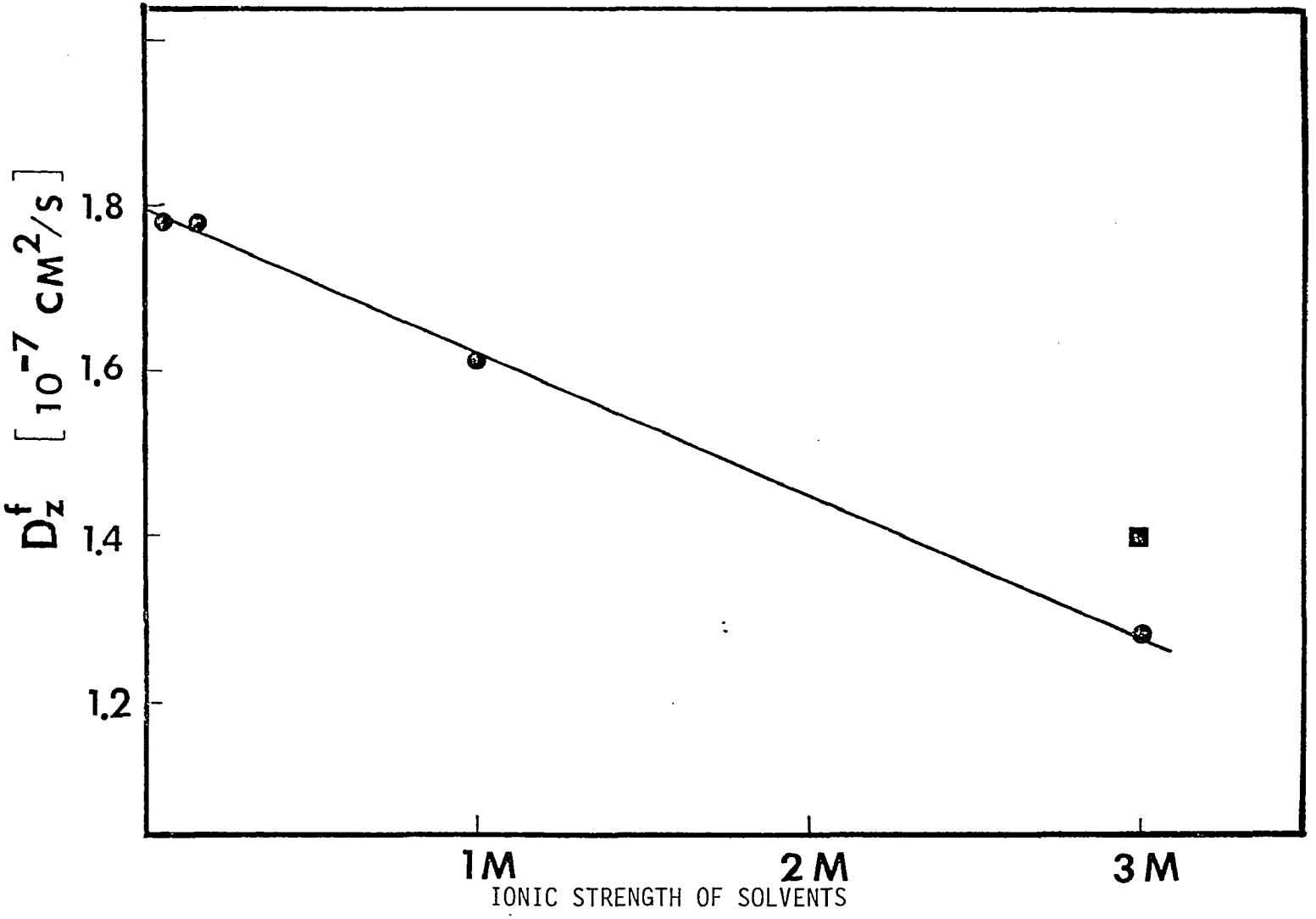

Fig. 13. The ionic strength dependence of the z-average free diffusion coefficient of gelatin solutions. T= 35°C, θ =90°.

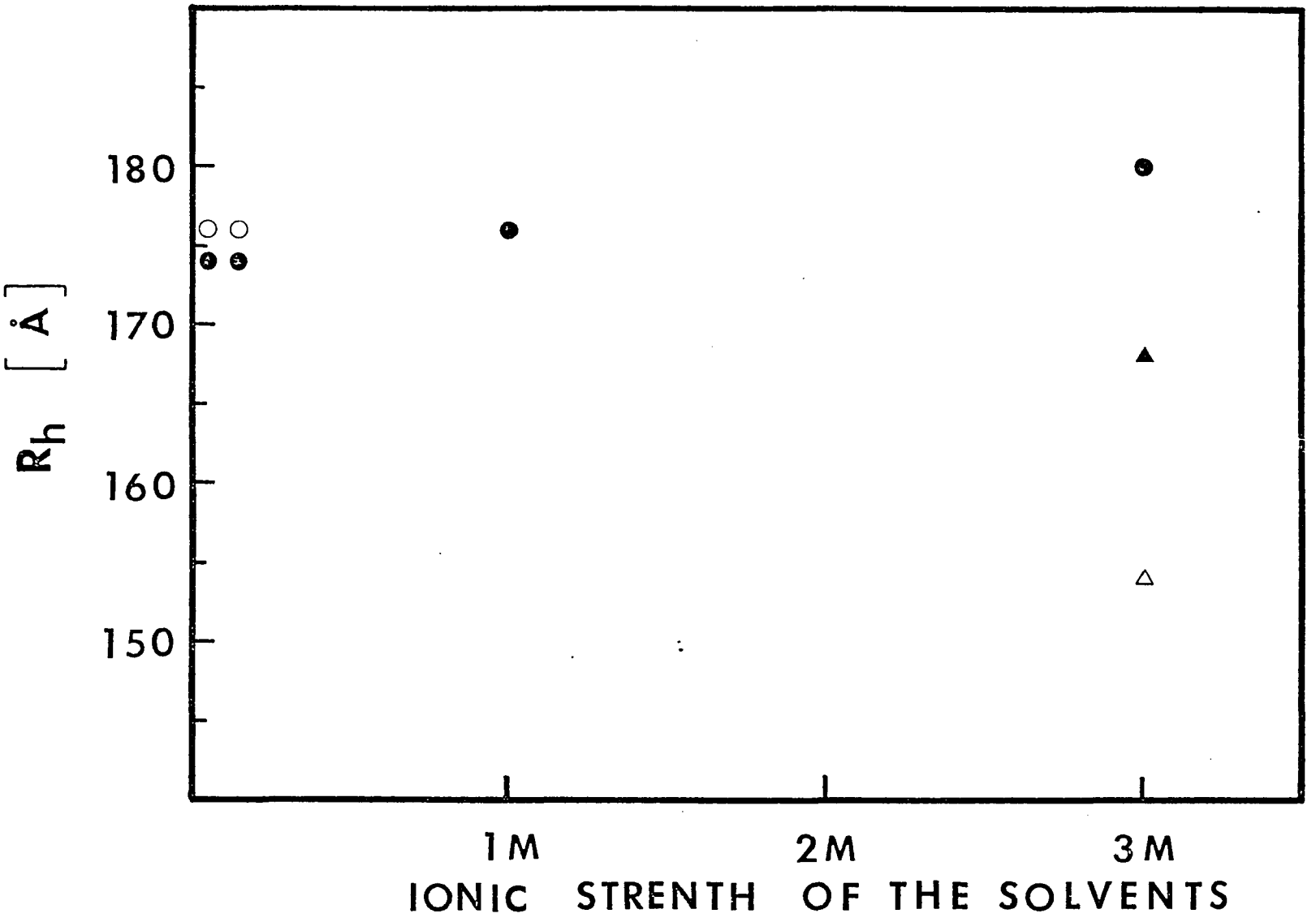

Fig. 14. The ionic strength dependence of the hydrodynamic radii of gelatin molecules.
T= 35°C, θ = 90°.

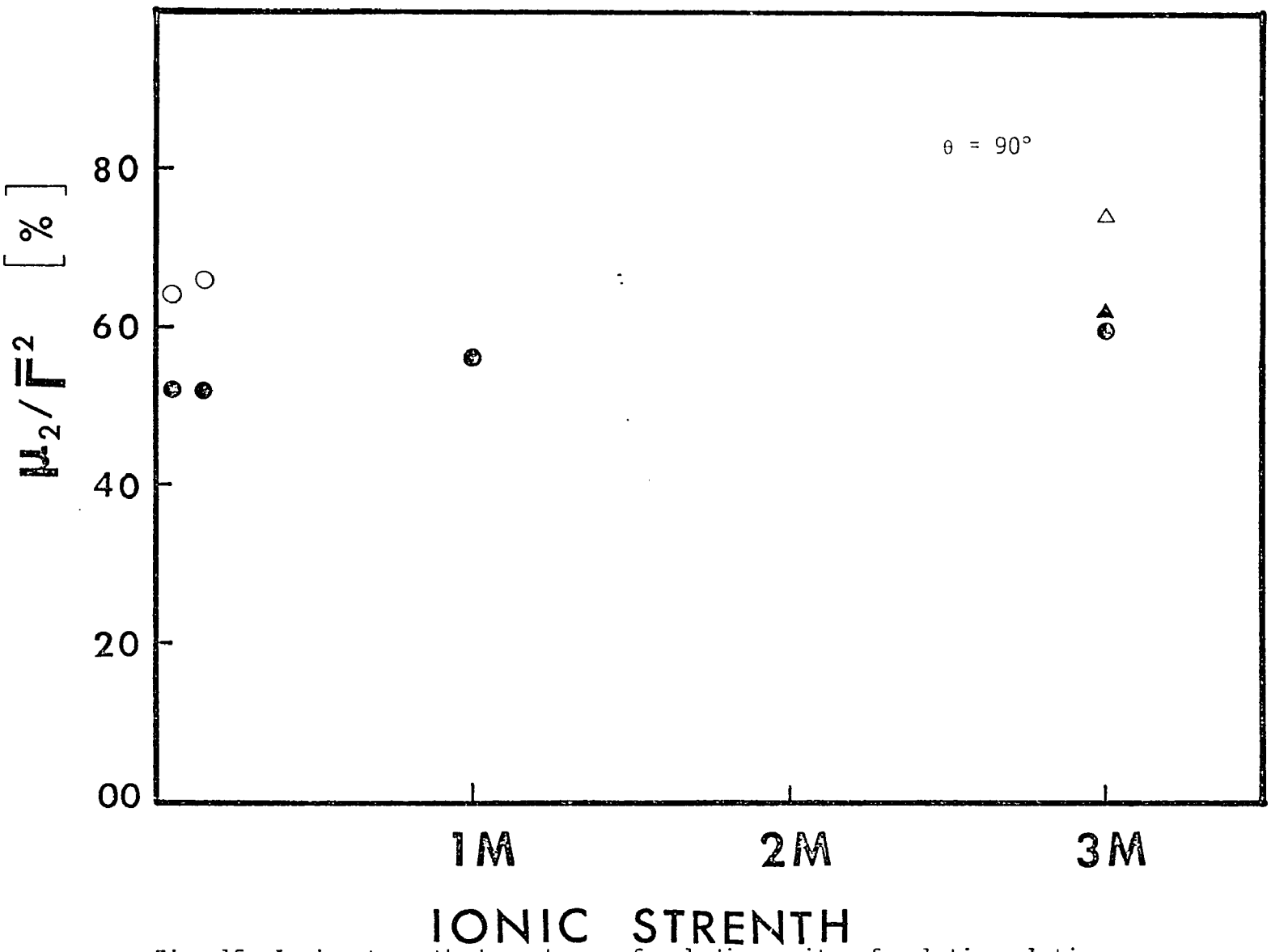

Fig. 15. Ionic strength dependence of polydispersity of gelatin solutions.

● : at 35° C in solvents of NaCl and .05M tris
○ : at 20° C in solvents of NaCl and .05M tris
▲ : at 35° C in solvents of $CaCl_2$ and .05M tris
△ : at 20° C in solvents of $CaCl_2$ and .05M tris

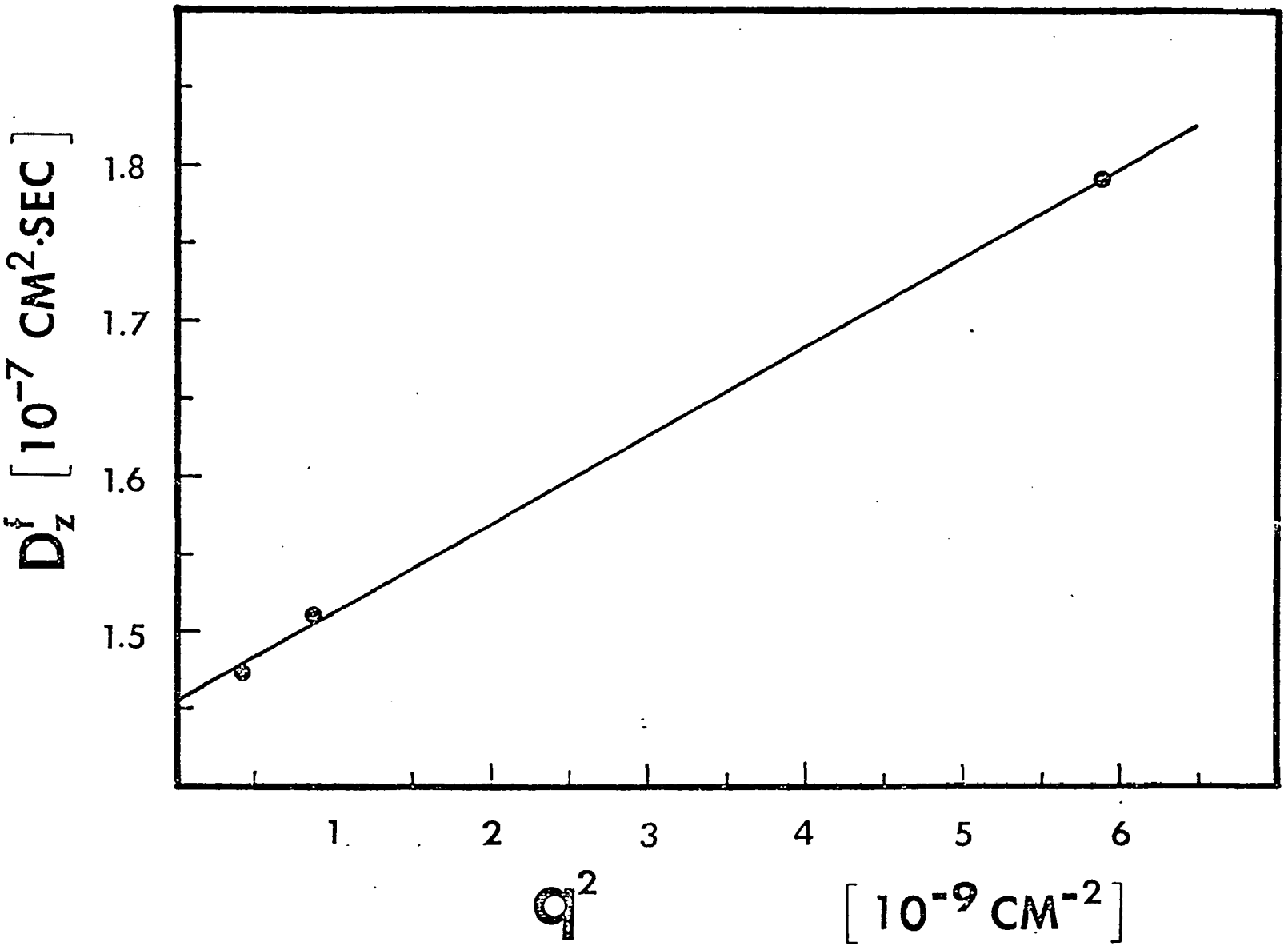

Fig. 16. q^2 dependence of z-average free diffusion coefficient of gelation solutions in 0.15M NaCl and 0.05M tris. T= 35°C

TABLE II

FREE DIFFUSION COEFFICIENTS AND HYDRODYNAMIC RADII

OF GELATIN MOLECULES

Solvents	35° C			20°C		
	$D_z^f(10^{-7}\frac{cm^2}{sec})$	$R_h(\mathring{A})$	$\mu_2/\langle\Gamma\rangle^2(\%)$	$D_z^f(10^{-7}\frac{cm^2}{sec})$	$R_h(\mathring{A})$	$\mu_2/\langle\Gamma\rangle^2(\%)$
0.05M NaCl, 0.05M Tris	1.78 ± 0.03	174	52±4	1.21 ± 0.03	176	68±4
0.15M NaCl, 0.05M Tris	1.77 ± 0.03	174	52±4	1.20 ± 0.03	176	68±4
1M NaCl, 0.05M Tris	1.61 ± 0.05	176	56±4			
3M NaCl, 0.05M Tris	1.28 ± 0.05	180	60±4			
1M $CaCl_2$, 0.05M Tris	1.40 ± 0.03	167	62±4	1.06 ± 0.03	163	74±4

TABLE III

RESULTS OF 1.25 MG/ML GELATIN SOLUTION WITH 0.15M NaCl
AND 0.05M TRIS SOLVENT

Scattering Angles	21.9°	31.8°	90°
q^2 (cm^{-2})	4.27×10^{9}	8.88×10^{9}	5.88×10^{10}
$\bar{\Gamma}$ (sec^{-1})	$0.063 \times 10^{+4}$	0.134×10^{4}	1.05×10^{4}
D_z^f (cm^2/sec)	1.48×10^{-7}	1.51×10^{-7}	1.79×10^{-7}
μ_2 (sec^{-2})	0.21×10^{6}	0.63×10^{6}	30.5×10^{6}

B. SEMI-DILUTE SOLUTIONS

For semi-dilute solutions, some of the correlation data are shown in Figs 17 to 21 along with their best single exponential fits. Note that the higher the concentration, the more the correlation spectra depart from their best single exponential fits. The diffusion coefficients calculated from the single exponential fits with total delay time $\cong 1.8\ \tau_c$ are plotted as function of concentrations in Fig. 22. The same results including results of higher concentrations are plotted in full logarithmic scales in Fig. 23. The diffusion coefficient at very low concentration is independent of concentration and then decreases rapidly with C, with linear behavior. However, when the concentration is high enough, it decreases slowly corresponding to a power law $D_{(c)} \propto C^{-1.67}$ which is contrary to De Gennes' prediction $D_c(c) \propto C^{0.75}$ but is similar to that for the self-diffusion coefficient of individual chain molecules of the polymer network with $D_s(c) \propto C^{-1.75}$.

Figs. 24 to 31 show the plotting of the first two order cumulants obtained from the cumulant analysis of the data from gelatin solutions. Note that for high concentration solutions, the cumulants from different order of polynomial fits do not converge to any common intercept.

4.4 DISCUSSION

A. DILUTE SOLUTIONS

At low concentrations, particles in solution undergo free diffusion. The diffusion coefficient is thus independent of concentration. However, at concentrations higher than the crossover concentration, the diffusion coefficient increases as the concentration

Fig. 17. Normalized correlation data for a 2.5 mg/ml uncentrifuged gelatin solution in 0.15M NaCl and 0.05M tris (Note 128 bin delay after bin 44).

T = 35° C , θ =90°

● : τ = 2 μsec/bin

▲ : τ = 5 μsec/bin

Solid lines : single exponential fits

H : The number of correlation times spanned by 44 bins

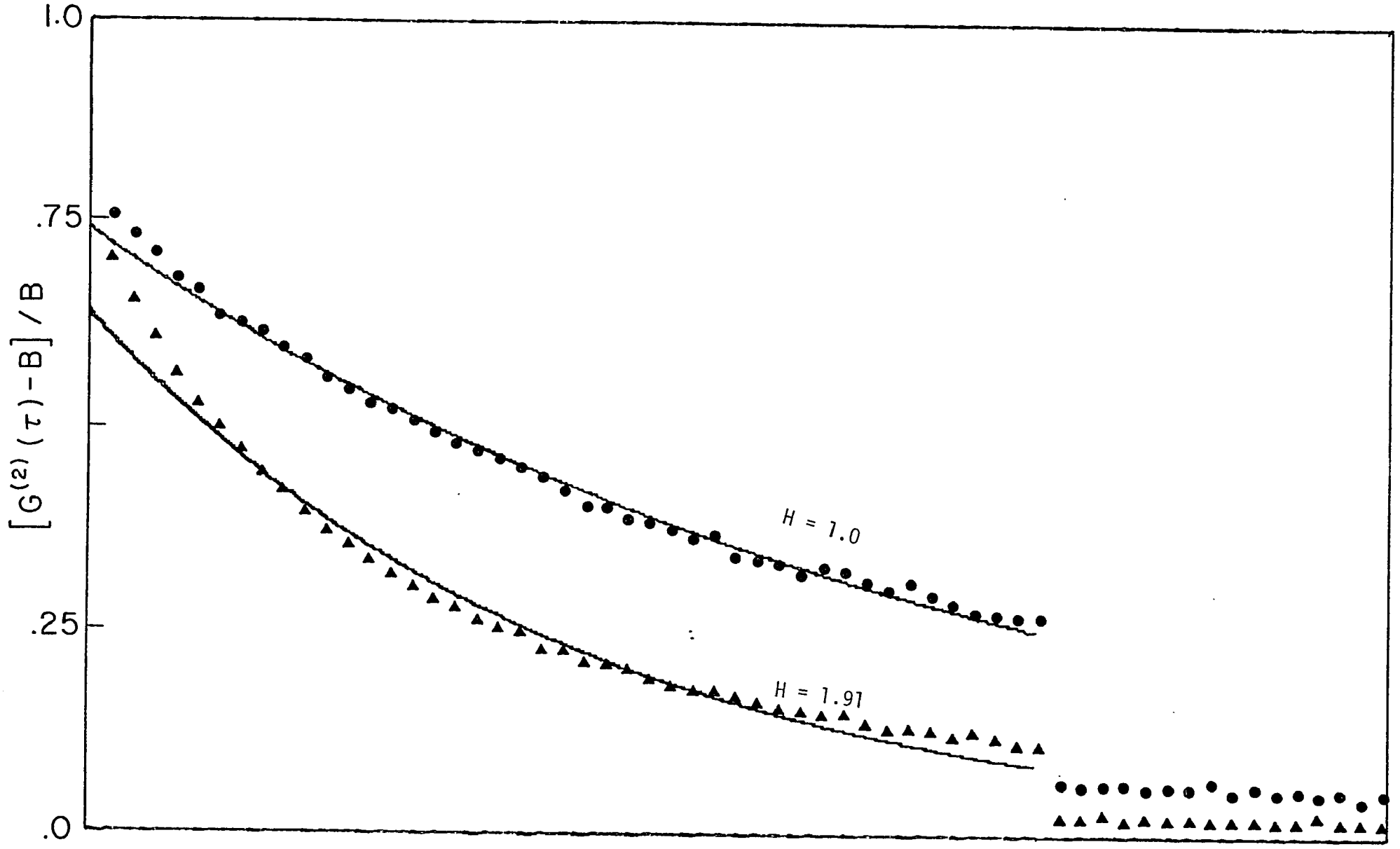
1.0
.75
.25
.0
$[G^{(2)}(\tau)-B]/B$
H = 1.0
H = 1.91

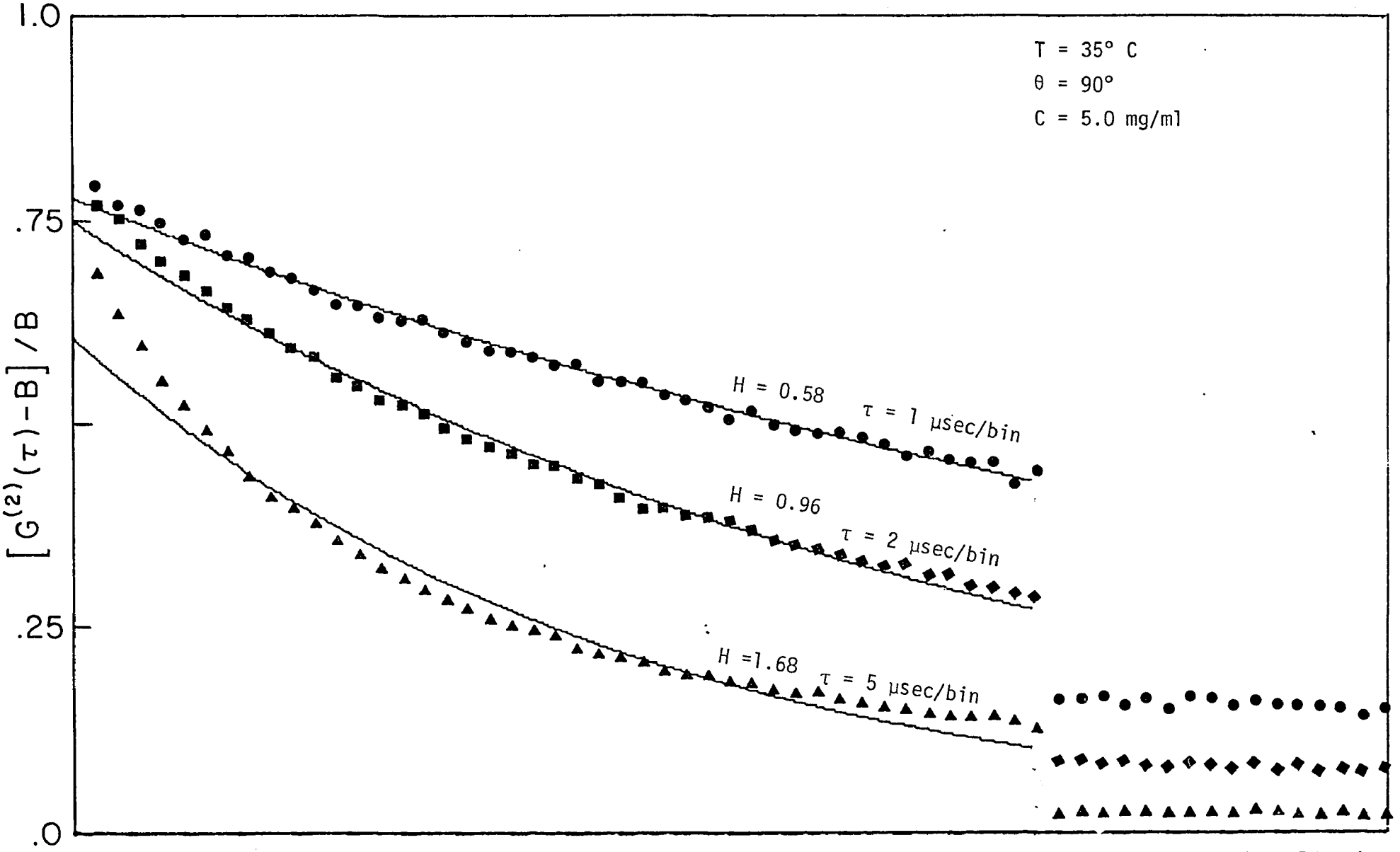

Fig. 18. Normalized correlation data for a 5.0 mg/ml uncentrifuged gelatin solution of 0.15M NaCl and 0.05M tris
Solid lines : single exponential fits, H : Number of correlation times spanned by 44 bins

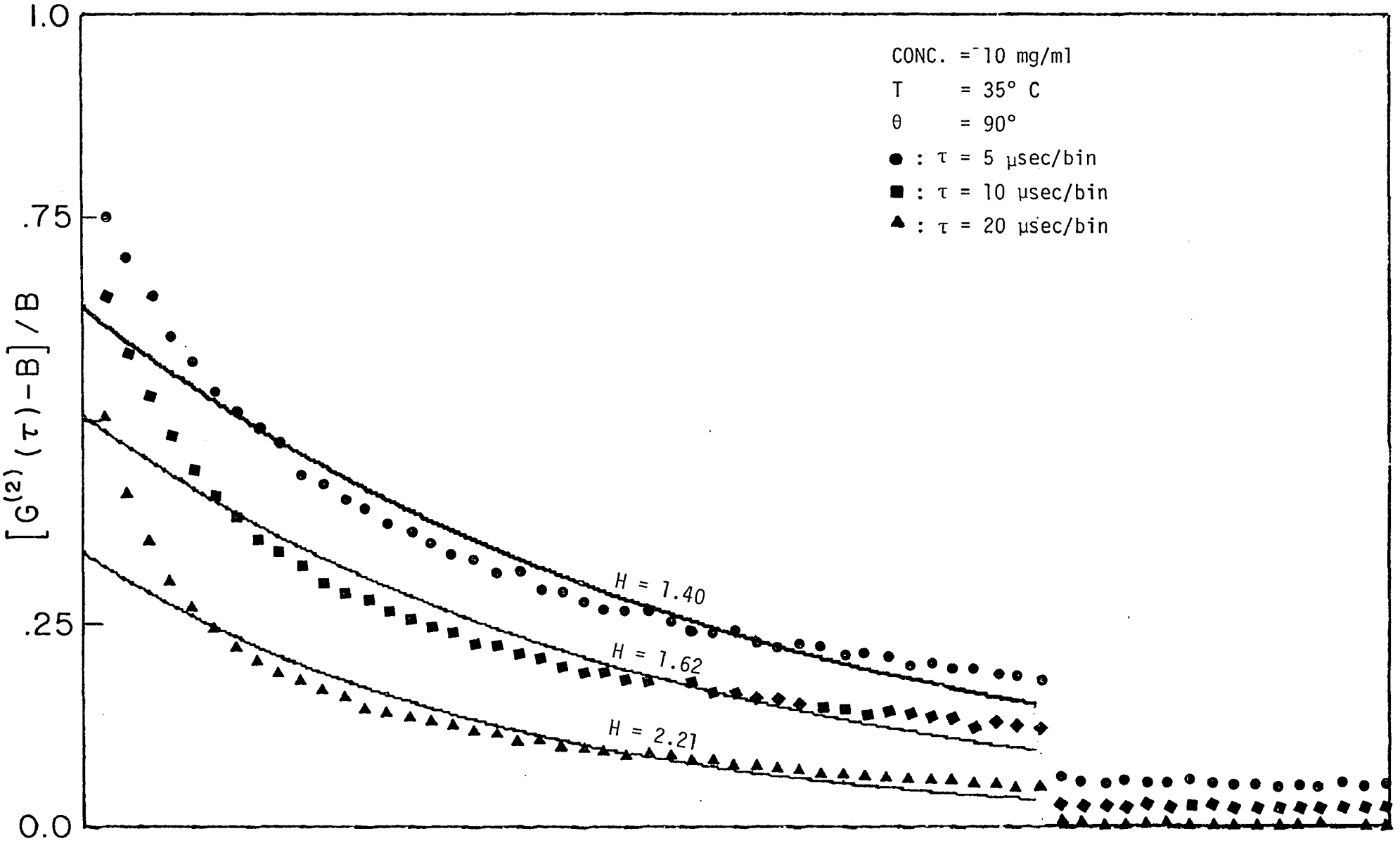

Fig. 19. Normalized correlation data for a 10 mg/ml uncentrifuged gelatin solution of 0.15M NaCl and 0.05M tris. Solid lines : single exponential fits, H : Number of correlation times spanned by 44 bins

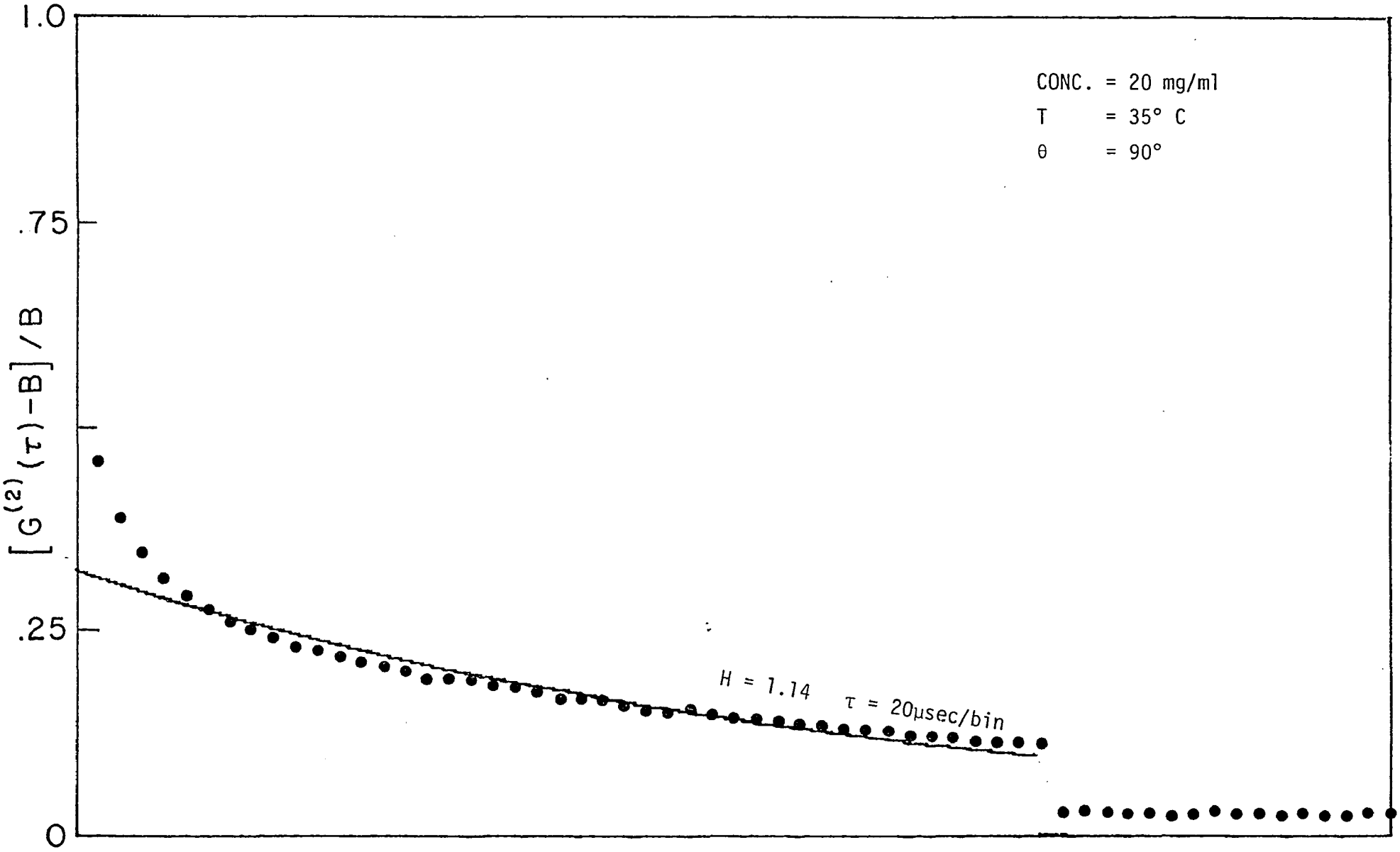

Fig.20. Normalized correlation data for a 20 mg/ml uncentrifuged gelatin solution of .15M NaCl & .05M tris.

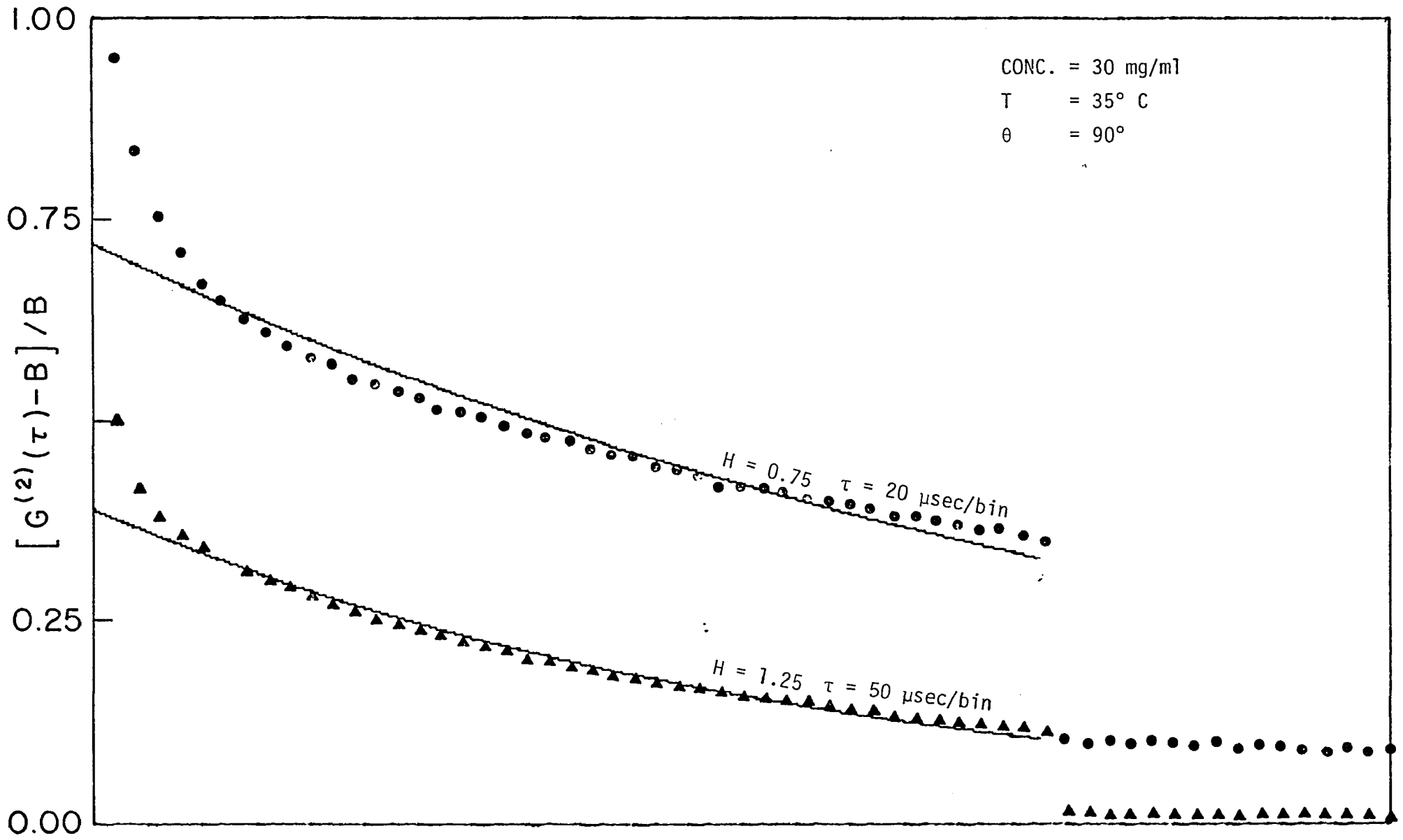

Fig.21 Normalized correlation data for a 30 mg/ml uncentrifuged gelatin solution of .15M NaCl & .05M tris.

Fig. 22. The concentration dependence of the diffusion coefficients of the gelatin solutions in 0.15M NaCl and 0.05M tris without being centrifuged. The diffusion coefficients were obtained by fitting the correlation data to single exponential functions. The error bars represent standard deviations of seven sets of experiments.
T= 35°C, θ= 90°

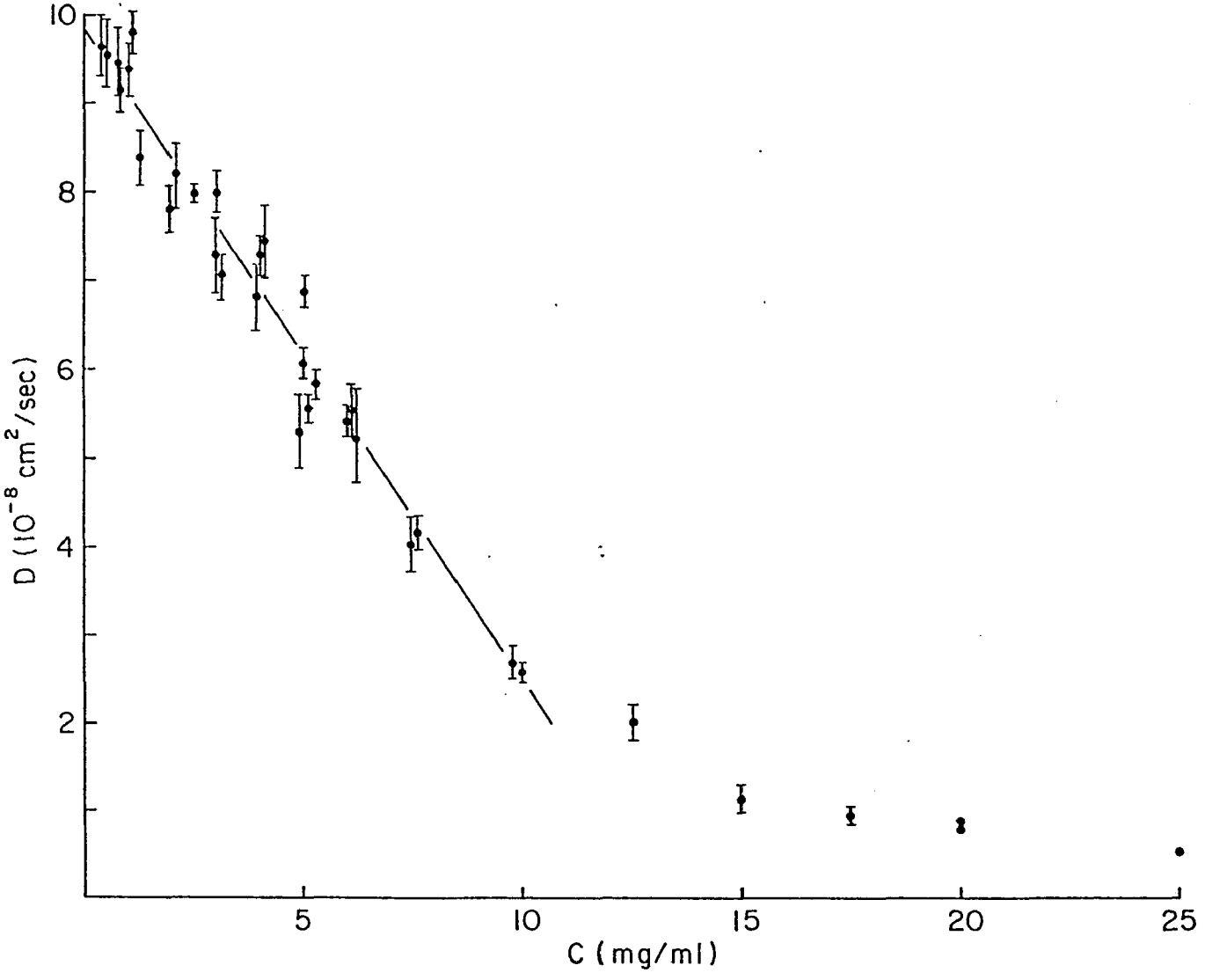
10
8
6
4
2
D (10^{-8} cm^2/sec)
5
10
15
20
25
C (mg/ml)

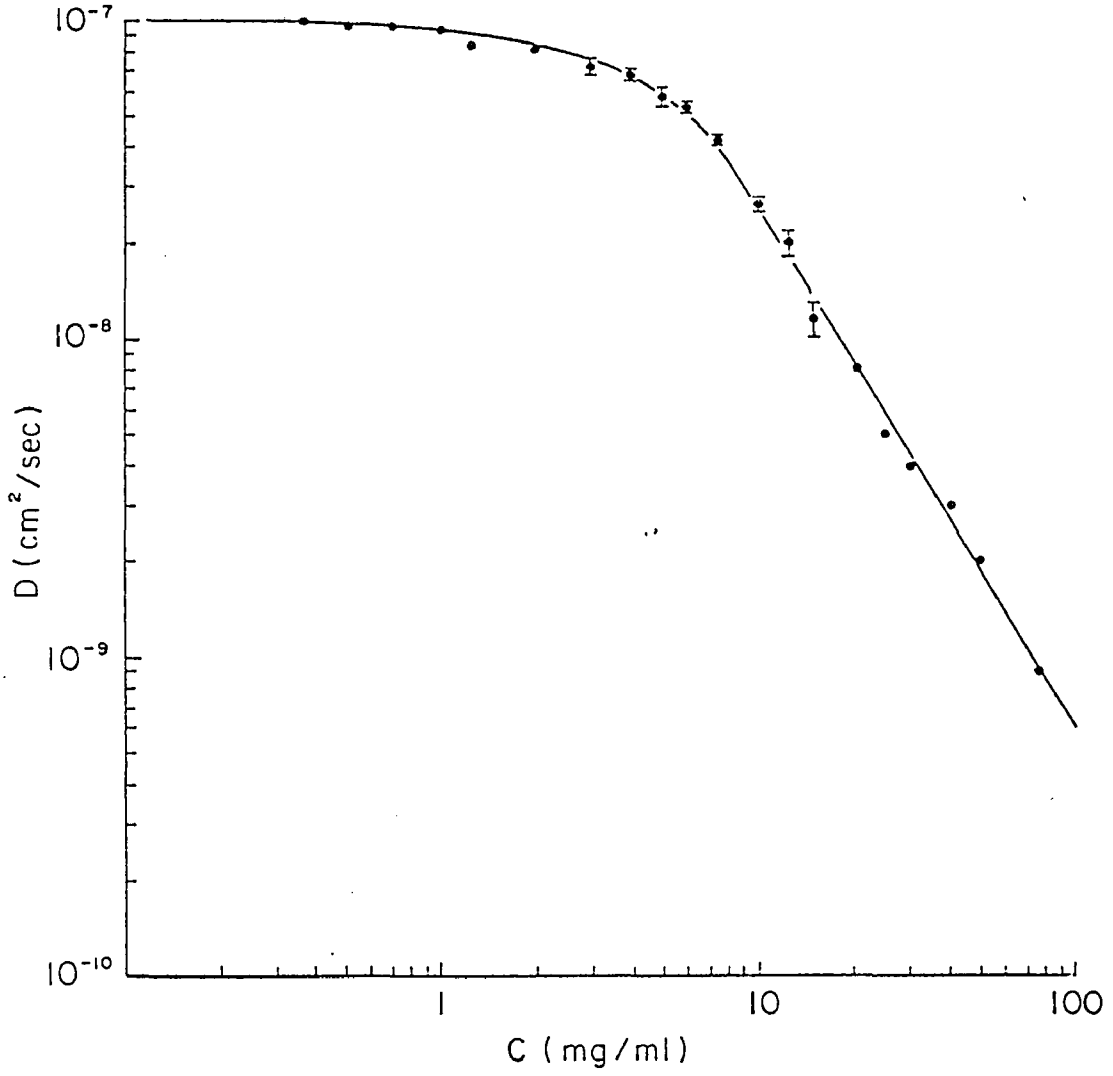

Fig. 23. Concentration dependence of diffusion coefficient of gelatin solutions in 0.15M NaCl and 0.05M tris without being centrifuged. T= 35°C, θ= 90°.
(Part of the data have been shown in Fig. 22.)

Fig. 24. First order cumulants from linear, quadratic and cubic fits to the correlation data of a 2.5 mg/ml uncentrifuged gelatin solution of 0.15M NaCl and 0.05M tris. $T = 35°$ C, $\theta = 90°$

⬡: Linear, ⊡: Quadratic, ⚠: Cubic

CONC. = 2.5 mg/ml
T = 35° C
θ = 90°
2.500
2.000
1.500
1.000
.500
.000
0.000
80.000
160.000
240.000
320.000
400.000
480.000
560.000
TMAX(USED

Fig. 25. Second order cumulants from quadratic and cubic fits to the correlation data of a 2.5 mg/ml uncentrifuged gelatin solution of 0.15M NaCl and 0.05M tris.

⬯ : Quadratic fit, △ : Cubic fit

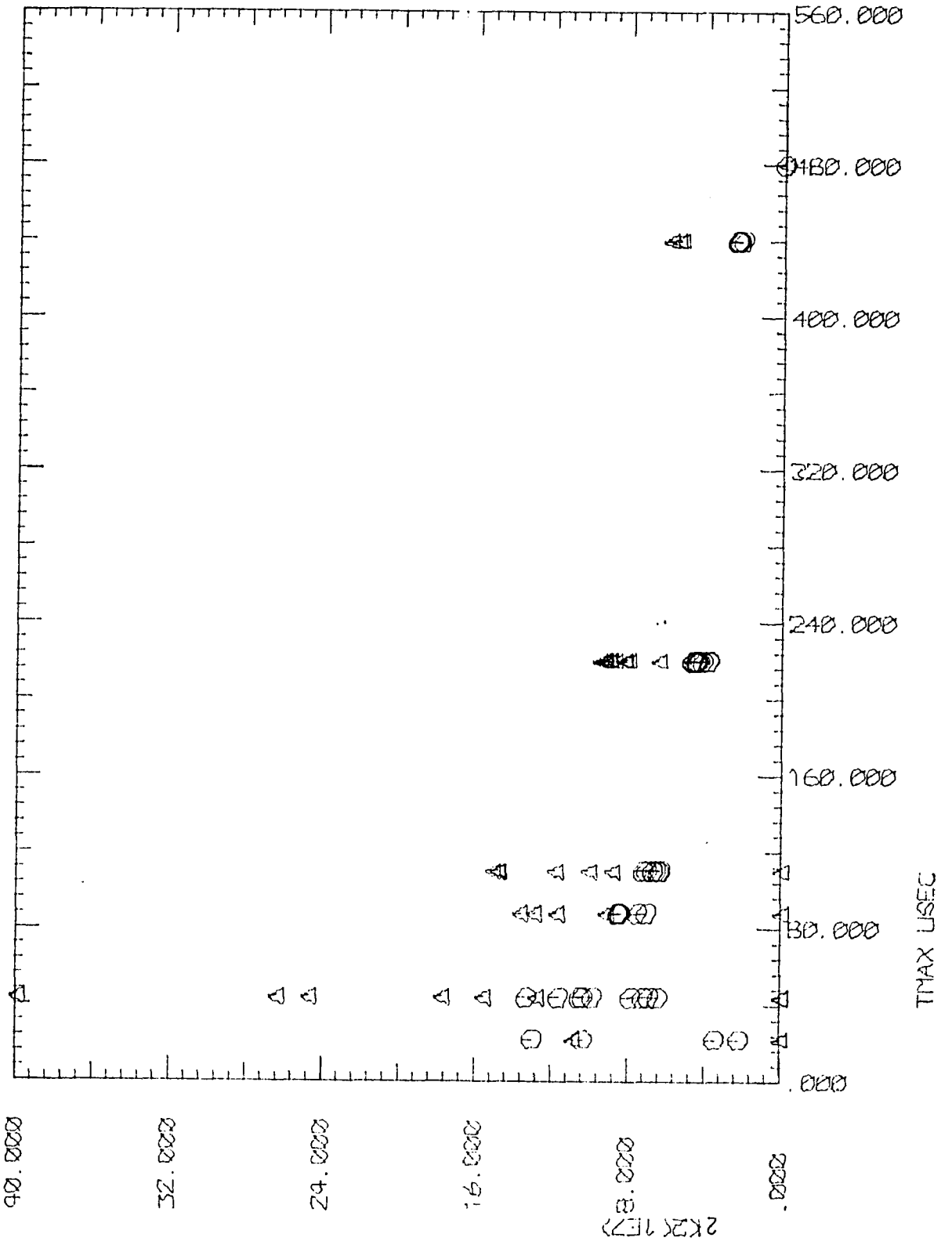
560.000
480.000
400.000
320.000
240.000
160.000
80.000
.000
TMAX USEC
40.000
32.000
24.000
16.000
8.000
.000
2K2K 1E7>

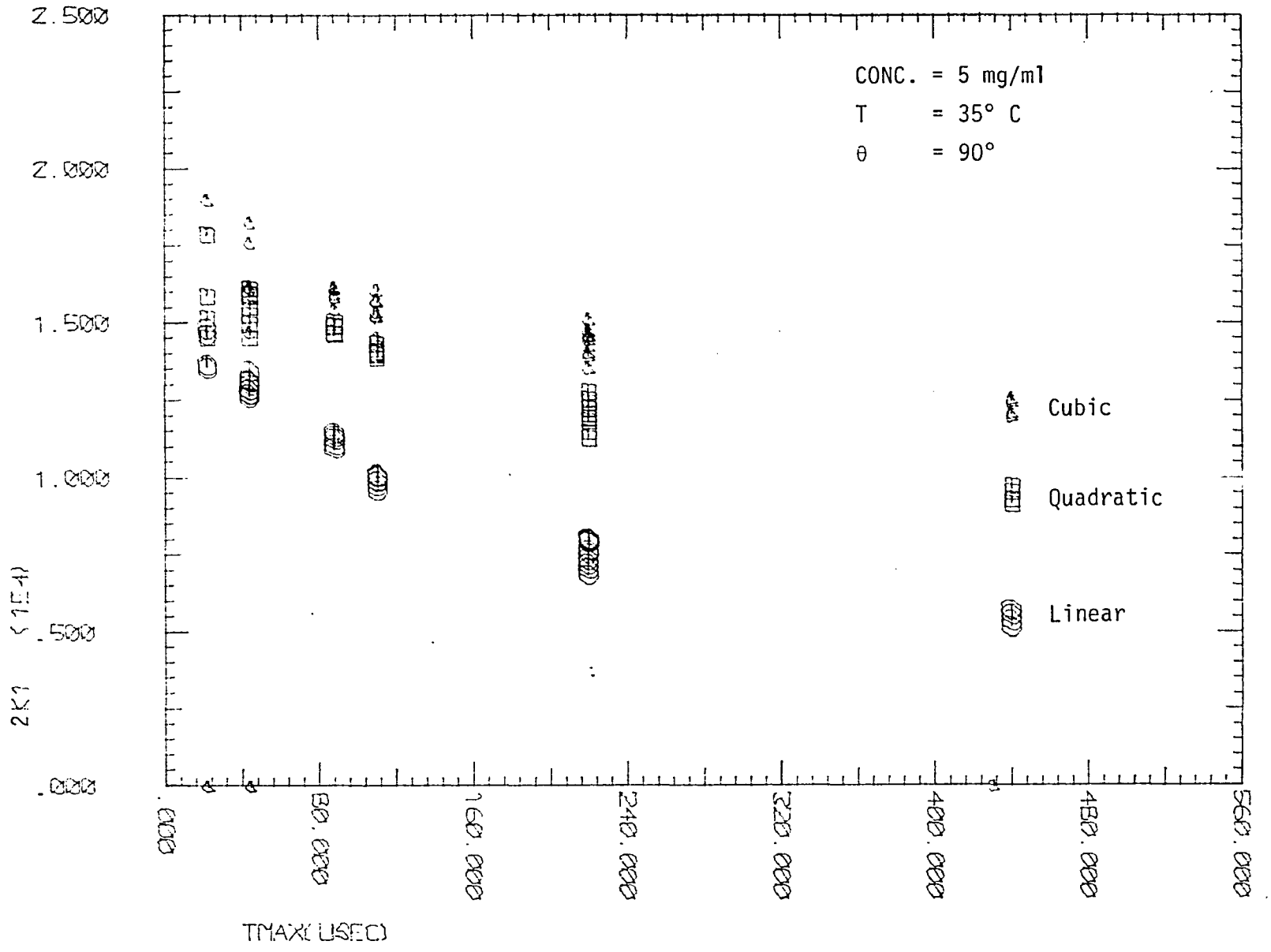

Fig. 26. First order cumulants from the correlation data of a 5 mg/ml uncentrifuged gelatin solution of .15M NaCl & .05M tris.

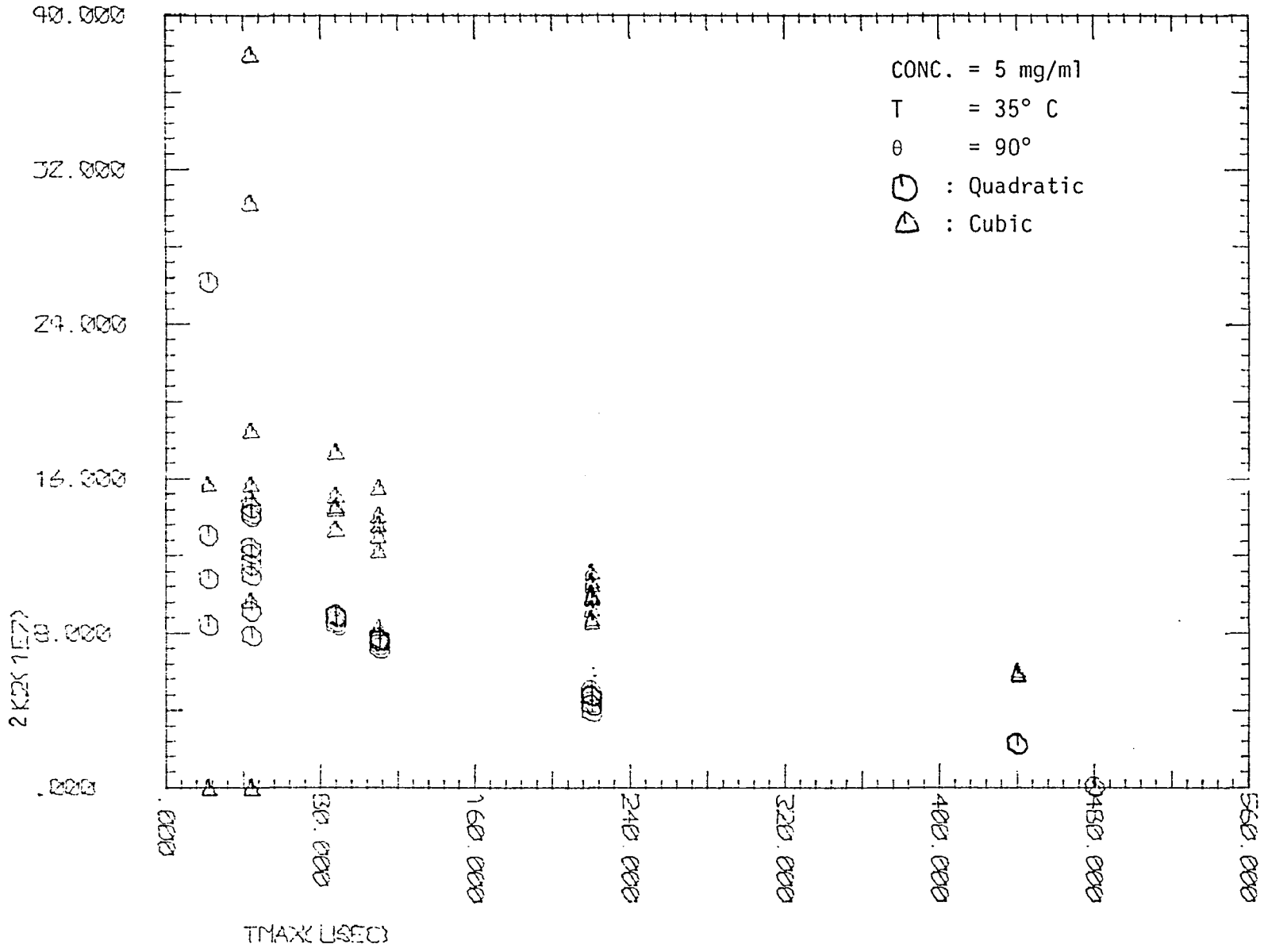

Fig. 27. Second order cumulants from the correlation data of a 5 mg/ml uncentrifuged gelatin solution of .15M NaCl & .05M tris.

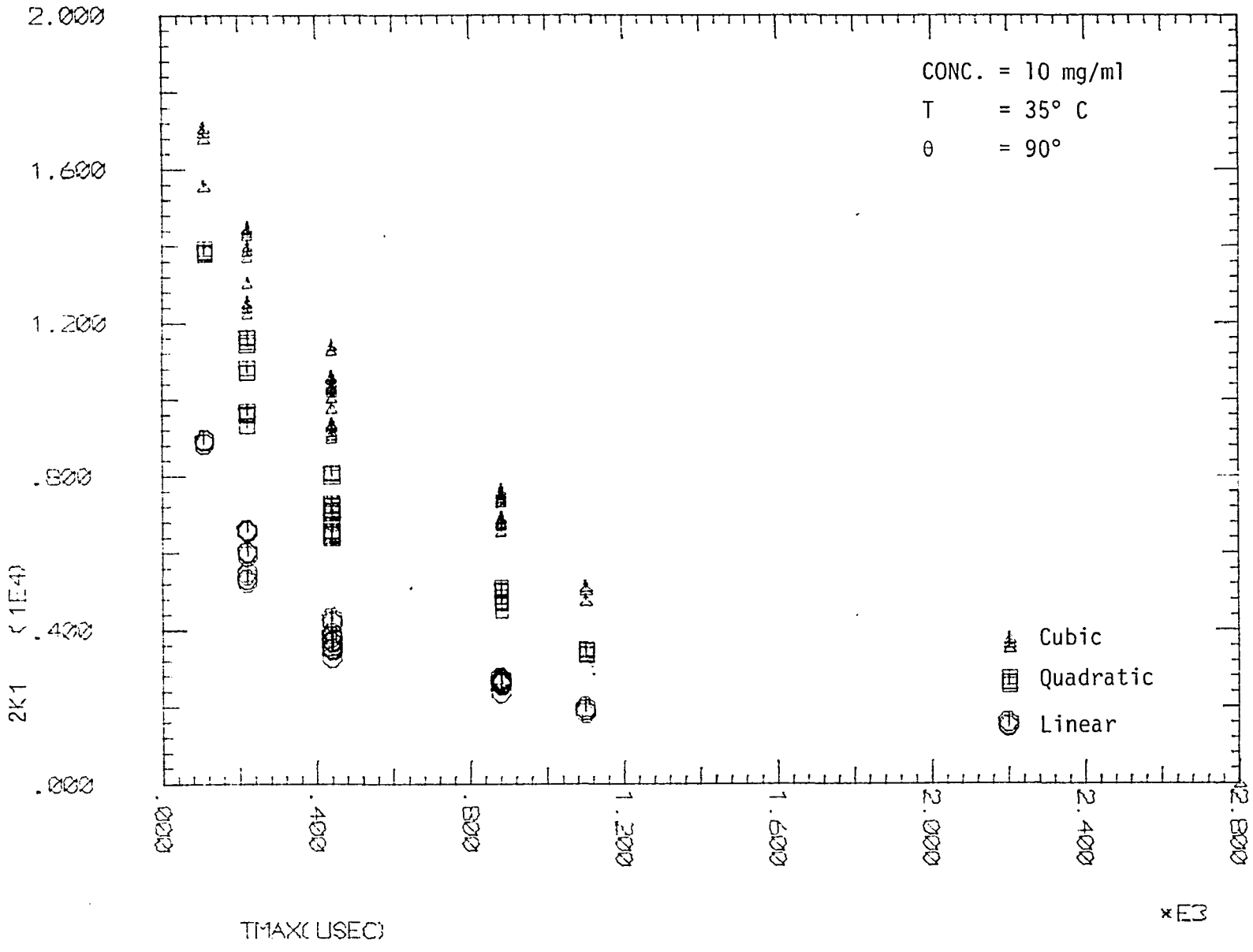

Fig. 28. First order cumulants from different order polynomial fits to the correlation data of a 10 mg/ml uncentrifuged gelatin solution of .15M NaCl & .05M tris.

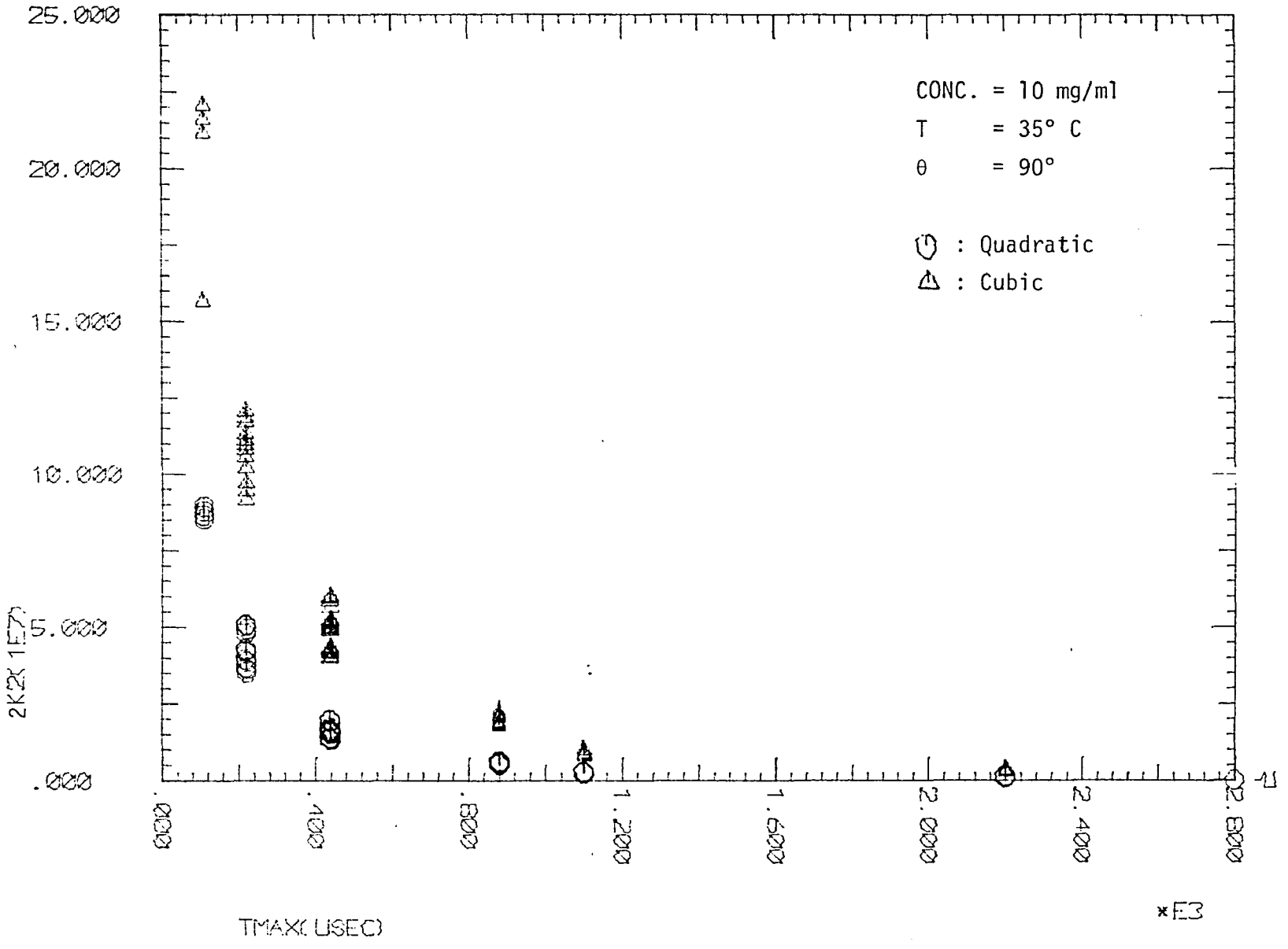

Fig. 29. second order cumulants from different order polynomial fits to the correlation data of a 10 mg/ml uncentrifuged gelatin solution of .15M NaCl & .05M tris.

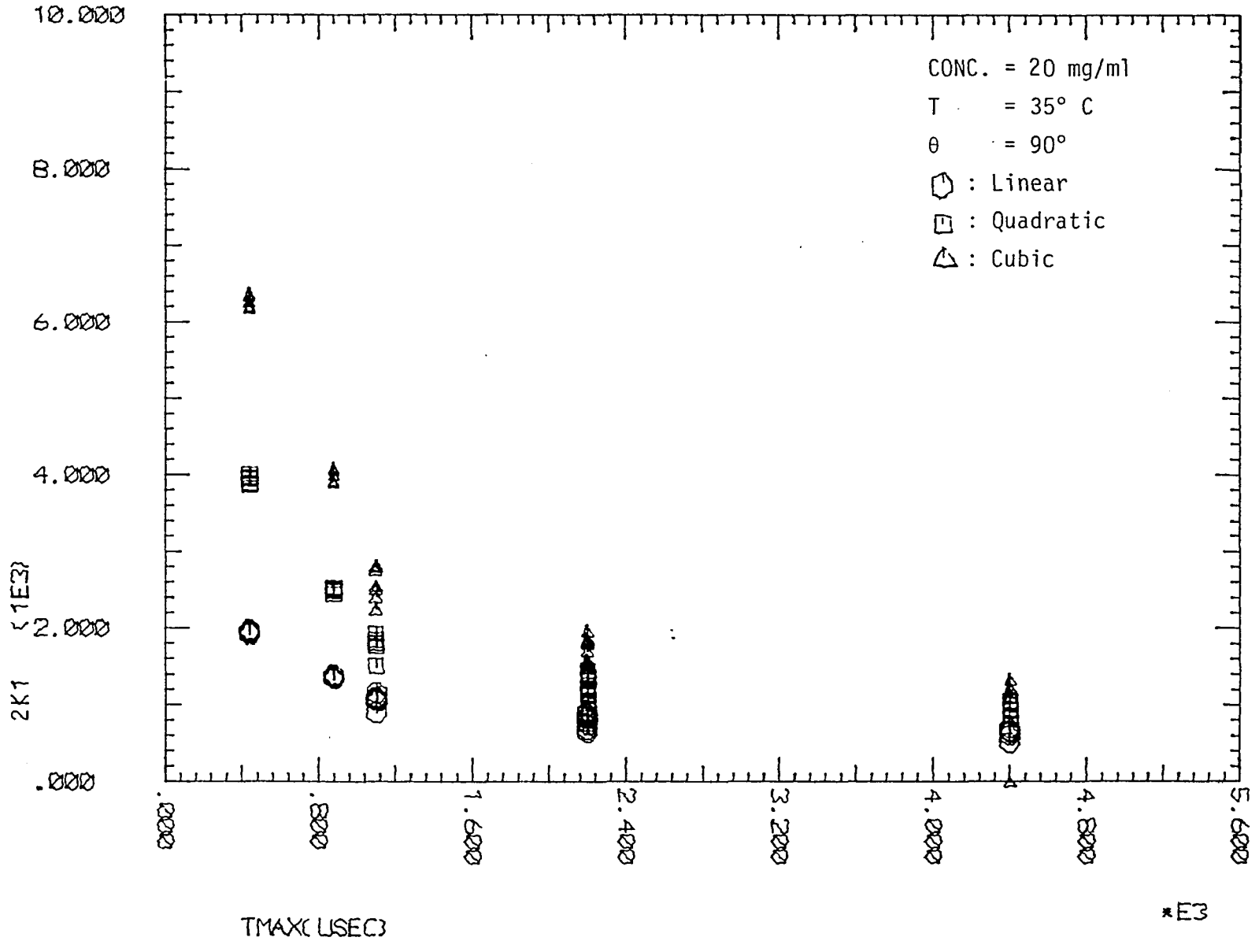

Fig. 30. First order cumulants from different order polynomial fits to the correlation data of a 20 mg/ml uncentrifuged gelatin solution of 0.15M NaCl and 0.05M tris.

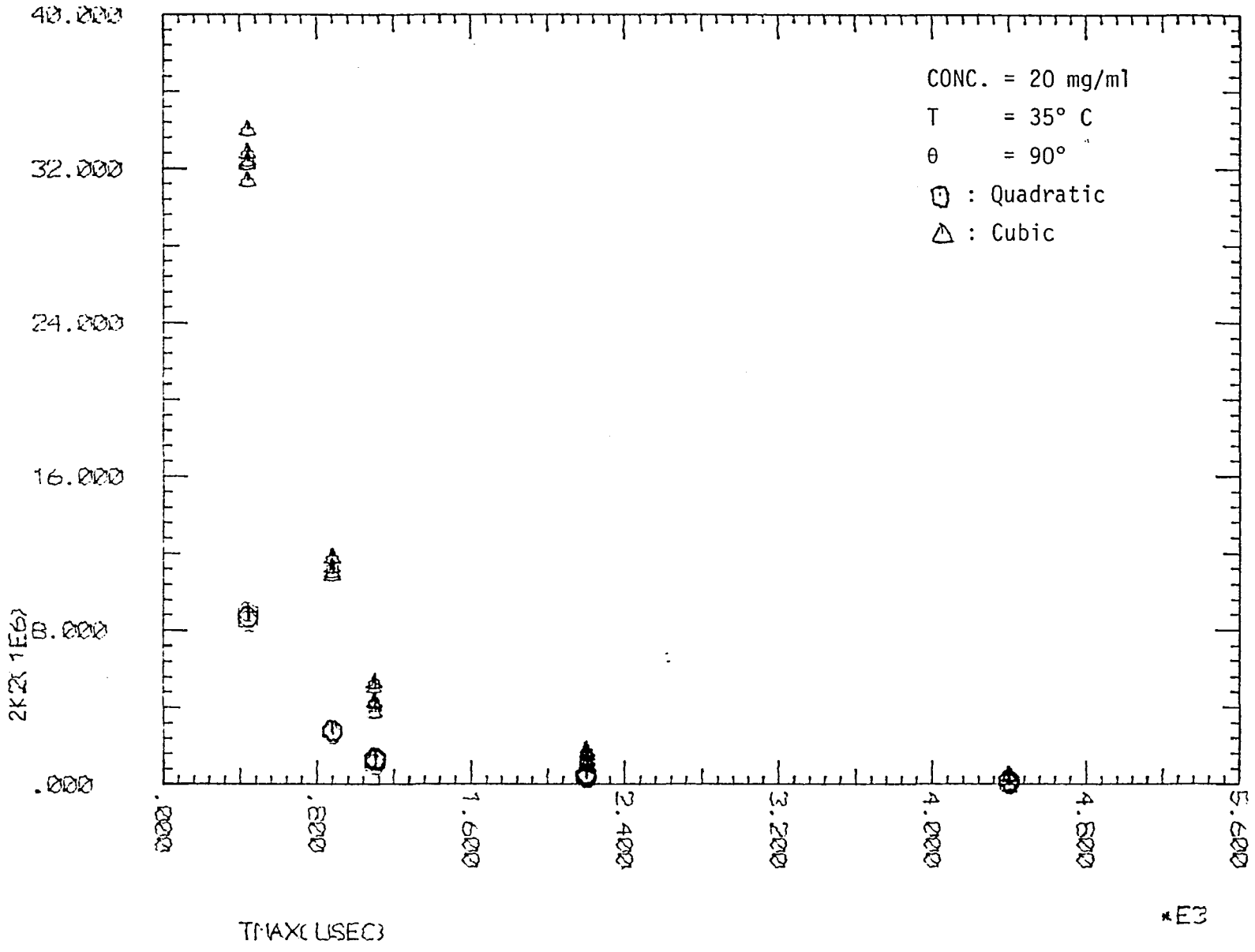

Fig. 31. Second order cumulants from different order polynomial fits to the correlation data of a 20 mg/ml uncentrifuged gelatin solution of 0.15M NaCl and 0.05M tris.

increases. This behavior is due to the increasing effects of interparticle interactions when the interparticle spacing becomes comparable to the particle size and particles in solution form a polymer network. The crossover concentration obtained is higher than its true value since the need to centrifuge samples to eliminate dust has also removed some big particles from the solutions and leads to an overestimate of the concentrations.

The polydispersity calculated from Eq. 26, using values of $\bar{M}_W$ and $\bar{M}_N$ measured at Kodak Laboratories is much lower than our experimental result. The discrepancy between these two values is due to the effect of centrifuging the sample in the correlation measurements and that Eq. 26 is valid only in the low limit of polydispersity.

The hydrodynamic radius of the gelatin molecules only increases a few angstrons when its temperature is lowered from 35°C to 20°C indicating that most of the aggregates are covalently linked and the hydrogen bonded or collagen-folded aggregates do not make a significant contribution even at low temperature (20°C). The increase in hydrodynamic radius when the ionic strength of the solution increases indicates that gelatin molecules do carry charges. At low ionic strength the chance for charged particles to collide and form hydrogen bonded aggregates is reduced by the repulsive Coulombic forces between the charges on the macromolecules. However, as the ionic strength is increased, the Coulombic interactions are screened out more and more completely by the charges on the ions and the macromolecules are more free to aggregate.

Boedtker and Doty failed to find any significant change in aggregates when the ionic strength was increased from 0.15M to 1M and concluded that electrostatic forces do not play an important role in the aggregation process. Our results instead indicate a large amount of charges carried by the molecules so that the ions in 1M NaCl solvent are not enough to screen out a significant fraction of the repulsive Coulombic forces and their instruments were unable to distinguish the small amount of change. Our results have also indicated that further increase in ionic strength has screened out the repulsive Coulombic interactions more completely and thus brought a significant increase in aggregation.

For a monodisperse sample of small particles with $qL<<1$, we expect the diffusion coefficient to be independent of q^2 or the decay rate to be proportional to q^2. Since our samples are polydisperse the z-average diffusion coefficient is proportional to q^2 with the proportionality depending on the polydispersity of the samples. This is because the smaller the scattering angle the more the light scattering is dominated by bigger particles. The first order cumulant which equals the z-average decay rate $\bar{\Gamma}$, and the second order cumulant μ_2 which indicates the polydispersity of the samples, are given by[66]

$$\bar{\Gamma} = \frac{\int_0^\infty \Gamma G(\Gamma)d\Gamma}{\int_0^\infty G(\Gamma)d\Gamma} = \frac{\int_0^\infty \Gamma G(R)dR}{\int_0^\infty G(R)dR} \qquad (45)$$

and

$$\mu_2 = \frac{\int_0^\infty (\Gamma-\bar{\Gamma})^2\, G(\Gamma)d\Gamma}{\int_0^\infty G(\Gamma)\, d\Gamma} = \frac{\int_0^\infty (\Gamma-\bar{\Gamma})^2\, G(R)dR}{\int_0^\infty G(R)dR} \qquad (46)$$

where $G(\Gamma)\, d\Gamma$ is the fraction of scattered intensity due to particles with decay rate $\Gamma = Dq^2$ in the range Γ to $\Gamma + d\Gamma$ and $G(R)dR$ is defined in a similar way with particle radius in the range R to R + dR. The

relation $G(\Gamma)d\Gamma = G(R)dR$ has been applied in the above equations. For particles small compared to the wavelength of the incident light G(R) is given by

$$G(R)dR = N(R)\, R^6\, f_q(R) \cdot dR \qquad (47)$$

where N(R) is the distribution function of particles with radius R and $f_q(R)$ is the form factor of the particles in the solutions. Substituting Eq. 47 into Eq. 45 and Eq. 46 and using the relation $\Gamma = Dq^2 = (kT/6\pi\eta R)q^2$ we can calculate $\bar{\Gamma}$ and μ_2 for a given model of particle distribution N(R) and particle shape for which the form factor $f_q(R)$ is known. The z-average free diffusion coefficient D_z^f is calculated from $\bar{\Gamma}/q^2$.

Two kinds of models, Gaussian and Rectangular, for the particle distribution functions have been applied to fit the results listed in Table III by assuming spherical particles with form factor given by[7]

$$f_q(R) = \left\{ \frac{1}{qR^3} [\sin(qR) - qR\cos(qR)] \right\}^2 \qquad (48)$$

Neither distribution, however, gives a prominent q^2 dependence in the calculated values of D_z^f and μ_2 nor is there any agreement between the calculated values of D_z^f and μ_2 with these measured values at a given value of q^2.

B. SEMI-DILUTE SOLUTIONS

Since the samples are highly polydisperse, the crossover concentration which is proportional to the molecular weight and inversely proportional to the cube of the radius of gyration of the particles cannot be well defined. However, in the very low concentration region the diffusion coefficient is independent of C since the particles in

the solutions are undergoing free diffusion motion. The polydispersity of the solutions makes the correlation spectra different from a single exponential decay. As the concentration increases, particles start to interact with each other through entanglements among themselves and more particles aggregate. The diffusion coefficient is thus decreasing with C.

The divergence of different order cumulants at $\tau_{max} = 0$ when the concentration is high enough plus the significant departure of correlation data from the single exponential fits in the first few channels indicate that some density fluctuations with very short decay time exist. Two alternative conjectures about the dynamics of macromolecular motions can be made to interpret the above behavior. The first is that the particles are becoming more and more aggregated as the concentration is increasing and when the concentration is high enough each aggregated particle forms a network itself and is executing network vibrations (internal modes) in addition to the diffusion motion. The second alternative is that some particles aggregate and the rest form a single network which is so loose that the rest of the particles (aggregated) can still move around, and undergo diffusion motions. The light scattering in both cases comes from a collective effect of density fluctuations due to vibrations of the polymer network and the diffusive motion of individual particles, especially those aggregated. The collective diffusion coefficient we have follows $D_{(c)} \propto C^{-1.67}$ and the polymerization index N - the average number of monomers of each aggregated particle - can be estimated by $N \propto C^{5}$.

DeGennes' prediction that the cooperative diffusion coefficient follows $D_c(c) \propto C^{0.75}$ in the semi-dilute region is true for a homogeneous polymer network formed by monodispersive chain molecules. Since the system is extremely polydisperse with aggregation increasing with concentration, we do not have a homogeneous polymer network, the correlation spectra are thus not a single exponential decay and the results from correlation measurements are quite different from DeGennes' predictions.

CHAPTER 5

GELS

5.1 SAMPLE PREPARATION AND EXPERIMENTAL PROCEDURE

Gelatin solids were added to a solvent of 0.15M NaCl and 0.05M Tris to make solutions of 50 mg/ml or 75 mg/ml concentrations and then kept at 4°C at least overnight allowing the solids to swell. The solutions were then rapidly heated to 40°C for an hour, stirred for several minutes, and transferred to cuvettes. Samples were then either loaded into the system for light scattering measurements or kept at 4°C for a period from overnight up to several days.

For the samples with formaldehyde, the crosslinking agent was added to the solution immediately after they were heated at 40°C for an hour. The solutions were then stirred for one to two minutes and then loaded into cuvettes. Light scattering measurements were started within an hour.

Since the scattered field from a gel is a non-Gaussian field, the clipping function of the correlator can not be applied. In taking correlation functions, the correlator was set to single prescaled mode and the total delay time of 44 channels was chosen to be near 1.8 correlation times. The prescale levels were set such that

$$\frac{\text{Number of counts per bin}}{\text{Prescale level}} = < 0.1$$

or

$$\frac{\text{Count rate of photopulses x Bin time}}{\text{Prescale Level}} = < 0.1$$

in order to make the probability of detecting two scaled counts in a bin time negligible.

Samples were allowed to sit in the system at 20°C for at least a week and light scattering measurements were performed every hour in the first two days and then once or twice a day. Most of the data were measured at

scattering angles of 90°. Some were measured at scattering angles of 21.9° and 31.8° when the samples had been kept in the system long enough and no significant changes in a short period of time were observed.

5.2 DATA ANALYSIS

Most of the previous studies on the autocorrelations of solid gels were analyzed and interpreted by the elastic continuum model which predicts a single exponential intensity autocorrelation function in the limit of $I_s >> I_o$. Although our solutions which formed the gels were highly polydispersive and relatively dusty, our intensity correlations of gels did fit to single exponential functions well. We therefore fit our data to a single exponential form and then calculated the average diffusion coefficient and the standard deviation from several autocorrelations with the same bin time taken at about the same time.

Besides the elastic continuum model, some predictions of the bounded particle model were also investigated. The intensity correlation function of the bounded particle model at very short delay time reduces from Eq. 36 to a single exponential function of delay time [55]

$$g^{(2)}(\tau) = 1 - \exp(-2Dq^2/\gamma) + \exp(-2Dq^2\tau) \qquad (49)$$

We thus have single exponential autocorrelation at short delay time for both the bounded particle model and the elastic continuum model which predicts a single exponential autocorrelation at all delay times. We therefore fit the data to mono- and multi-exponential forms.

$$G^{(2)}(\tau) = B + A \exp \frac{\tau}{\tau_c} \qquad (50)$$

and

$$G^{(2)}(\tau) = B[1 + \exp(B_o + B_1\tau + B_2\tau^2 + \ldots)] \qquad (51)$$

using the method of least squares fit discussed in Chapter 2. For the case of prescaling, the background level B was calculated from the total number of counts N and the total number of prescaled counts N_p by the equation

$$B = N N_p/(T/\Delta T) \qquad (52)$$

where T is the experimental duration and ΔT is the bin time.

Note that Eq. 36 for the autocorrelation of the bounded particle model can be expanded as

$$g^{(2)}(\tau) = 1 - \exp(-2Dq^2/\gamma) + \exp\left[(-2Dq^2/\gamma)\left(\sum_{n=1}^{\infty} \frac{(-\gamma\tau)^n}{n!}\right)\right]$$

or

$$g^{(2)}(\tau) = 1 - \exp(-2Dq^2/\gamma) + \exp\left[2Dq^2 \sum_{n=1}^{\infty} \frac{(-\gamma)^{n-1}}{n!}\, \tau^n\right]$$

or

$$g^{(2)}(\tau) = B_o + \exp \sum_{n=1}^{\infty} B_n\tau^n \quad . \ . \ . \ . \qquad (53)$$

where $B_n = \frac{-\gamma^{n-1}}{n!}$ and B_o is independent of delay time. Note that the ratio of the coefficients of two consecutive terms in the exponential $B_n/B_{n-1} = \frac{-\gamma}{n}$. We have $\frac{B_n}{B_{n-1}} \cdot n = -\gamma$ independent of delay time.

Note that the autocorrelations of the bounded particle model and the elastic continuum model, i.e. Eq. 36 and Eq. 39 at $\tau = 0$ become

$$g^{(2)}(o) = 2 - \exp(-2Dq^2/\gamma) \qquad (54)$$

and

$$g^{(2)}(o) = 1 + 2\,\frac{I_o}{I_s} \qquad (55)$$

respectively. Thus values of $\frac{A}{B}$ calculated from correlation data by

$[C(\tau)-B]/B$ at $\tau = 0$ limit or the intercepts of correlation functions at $\tau = 0$ are proportional to $1 - \exp(-2Dq^2/\gamma)$ and $2\ I_o/I_s$ respectively. Since γ increases and I_o/I_s decreases as gelation progresses, both models predict a decreasing of A/B during the gelatin process and the correlation function is nearly flat when the gelation is completed.

The static component of the scattered light depends on q^2 according to the Ornstein Zernike approximation through the relation[7]

$I_s \propto \frac{1}{1+\xi^2q^2}$ where ξ is called the correlation length which characterizes the range of the correlations between the density fluctuations at different positions. We have

$$\frac{I_o}{I_s} \propto 1 + \xi^2q^2$$

Both models predict a q^2 dependence of A/B in the forms of $1 - \exp(-2Dq^2/\gamma)$ and $1 + \xi^2q^2$ respectively. By using the power expansion for the exponential term we have

$$1 - \exp(-2Dq^2/\gamma) = 1 - \sum_{n=0}^{\infty} \frac{-2Dq^2/\gamma}{n!} = 2Dq^2/\gamma$$

where the higher order terms were neglected. Thus both models predict that A/B is proportional to q^2.

For the samples with formaldehyde, the relaxation time τ_c became shorter with age. Thus we compared the correlation functions with decreasing delay time such that 44 channels cover approximately the same number of relaxation times. Instead we could also change the number of delay channels in the fitting procedure. Since the relaxation time also depended on q^2, the q^2 dependence of the cooperative diffusion coefficient was also investigated in a similar way.

5.3 EXPERIMENTAL RESULTS

Fig. 32 shows the correlation functions of a gelatin solution of 75 mg/ml in 0.15M NaCl and 0.05M Tris at 35°C which was later formed into a gel by lowering its temperature to 20°C. The best single exponential fits are also shown in the same figure. Autocorrelations obtained at a scattering angle $\theta = 90°$ from a 70 hour old gel at 20°C with 75 mg/ml concentration are shown in Fig. 33 along with their best single exponential fits. Similar curves for gels with formaldehyde are shown in Fig. 34. Fig. 35 shows the autocorrelation taken on 31.8° scattering angle along with their best single exponential fits. Note that those correlations with 44 channels covering less than 1.8 relaxation times are fit well by a single exponential function except the first channel which was not included in the fit. The intercepts of the autocorrelations are decreasing with age and the scattering angles, and the correlation functions become almost flat for those gels which were very old.

The ratios $\frac{B_n}{B_{n-1}} \cdot n$ from the multi-exponential fit of Eq. 53 were calculated and do not give any evidence of being constant. The variance in time of the average decay rate of the correlation functions of gels with concentrations 75 mg/ml and 50 mg/ml are plotted in Fig. 36 to Fig. 39. For gels without formaldehyde the decay rate reached a terminal value several hours after its temperature was changed to 20°C either from 40°C (in the liquid state) or 4° (in the solid state) and then stayed approximately at that value. For gels with formaldehyde the decay rate of the correlation function continuously increased in time. The q^2 dependence of the decay rate of

96

Fig. 32. Normalized correlation data for a 75 mg/ml gelatin solution in 0.15M NaCl and 0.05M tris without being centrifuged (Note 128 bin delay after bin 44). T =35°C, θ=90°.

♣ : τ= 200 μsec/bin, H= 1.0

● : τ=1000 μsec/bin, H= 3.5

H : Number of correlation times spanned by 44 bins

Solid lines : single exponential fits

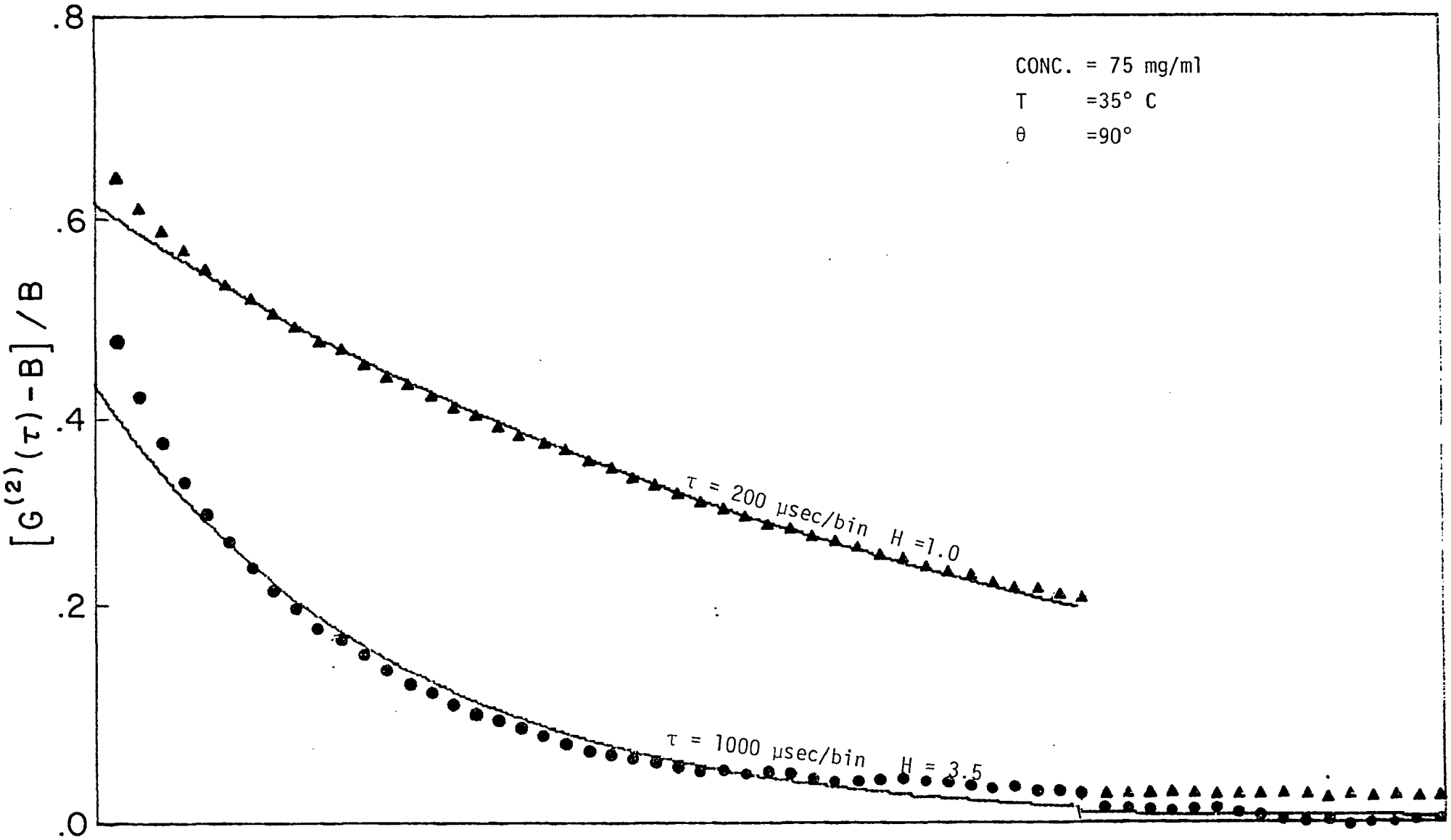
.8
.6
.4
.2
.0
$[G^{(2)}(\tau)-B]/B$
CONC. = 75 mg/ml
T =35° C
θ =90°
τ = 200 μsec/bin H =1.0
τ = 1000 μsec/bin H = 3.5

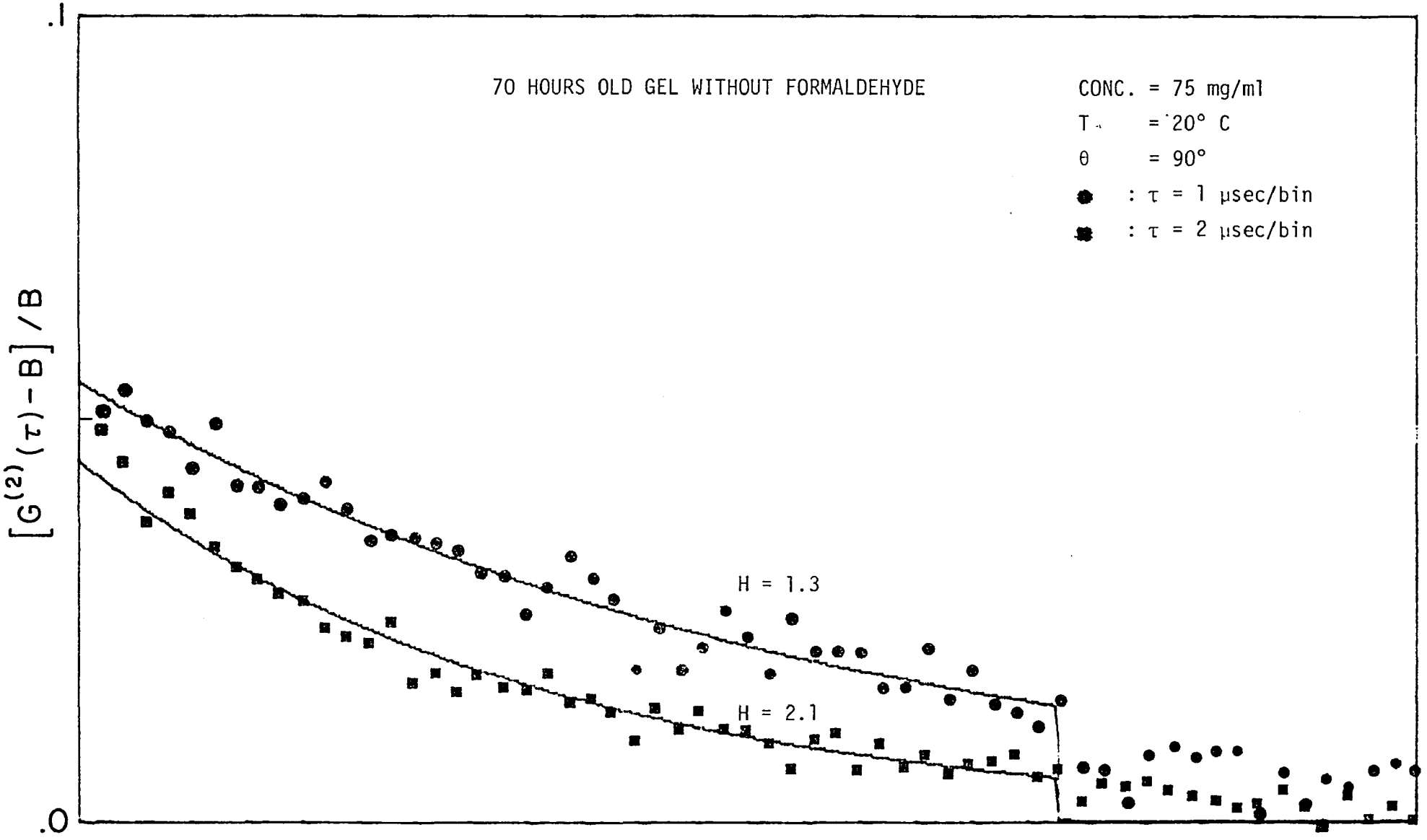

Fig. 33. Normalized correlation data of a 70 hour old gel of 75 mg/ml concentration in 0.15M NaCl and 0.05M tris. Solid lines : single exponential fits

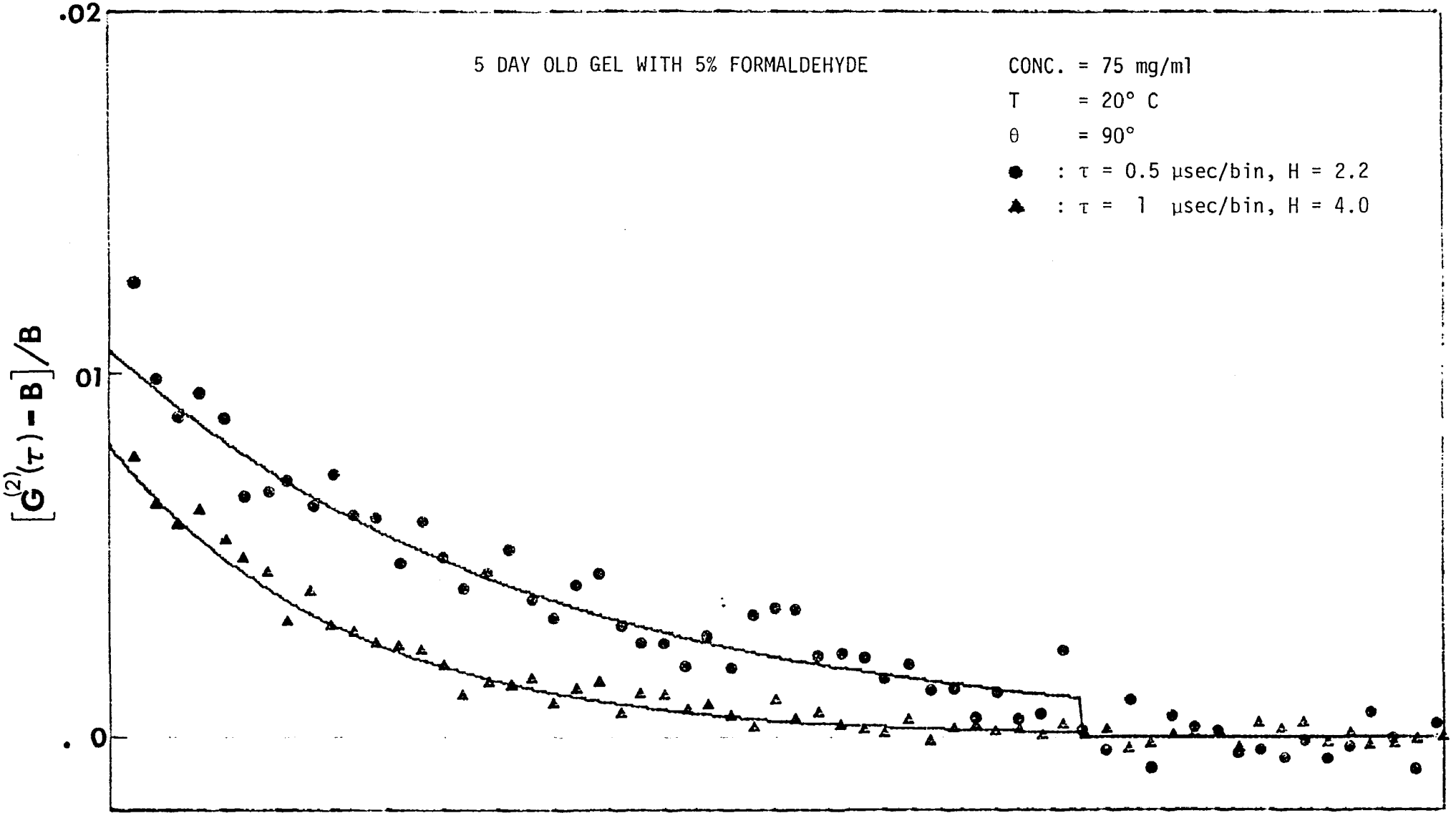

Fig. 34. Normalized correlation data of a 5 day old gelatin gel of 75 mg/ml concentration and 5% formaldehyde in 0.15M NaCl and .05M tris. Solid lines : Single exponential fits, H : Number of correlation times

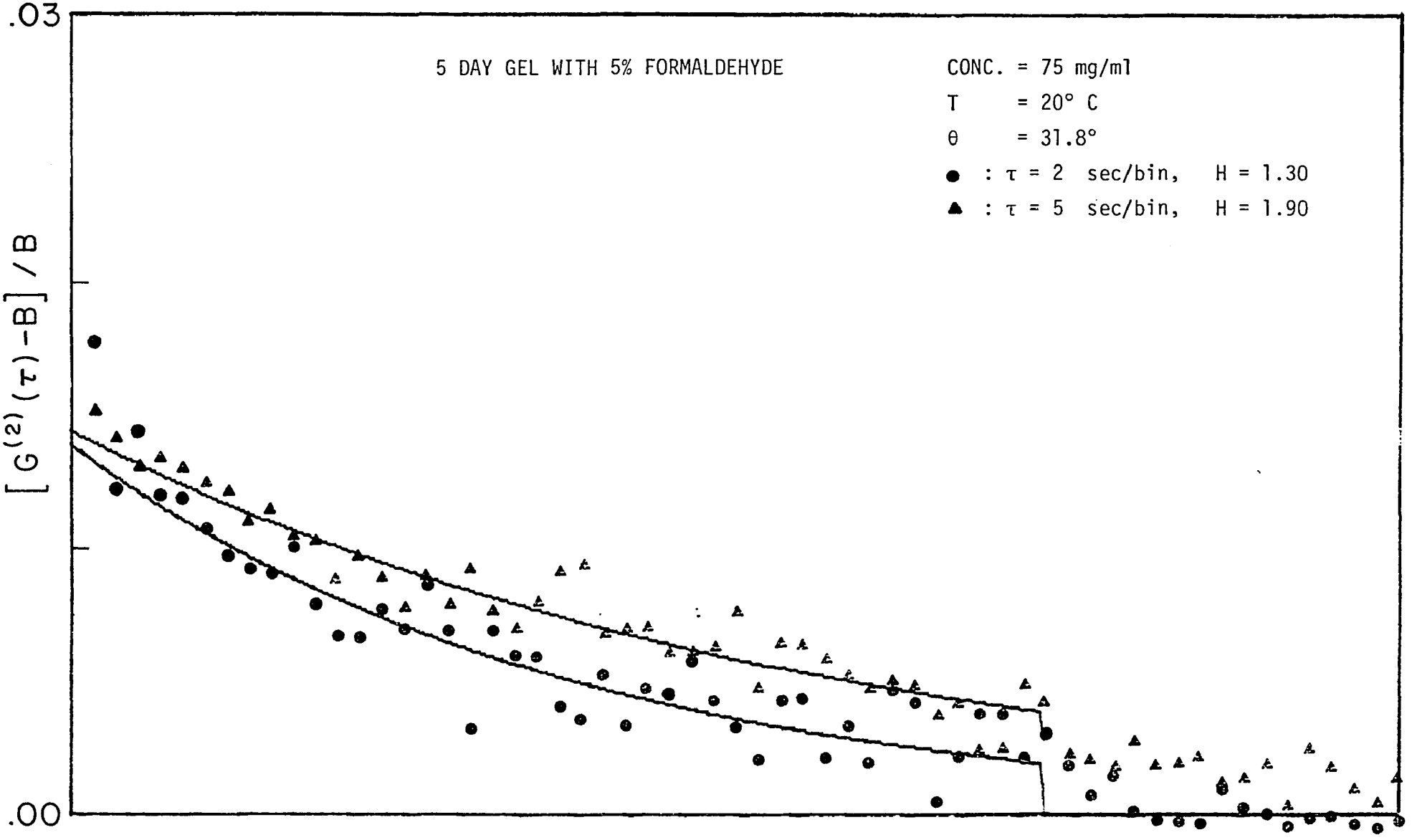

Fig. 35. Normalized correlation data for a 5 day old gelatin gel of 75 mg/ml concentration & 5% formaldehyde in .15M NaCl & .05M tris. Solid lines : single exponential fits, H : number of correlation times spanned by 44 bins

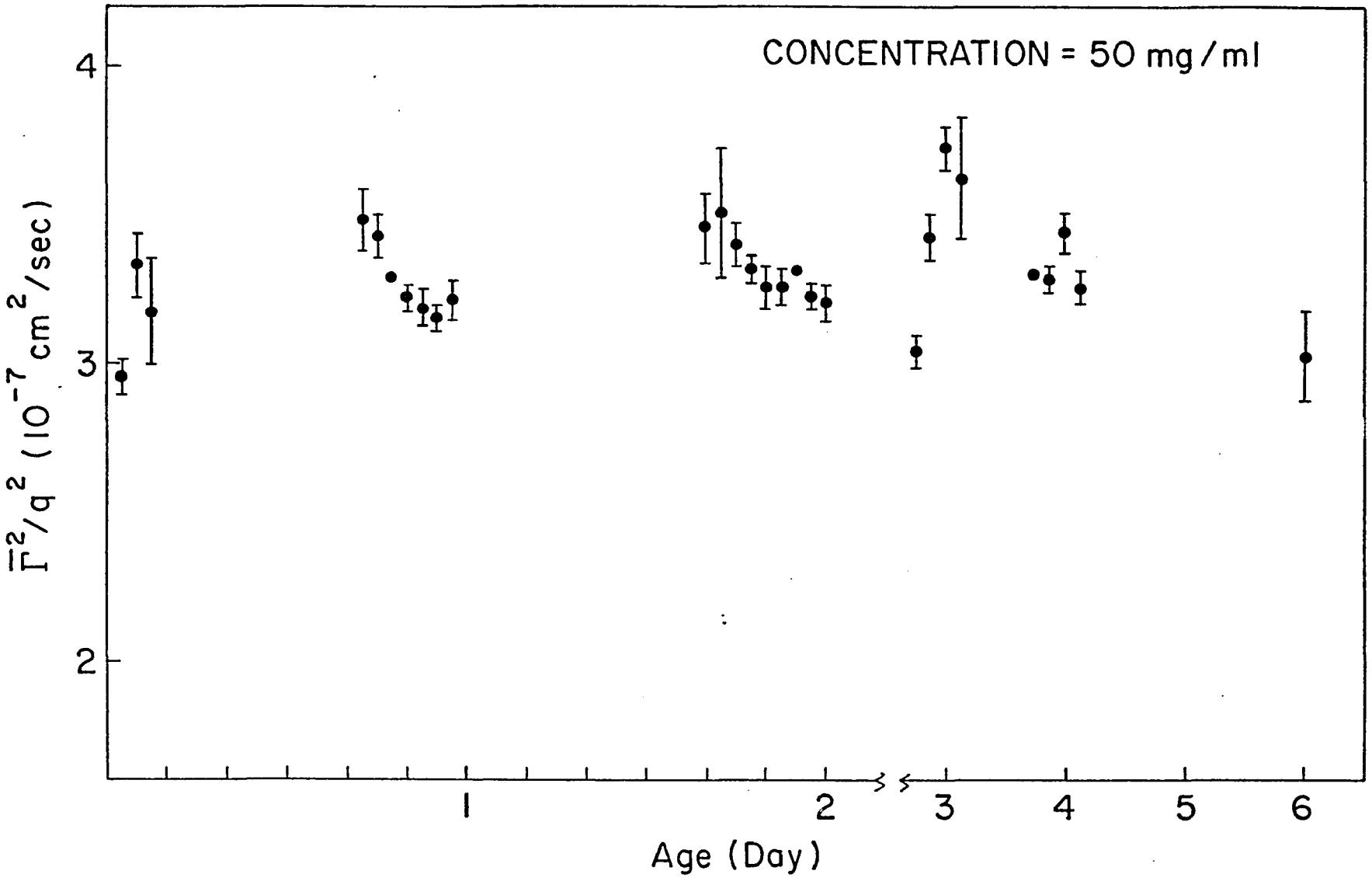

Fig. 36. The change in the decay rate of the intensity correlation functions in age for a 50 mg/ml gelatin gel in 0.15M NaCl and 0.05M tris. T= 20°C, θ=90°.

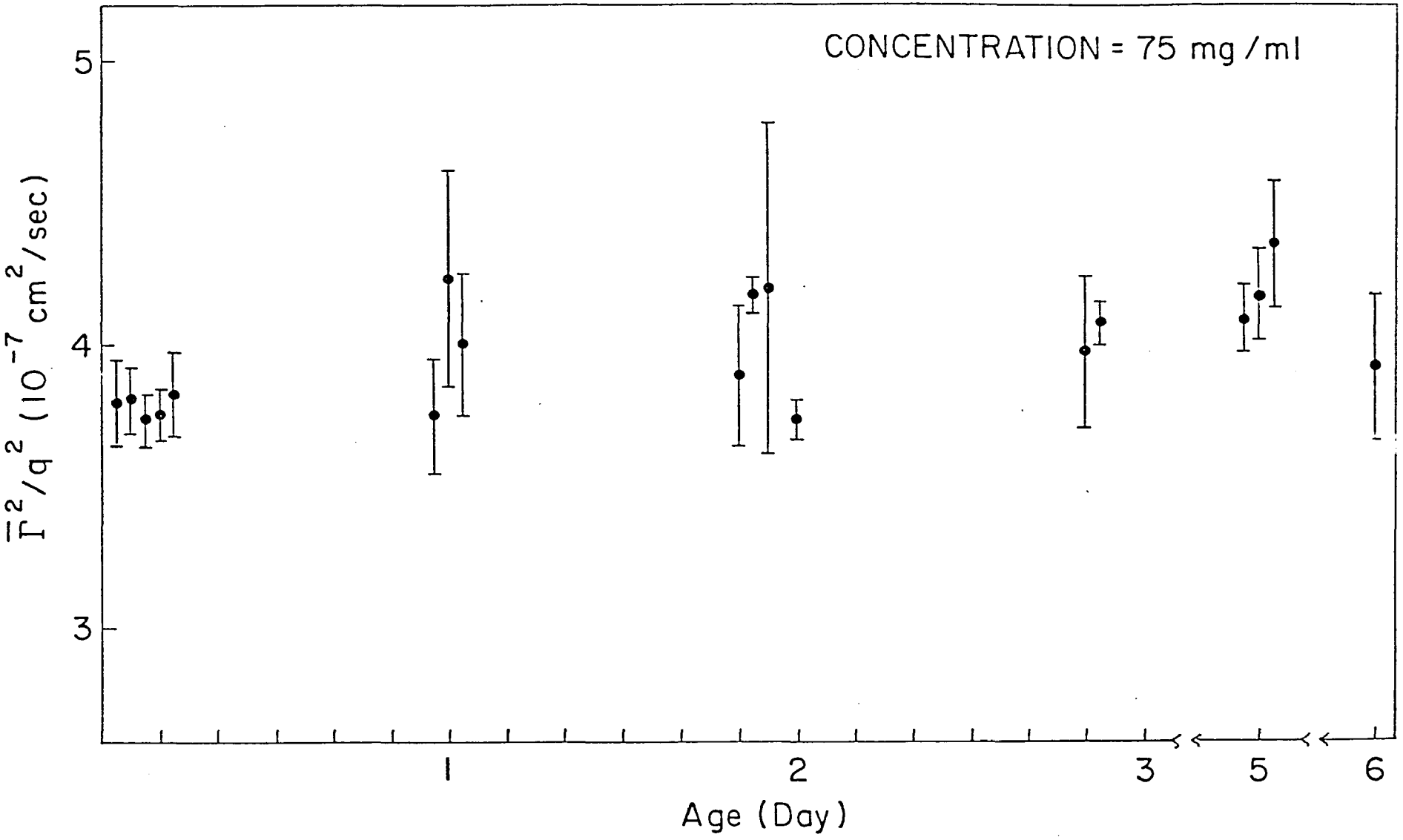

Fig. 37. The change in decay rate of intensity correlation functions in age for a 75 mg/ml gel in 0.15M NaCl and 0.05M tris. T= 20°C, θ=90°.

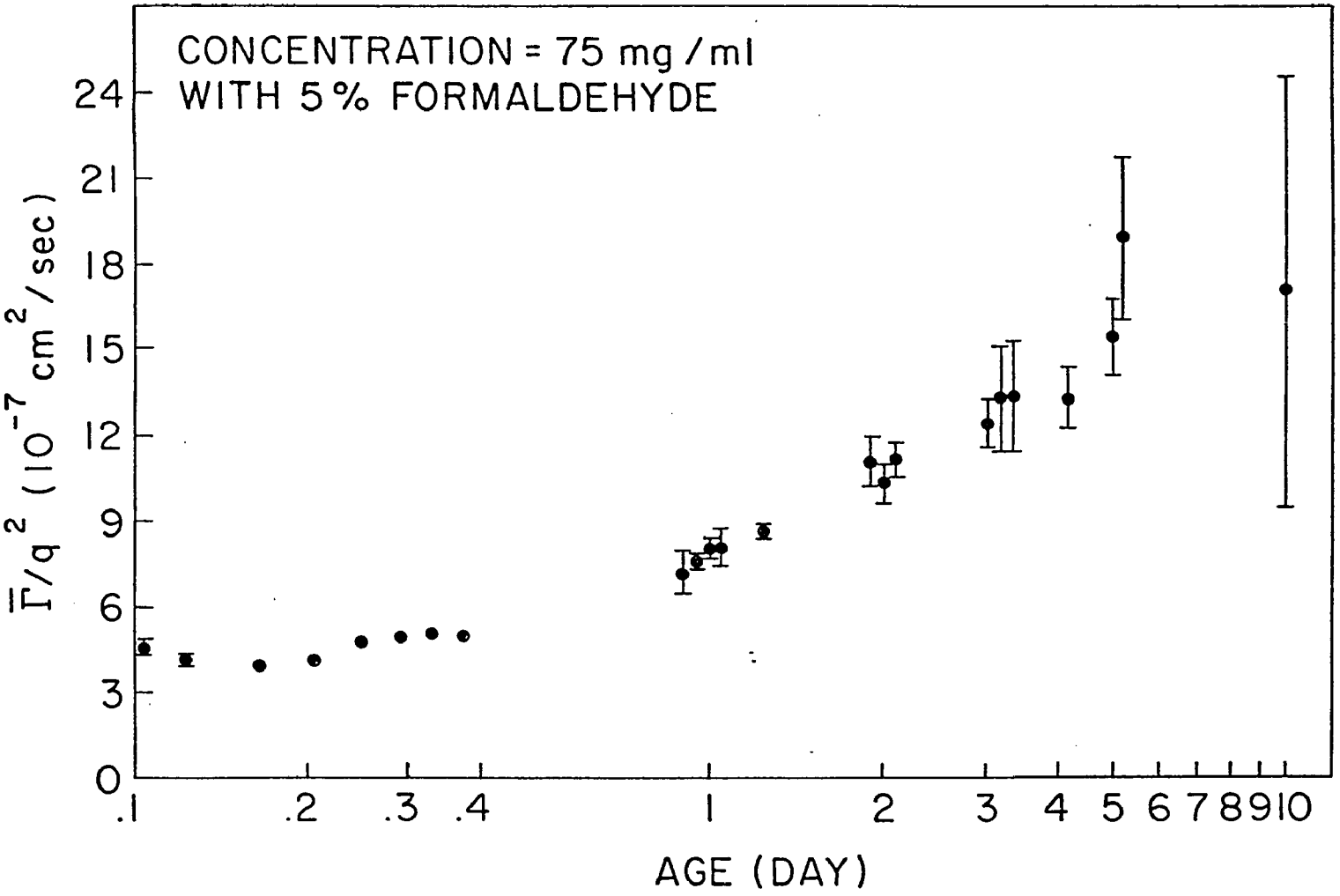

Fig. 38. The change in decay rate of the intensity correlation functions in age for a 75 mg/ml gel in 0.15M NaCl, 0.05M tris and 5% formaldehyde. T= 20°C, θ =90°.

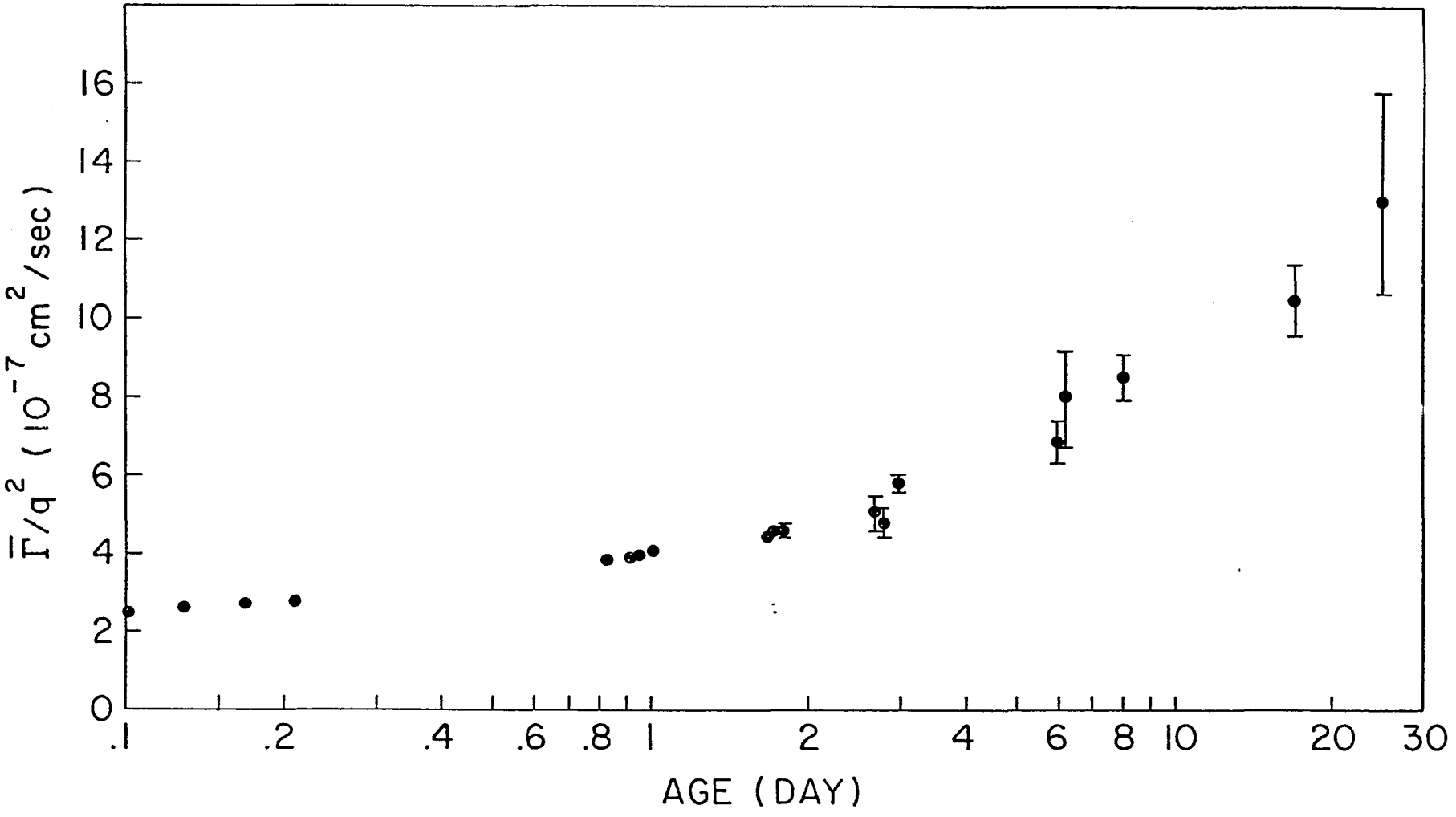

Fig. 39. The change in decay rate of the intensity correlation functions in age for a 50 mg/ml gel in 0.15M NaCl, 0.05M tris and 5% formaldehyde. T= 20°C, θ=90°.

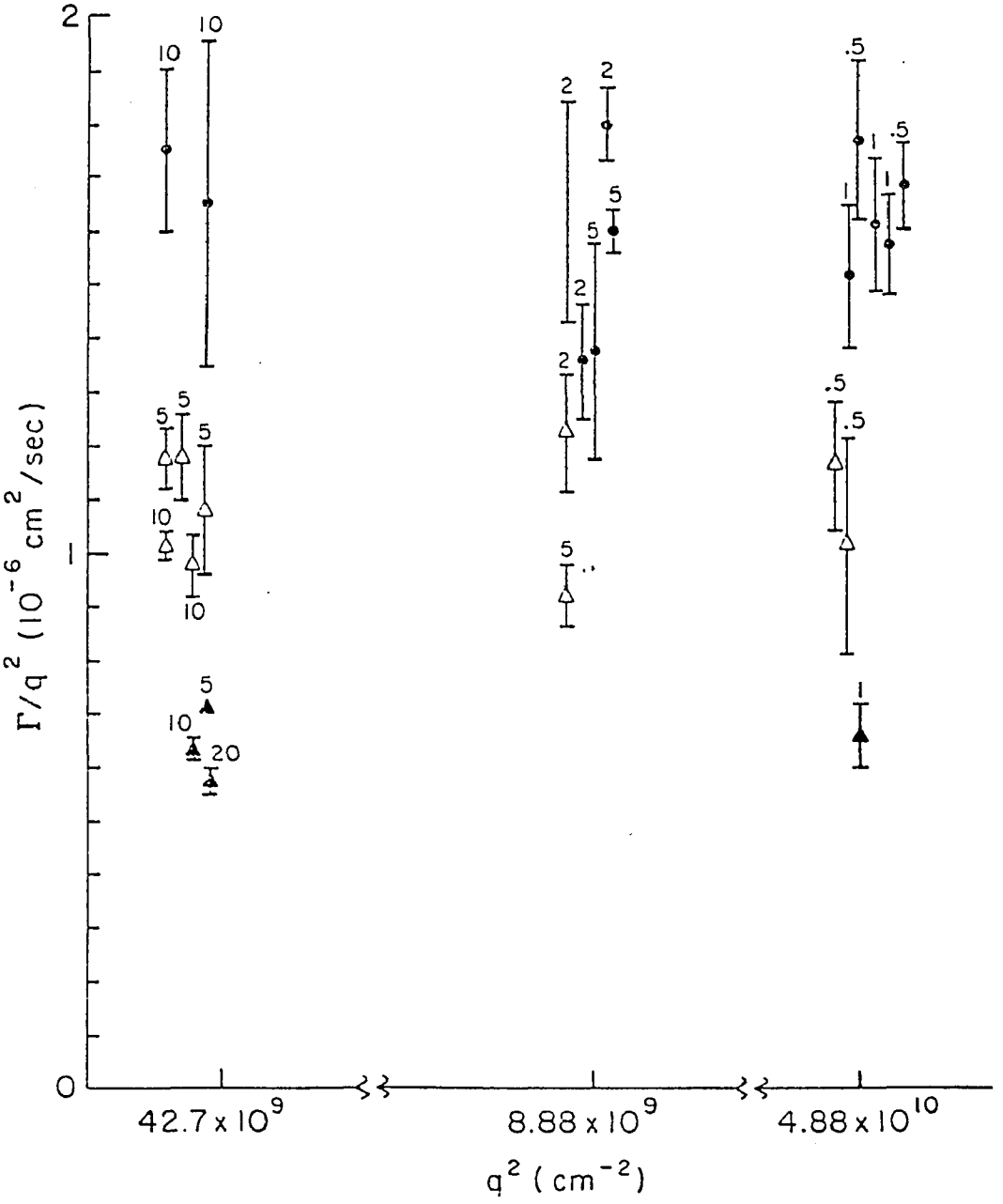

Fig. 40. q^2 dependence of the decay rates of the correlation functions of gels with formaldehyde

● : 75 mg/ml & 5% formaldehyde, T= 20°C, 5 day old sample

Δ : 50 mg/ml & 5% formaldehyde, T= 20°C, 7 day old sample

▲ : 50 mg/ml & 5% formaldehyde, T= 20°C, 18 day old sample

106

Fig. 41. The age and q^2 dependences of the initial amplitude A/B of the intensity correlation functions of gels. T= 20°C
: 50 mg/ml gel in 0.15M NaCl, 0.05M tris and 5% formaldehyde
* : 75 mg/ml gel in 0.15M Nacl, 0.05M tris and 5% formaldehyde

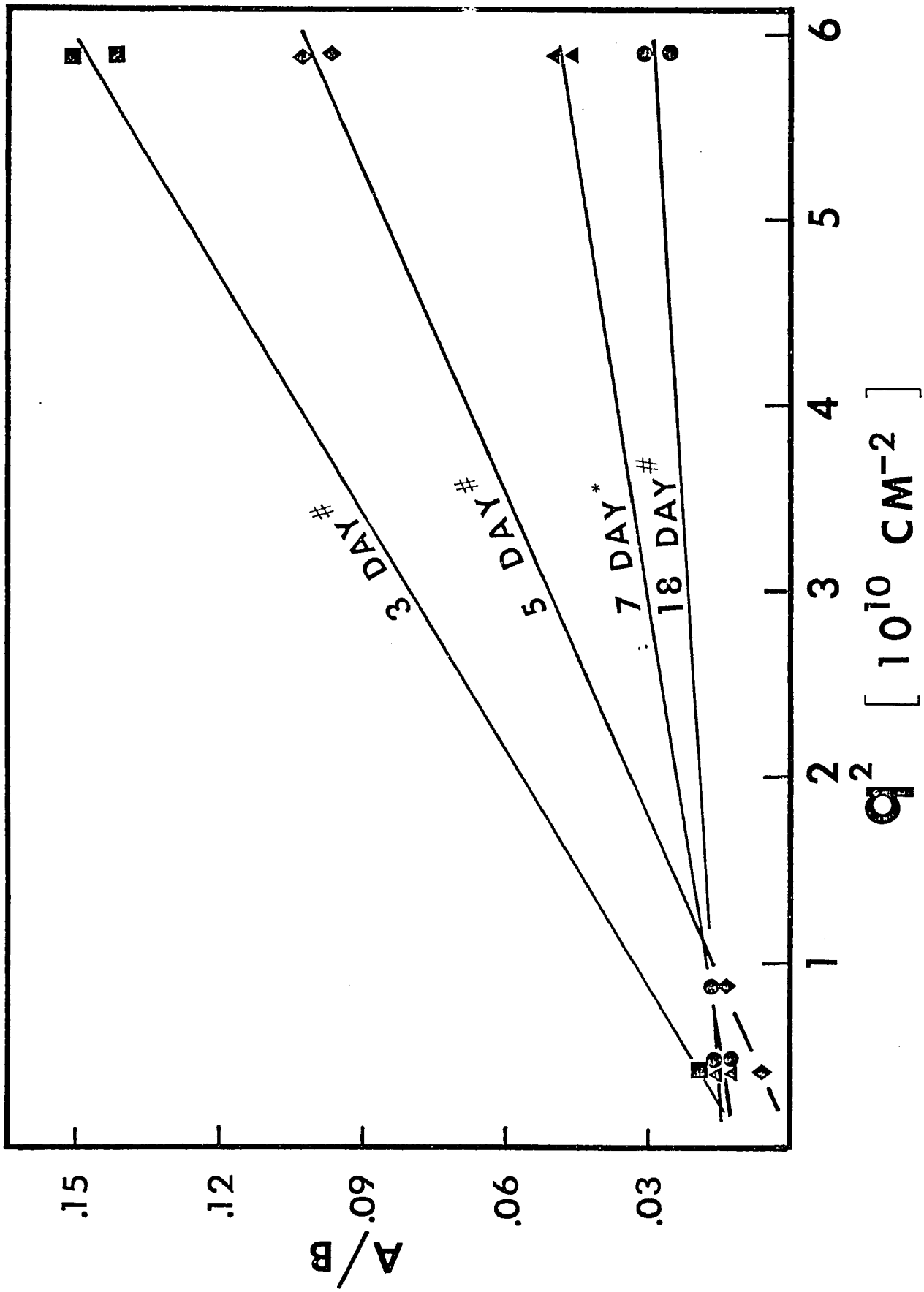
A/B
.15
.12
.09
.06
.03
1
2
3
4
5
6
q^2 [10^{10} CM^{-2}]
3 DAY#
5 DAY#
7 DAY*
18 DAY#

the correlation function of gels kept at 20°C for several days are shown in Fig. 40. The diffusion coefficient is independent of q^2 (or the decay rate is proportional to q^2). A summary of some results is shown in Table IV.

Fig. 41 shows the q^2 dependence of A/B. Note that A/B is proportional to q^2 and the slope of the straight line decreased with age. Therefore the correlation length becomes shorter and shorter for gel with formaldehyde.

5.4 DISCUSSION

Polymers in gelatin solution under appropriate conditions form interchain contacts or cross-links stabilized by either primary or secondary bonds. As long as the number of interchain contacts is below some initial number per polymer chain, the polymer system retains its stability. When the critical point is reached there is a transition which corresponds to the formation of an infinitely large permanent network of polymer chains. This network is insoluble and the entire polymer-solvent system forms a gel.

For gels without a crosslinking agent such as formaldehyde, the network system is stabilized by secondary forces such as hydrogen bonds, exhibiting a strong dependence upon the solvent environment and the system temperature. The whole system represents a delicate balance between solute-solvent and solute-solute interactions. The system under certain circumstances reaches equilibrium within several hours and the diffusion coefficient reaches its final value which is much higher than it is in the liquid state. It is able to have a reverse gel to gelatin transition by simply increasing its temperature above the melting point.

TABLE IV

THE DECAY RATES OF THE CORRELATION FUNCTIONS

FOR GELATIN GELS

	$\Gamma/q^2(10^{-10}cm^2/sec)$ at 35°C in liquid state	$\Gamma/q^2(10^{-7}cm^2/sec)$ at 20°C in solid state
2.0% Gel without Formaldehyde	145.40	1.26 ± 0.3
5.0% Gel without Formaldehyde	41.32	3.3 ± 0.3
7.5% Gel without Formaldehyde	14.50	4.0 ± 0.3

Table IV shows that as the concentration increases the diffusion coefficient decreases in the solution state but increases in the gel state. This result indicates that as the concentration increases, more and bigger aggregates are formed in solutions; however less ordered network gels with more interchain contacts and smaller crystallite sizes are formed in solid gels.

Formaldehyde, a crosslinking agent, creates covalent bonded crosslinks or interchain contacts. A gel with this agent added becomes stiffer with age since more and more covalent bonds are created in time. As a result, the gel-gelatin transition cannot be carried out for an old gel with a crosslinking agent by simply increasing its temperature. Since more and more crosslinks are created in time, portions of polymer that are either between two crosslinks or interchain contacts in the elastic continuum model or that are bound by the surrounding network in the bouded particle model become smaller and smaller. In Chapter 2, we showed that the diffusion coefficients defined in Eq. 36 and Eq. 39 are equivalent to the free diffusion coefficients of the effective individual particles defined as the portions of polymer mentioned above. Both models thus predict that the diffusion coefficient or the decay rate of the correlation functions increases in time which is in agreement with our results.

In section 2, we have shown theoretically that both models predict a decrease of $g^{(2)}(0)$ during the gelation process while A/B, which equals $g^{(2)}(0)-1$, is proportional to q^2. Our results are also in agreement with these predictions. The increase in time of the average decay rate of the correlation functions or the cooperative

diffusion coefficient for gels with formaldehyde can also be interpreted by both models. However, the bounded particle model predicts that the ratio of two consecutive coefficients in the multi-exponential fit will be constant, which is not supported by the data. In contrast, the elastic continuum model has a single exponential correlation function which is in agreement with our results but is in disagreement with the bounded particle model except at very short delay times. In addition, the elastic continuum model also predicts a q^2 scattering which has been proven to be true. We therefore conclude that the elastic continuum model provides an appropriate description of the dynamics of the gel's polymer network and that the bounded particle model is limited to the region of very short relaxation times. The correlation lengths of a gel with formaldehyde, calculated by the elastic continuum model, become shorter with age as expected and are listed in Table V.

TABLE V

THE AGE DEPENDENCE OF THE COOPERATIVE DIFFUSION COEFFICIENTS AND CORRELATION LENGTHS OF GELS WITH FORMALDEHYDE

Sample	4FG 75 mg/ml gel 5% Formaldehyde	5FG 50 mg/ml gel 5% Formaldehyde		
Age	5 day	3 day	7 day	18 day
$D(10^{-7}cm^2/sec$	8.75 ± 0.75	3.00 ± 0.50	3.25 ± 0.50	5.50 ± 0.70
ξ (cm)	1.23×10^{-6}	1.54×10^{-6}	0.736×10^{-6}	0.510×10^{-6}

CHAPTER 6

COLLAGEN

6.1 SAMPLE PREPARATION AND EXPERIMENTAL TECHNIQUES

Dried collagen from different sources prepared by the Hoffman La Roche Research Laboratory was added to 0.05M acetic acid to make up the collagen solutions. The mixture was stirred with a magnetic stirrer at 4°C for 36 hours and then centrifuged at a speed of 50,000 g for three hours at the same temperature. The supernatant of the centrifuged collagen solutions was then either directly dialyzed against a dialyzing buffer or purified by the density gradient technique and then dialyzed.

Samples which were not to be purified by the density gradient technique had a concentration of 1 mg/ml in the initial mixtures. Repeated centrifugations removed a large amount of inhomogeneities and dust. The concentration in the solutions ready for correlation measurements were estimated to be around 0.5 mg/ml.

The density gradient technique was employed to remove collagen aggregates which were not removed by centrifugation. We first created in centrifuge tubes the density gradient with sucrose concentration varying from 30% at the bottom to 10% at the top using a density gradient maker. The total amount of the sucrose solution in each tube was 12 ml. 1.5 ml supernatant from the centrifuged collagen solution was then loaded carefully on top of the sucrose solution in each centrifuge tube without disturbing the gradient. These tubes were then centrifuged at a speed of 120,000 ~ 200,000g for 44 hours at 4°C using Beckman L2-65B ultracentrifuge and SW40Ti rotor.

The centrifuged solution in each tube was then separated into different fractions. The comparable fractions from different tubes were combined together to form each sample which was then loaded into dialyzer tubing and dialyzed against the buffer.

The dialyzing buffer was an aqueous solution of 0.05M tris, 0.02M NaCl and 0.005M $CaCl_2$ with a pH of 7.6. In each case, the total amount of dialyzed sample was less then 5 ml and was dialyzed against 750 ml buffer each time. The dialyzing buffer was replaced with fresh buffer every 12 hours, repeated four times. The samples were then centrifuged at a speed of 50,000 g for three hours at 5 to 10°C. The supernatants were then transferred to the cuvettes and centrifuged in a RC2 Sorvall centrifuge at a low speed of 10,000 g or less overnight with a well balanced rotor. This final centrifugation was to settle down the residual collagen aggregates and dust in the sample to the bottom of the cuvette which was removed and loaded into the thermostated bath before the light scattering measurements.

Samples to be passed through the density gradient purification had 6 mg/ml concentration in the initial mixture. At the first centrifugation the concentration of the supernatant was estimated to be less than 3 mg/ml. The final concentration of the sample, ready for measurement, was less than or equal to 0.5 mg/ml

Before the collagen sample was loaded, the apparatus was calibrated at scattering angles of 31.8° and 90° with a polystyrene sample of known particle size. The laser output was also adjusted to a single longitudinal mode monitored with a piezoelectric spectrum analyzer. Correlation functions of collagen solutions were then measured at 20°C for 31.8° and 90° scattering.

The difficulty in removing all the dust from the sample made the scattering intensity fluctuate significantly at low scattering angles. The low concentration of collagen also intensified the fluctuation. Therefore, at low scattering angle many short experiments were performed and

only those with average count rate and $\mu_2/\langle\Gamma\rangle^2$ - an indication of polydispersity of the sample - below certain values were accepted.

At large scattering angle, the count rate was extremely low, so that we had to collect data for a long experimental duration to obtain statistically acceptable results. Since the scattering from oversized particles is directed strongly into low angles, long collection times are possible without overflow and the validity of the measured diffusion coefficients is greater than at small angles.

6.2. DATA ANALYSIS

A. VISCOSITY

The Broersma equations (eq. 18 and 19) show that both the translational and rotational diffusion coefficients are inversely proportional to the shear viscosity η. However, the ratio of D_T and D_R is independent of the viscosity and is given by:

$$\frac{D_T}{D_R} = \frac{1}{9L^2} \frac{\delta^{-\frac{1}{2}}(\gamma_{11}+\gamma_{\perp})}{\delta - \xi} \qquad (56)$$

where δ, ξ, γ_{11} and $\gamma_{\perp}$ were defined in section 2.4 and depends only on the length L and diameter d of the particles. D_T/D_R is thus a function only of L and d. Furthermore, since the diameter d is very small compared with the length L, the variance in d does not create any significant change in D_T/D_R. Thus D_T/D_R depends only on the length L. For a given L, we calculated the corresponding D_T/D_R and the results are listed in Table VI.

The viscosity η of our sample was not well defined due to the intrinsic viscosity[91,92] of the collagen molecules and the residual sucrose introduced during the density gradient purification process and incompletely removed by the dialyzing process. In analyzing our data, we used the ratio

TABLE VI

VALUES OF D_T/D_R AND THE RATIO OF THE SCATTERED INTENSITIES OF B_o, B_2, B_4 and B_{tot} FOR DIFFERENT MOLECULAR LENGTHS

Length (Å)	D_T/D_R (10^{-11}cm^2)#		90° Scattering *			31.8° Scattering *	
	d=13.6Å	d=14Å	$\frac{B_2}{B_o}$	$\frac{B_4}{B_o}$	$\frac{(B_2+B_4)}{B_{tot}}$	$\frac{B_2}{B_o}$	$\frac{B_4}{B_o}$
2500	8.30	8.31	0.253	0.004	0.997	0.005	0
2550	8.63	8.64	0.275	0.005	0.996	0.005	0
2600	8.97	8.97	0.299	0.006	0.995	0.005	0
2650	9.31	9.32	0.324	0.007	0.995	0.006	0
2700	9.65	9.66	0.351	0.008	0.994	0.006	0
2715	9.76	9.77	0.361	0.009	0.994	0.007	0
2725	9.83	9.84	0.365	0.009	0.993	0.007	0
2750	10.01	10.02	0.379	0.010	0.993	0.007	0
2800	10.37	10.38	0.410	0.011	0.992	0.007	0
2850	10.74	10.75	0.441	0.013	0.991	0.008	0
2900	11.11	11.12	0.475	0.015	0.990	0.009	0
2950	11.49	11.50	0.487	0.018	0.988	0.010	0
3000	11.88	11.89	0.529	0.020	0.980	0.010	0

Calculated from Eq. 56

* From Ref. 62

D_T/D_R which is independent of viscosity instead of D_T or D_R individually, to determine the particle length L via the Broersma equations. D_T was first independently calculated from the data at low scattering angle (31.8°). From the data at 90° scattering angle, we found a set of D_T and D_R by trying different values of L and D_R such that D_T was equal to that obtained from low scattering angle data, and D_T/D_R was equal to that predicted by the Broersma equations. The details are described in the next section.

B. DATA FITTING

The autocorrelation function for solutions of monodisperse rigid rod particles was discussed in chapter 2. It can be written as

$$g^{(1)}(\tau) = \frac{1}{\sum_{\substack{\ell=0 \\ \text{even}}}^{\infty} B_\ell} \sum_{\substack{\ell=0 \\ \text{even}}}^{\infty} B_\ell \exp\{-[D_T q^2 + \ell(\ell+1)D_R]\tau\} \tag{57}$$

$$B_{tot} = \sum_{\substack{\ell=0 \\ \text{even}}}^{\infty} B_\ell \tag{58}$$

where $B_\ell = (2\ell+1)\{\frac{1}{h}\int_0^h \frac{J_\ell(x)}{x}\, dx\}^2$

$J_\ell(x)$ are Bessel functions and h equals $qL/2$. The values of B_ℓ in terms of h have been calculated by Pecora[61] and also by Cummins.[62] In table VI we listed some of these values corresponding to several different lengths L of the macromolecules.

Note that at a 31.8° scattering angle, B_o contributes more than 99% of B_{tot}. Thus correlation data for this case was fitted to the single exponential function as discussed in section 4.2A. The result obtained was the translational diffusion coefficient D_T.

At a 90° scattering angle both B_o and B_2 make considerable contributions. Since they make up more than 99% of B_{tot}, the correlation functions can be written as

$$g^{(1)}(\tau) = [\exp(-D_T q^2 \tau)]\,[B_o + B_2 \exp(-6D_R\tau)] \tag{59}$$

and

$$g^{(2)}(\tau) = 1 + [\exp(-2D_T q^2 \tau)]\,[B_o + B_2 \exp(-6D_R\tau)]^2 \tag{60}$$

The normalized correlation data $\frac{C(\tau)-B}{B}$ can be related to the correlation function by

$$\frac{C(\tau)-B}{B} = \frac{A}{B}(\exp -2D_T q^2\tau)\left[1 + \frac{B_2}{B_o}\exp(-6D_R\tau)\right]^2 \tag{61}$$

There are two ways to fit correlation data for 90° scattering. The first is to calculate from the data, the derived function:

$$Y(\tau) = \sqrt{\frac{C(\tau)-B}{B}\exp(2D_T q^2\tau)\cdot\frac{B}{A} - 1} \tag{62}$$

using the value of D_T from the low angle scattering and fit it to the single exponential function $\frac{B_2}{B_0}\exp(-6D_R\tau)$ as discussed in chapter 4.
An initial value for the parameter A/B corresponding to each value of B_2/B_o can be found by

$$\frac{C(o)-B}{B} = \frac{A}{B}\left(1 + \frac{B_2}{B_o}\right)^2 \tag{63}$$

where $\frac{C(o)-B}{B}$ can be obtained by fitting the very first few channels of the correlation functions to a multiexponential function as discussed previously. The parameters obtained in this single exponential fit are D_R and B_2/B_o. This process is iterated until a set of D_R and B_2/B_o is obtained such that B_2/B_o is sufficiently close to the initial value assigned to calculate A/B.

The physical properties obtained from this analysis are the rotational diffusion coefficient D_R and the particle length L which is determined from B_2/B_o.

Alternatively Eq. 61 can be written as

$$Z(\tau) = \frac{C(\tau)-B}{B} / \left[1+ \frac{B_2}{B_o} e^{-6D_R\tau}\right]^2 = \frac{A}{B} \exp\left(-2D_T q^2 \tau\right) \qquad (64)$$

By knowing D_R, the derived function of the correlation data can be fitted to a single exponential function and D_T can be obtained. Different values of D_R were tried for a given particle length L and a D_T and D_T/D_R corresponding to each D_R was found. This process was continued until a set of L and D_R were found such that D_T was equal to the value obtained at a 31.8° scattering angle and D_T/D_R was equal to the value predicted by the Broersma equations at the same value of particle length L.

6.3 EXPERIMENTAL RESULTS

Fig. 42 shows the correlation function taken at 31.8° scattering angle of a rat skin collagen solution without density gradient purification. The correlation function departs from the best single exponential fit significantly and the decay rate which, in the case of collagen monomer solution equals $2D_Tq^2$ at 31.8° scattering angle is extremely small. These indicate that the solution still contained collagen aggregates, inhomogeneities and dust.

The correlation functions of a collagen solution which has been purified by the density gradient technique are shown in Fig.43 and Fig.44 for 31.8° and 90° scattering angles respectively. The correlation function at 31.8° scattering angle fitted well to a single exponential function indicating the monodispersity of the sample. $7.20 \pm 0.16 \times 10^{-8} cm^2/sec$ was

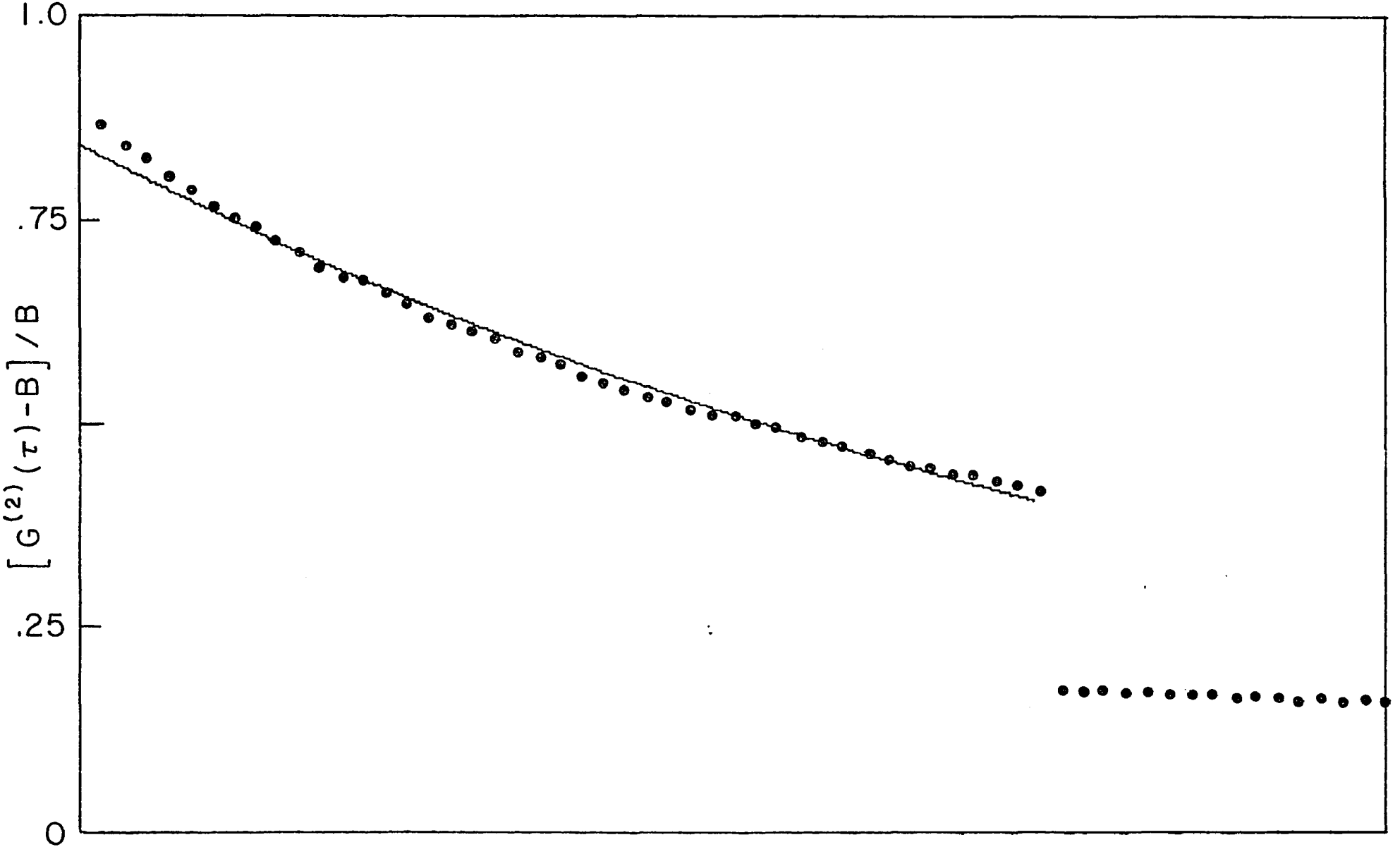

Fig.42. Normalized correlation data for a rat skin collagen solution without being purified through sucrose gradient separation. T= 20°C, θ= 31.8°. H= 0.69, τ= 50 μsec/bin

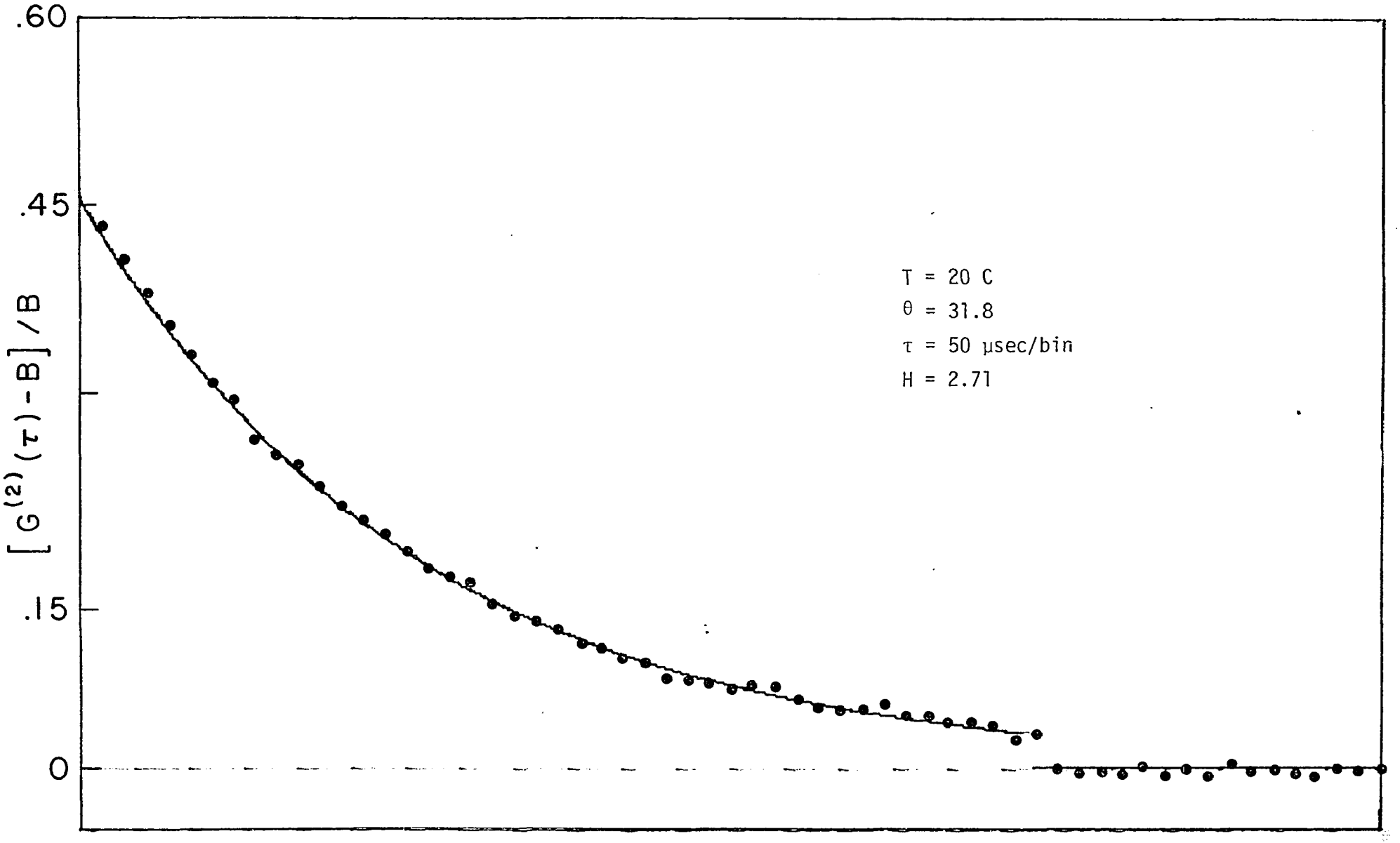

Fig. 43. Normalized correlation data for a rat skin collagen solution purified through sucrose gradient separation. τ = 50 μsec/bin, solid line: single exponential fit

122

Fig. 44. Normalized correlation function of a rat skin collagen solution purified through sucrose gradient separation.
T= 20°C, θ= 90°, τ= 5 μsec/bin, H= 2.17
Solid line: theoretical fit to eq. 61 with A/B = .251, B_2/B_0= 0.361, D_R= 735 sec^{-1} and D_T= 7.242X10^{-8} cm^2/sec

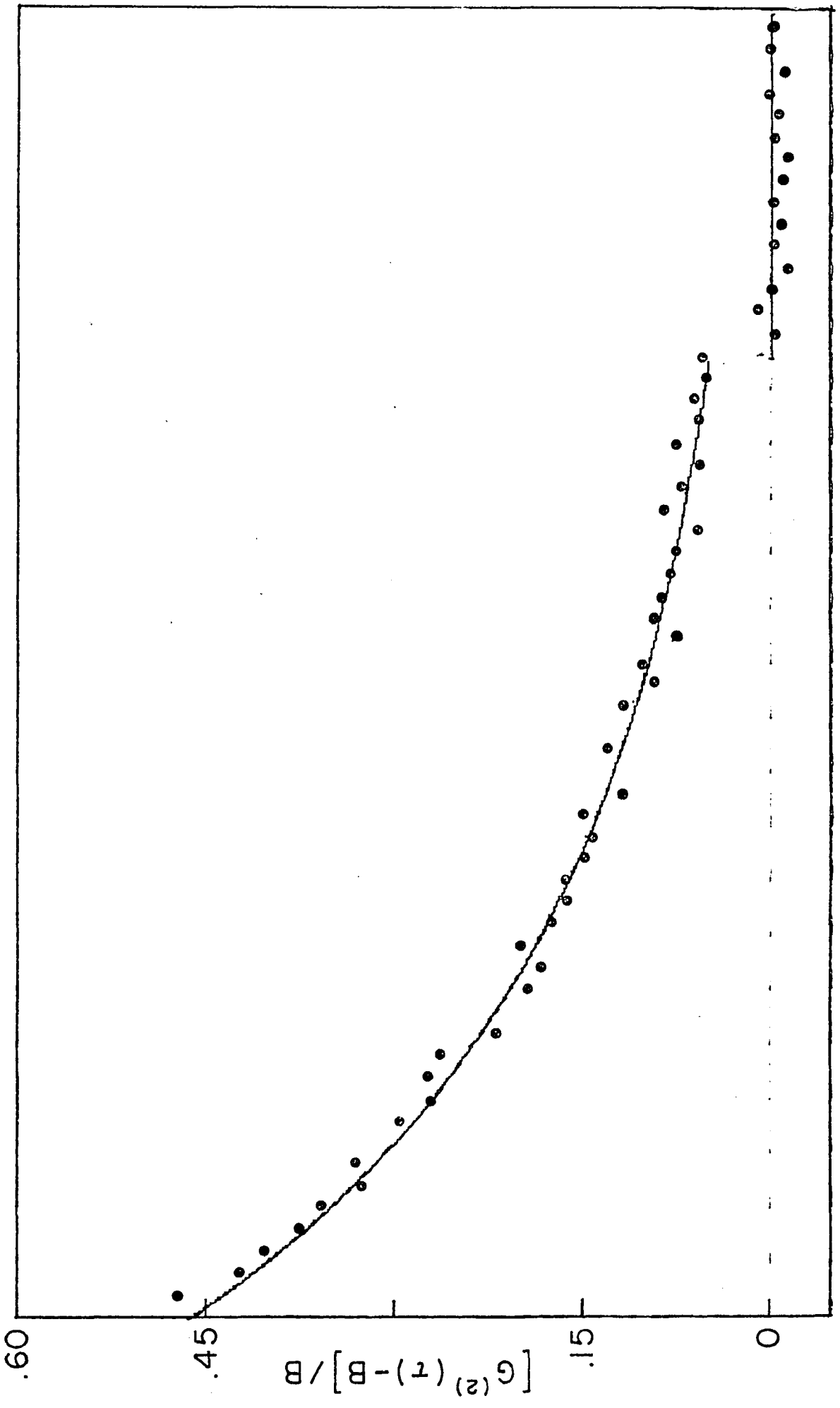
.60
.45
.15
0
$[G^{(2)}(\tau)-B]/B$

obtained for the translational diffusion coefficient by fitting these data to single exponential form as discussed in the last section.

The data for 90° scattering angle was analyzed mainly by the second method described in the last section. A preliminary check using the first method was performed. The results from both methods are in general agreement with each other. We only present the results using the second method in which we found sets of L and D_R such that the calculated D_T was restricted to $7.20 \pm 0.16 \times 10^{-8}$ cm^2/sec and D_T/D_R was equal to that calculated by the Broersma equations at the same particle length L. We obtained 2715 ± 100Å for the particle length and 735 ± 50 sec^{-1} for the rotational diffusion coefficient D_R. The theoretical fit to the correlation function with D_T = 7.20×10^{-8} cm^2/sec and D_R = 735 sec^{-1} is also shown in Figs.43 and 44.

For collagen monomers 2715Å in length and 13.6Å in diameter at 20°C in distilled water, the translational diffusion coefficient calculated from the Broersma equations is 8.47×10^{-8} cm^2/sec. The ratio of this value and our results of 7.20×10^{-8} cm^2/sec gives the relative viscosity η of our sample. The viscosity of the sample was then found to be 1.18 cp. The corrected rotational diffusion coefficient in 20°C distilled water is 865 sec^{-1}.

6.4 DISCUSSION

The primary result of our measurements is a determination of the ratio of the translational and rotational diffusion coefficients which in turn determines the length of the collagen molecules through the Broersma equations. The advantage of this procedure is to bypass

the shear viscosity η when it is not exactly known. All our analysis is, of course, dependent on the validity of the Broersma equations which may apply only to rigid rodlike molecules.

The results of some previous physical studies on tropocollagen solutions by the techniques of electron microscopy, electric birefringence and intensity fluctuation spectroscopy are listed in Table VII. The calculation of D_R or D_T from the directly measured correlation functions of non-zero degree scattering is first carried out here. All previous studies indicate that collagen molecules have a diameter between 13.6Å and 14Å and a length between 2500Å and 3000Å. Our results yield a length (2715 ± 100Å) which is in generally good agreement with the results of previous studies. As pointed out by Thomas and FLetcher,[28] the lengths obtained from dynamic measurements and the use of the Broersma equations are all somewhat smaller than the lengths obtained from electron microscopy. Fletcher attributed the discrepancy to the slight flexibility and the small diameter of collagen molecules. The Broersma equations, as any hydrodynamic relationship, strictly apply only to situations in which the dimensions of the scattering particles are very much greater than the dimensions of the solvent molecules. The 13.6Å diameter of a collagen molecule is only several times greater than the diameter of a water molecule. The flexibility, of course, makes the apparent length of molecules measured in solution less than the electron microscopic length. In addition, the electron microscopic technique may also stretch the particle and make the measured length longer than it is in solution.

TABLE VII

THE RESULTS OF CURRENT PHYSICAL STUDIES IN TROPOCOLLAGEN SOLUTIONS

Investigator	Technique[a]	D_T[b] ($10^{-8}\frac{cm^2}{sec}$)	D_R[b] (sec^{-1})	Length[c] (Å)	Conditions
Present work	DLS	8.47 ± .20	865 ± 60	2715 ± 100	Rat skin collagen,0.5 mg/ml in 0.02M NaCl,0.005M$CaCl_2$, 0.05 M Tris at pH=7.6
Thomas[28] & Fletcher	DLS		1082 ± 30[d]	2530 ± 70	Rat tail tendon (RTT) 0.8-5.4 mg/ml in .09M HAC
G. Fletcher[27]	DLS	8.6 ± 0.2			RTT,0.1-1 mg/ml in 0.5M calcium acetate or 0.1M calcium chloride
J. Bernengo[25] et al	EB		1040 ± 60	2560 ± 150	Calf skin collagen(CSC) 0.012-0.1 mg/ml in 0.1M HAC
"	EM			2940 ± 40	"
B. Obrink[23]	DLS	7.8			Lathyritic collagen, 0.8-3.2 mg/ml in phosphate buffer at pH = 7.4
Ananthanarayanan[24] et al	EB		810	2790	CSC, 0.05-0.4 mg/ml in 0.01M HAC
"	EM			2850	"
Yoshioka[85] et al	EB		972 ±324	2620	RTT, 01.-0.2 mg/ml in 0.02M HAC
C. Tanford[3]	Sedimentation & Light Scattering	6.9			Using Dot'y conclusion[32]

a. DLS, depolarized light scattering; EB, electric birefringence; EM, electron microscopy

b. Corrected to scattering in water at 20°C

c. From Broersma equations (Eq. 18 and Eq. 19) with d = 13.6Å)

d. Extrapolated to zero concentration

The purification by the density gradient technique gave very good monodisperse samples. However, since 10 to 30% sucrose solutions were used in the process, extensive dialysis was needed to remove the sucrose from the sample completely. As a result, the viscosity of the samples was higher than that of the pure solvent by an indeterminate amount. Therefore, the normal procedure of determining D_T from low angle scattering and D_R from high angle scattering individually does not give reliable results in this case. Our technique, based on the ratio D_T/D_R, solves this problem and provides a reasonable input for the evaluation of molecular dimensions through the Broersma equations.

The centrifugation of the samples within the cuvettes prior to the measurement of autocorrelation functions was found to be essential. It settled the residual collagen aggregates and dust in the sample to the bottom of the cuvettes. The limitation of this technique is the need to physically move the cuvettes from the centrifuge to the spectrometer, thereby agitating the contents somewhat. The only improvement on this technique would be to build the centrifuge into the spectrometer and measure the correlation function in situ. However, meeting the joint requirements of centrifugation and the optical access necessary to do photon correlation spectroscopy at different scattering angles is a formidable task. Therefore, the samples obtained by our technique were tropocollagen solutions as clean and monodisperse as can be obtained from available technology.

CHAPTER 7

CONCLUSIONS

In the present study, we employed the technique of intensity fluctuation spectroscopy, mainly measuring the intensity autocorrelation functions of different systems, to study the collagen-gelatin and gel system. Various hydrodynamic properties were then derived from these correlation data. We have successfully characterized the z-average diffusion coefficients, polydispersities, hydrodynamic radii and other hydrodynamic properties of gelatin molecules in different concentration regions. The molecules were found to execute free diffusion motion at low concentrations and form polymer networks at high concentrations. The aggregates of the molecules were mainly due to covalent crosslinks with polymerization index $N \propto C^5$. For gelatin gels, single exponential correlation functions were obtained and the elastic continuum model was found to describe all the observed properties better than the bounded diffusion model.

The purification of collagen solution by the density gradient technique gave very good monodisperse samples. The calculations of D_T and D_R from the directly measured correlation functions of non-zero degree scattering were first carried out in the present study. A new approach to simultaneously determine the translational and rotational diffusion coefficients was used to estimate the length of macromolecules without knowing the viscosity of the solutions. In fact this procedure may provide a new way of determining the shear viscosity of the solvents and the intrinsic viscosity of the polymers. In our study of tropocollagen solutions we obtained a reasonable value for the molecular

length and a 1.18 cp for the viscosity of the collagen solutions compared to 1.05 cp for the pure solvent. We attributed the high viscosity to the presence of sucrose residues which were not removed in the dialyzing process. In fact the high value of the viscosity may be due to the intrinsic viscosity of the collagen molecules whose high viscosity has been known for a long time. Therefore a further study suggested is to repeat the present measurement dialyzing the sample more completely after it is purified by the sucrose gradient separation.

Intensity fluctuation spectroscopy has been proven to be a powerful and successful technique to study the hydrodynamic properties of the collagen-gelatin and gel system. We suggest that a more complete picture would result from relating our measurements to macroscopic measurements not available in our laboratory such as the longitudinal compressional modulus, friction constant between the polymer chains the their surrounding fluid, sedimentation constant, osmotic pressure, etc.

REFERENCES

1. A. Veis, "The Macromolecular Chemistry of Gelatin," Academic Press, New York 1964.

2. D. Eyre, Science, Vol. 27, 1315 (1980).

3. C. Tanford, "Physical Chemistry of Macromolecules," John Wiley & Sons, New York 1967.

4. B. Zimm, J. Chem. Phys., 16, 1099 (1948).

5. H. Z. Cummins and H.L. Swinney, in "Progress in Optics," Vol. 8 E. Wolf, Ed., p. 133-200, Amsterdam, North Holland Publishing Co. 1970.

6. H. Z. Cummins and E.R. Pike, "Photon Correlation, Light Beating Spectroscopy and Velocimetry," Plenum, New York 1974.

7. B. Berne and R. Pecora, "Dynamic Light Scattering," John Wiley & Sons, New York 1976.

8. H. Z. Cummins and E.R. Pike, "Photon Correlation and Light Beating Spectroscopy," Plenum, New York 1976.

9. B. Chu, "Laser Light Scattering," Academic Press, New York 1974.

10. S. E. Bresler, P. A. Finogenov and S. Y. Frenkel, Reports Acad., U.S.S.R., Moscow 72, 555 (1950).

11. M. B. Mathews, E. Kulonon and A. Dorfman, Arch. Biochem. Biophys. 52, 247 (1954).

12. A. Veis, D. N. Eggenberger and J. Cohen, THIS Journal, 77, 2368 (1955).

13. M. B. M'Ewen and M.I. Pratt, "Nature and Structure of Collagen," J. T. Randall, p. 158-168, Academic Press, New York 1953.

14. P. M. Gallop, Arch. Biochem, Biophysics, 54, 486, 501 (1955).

15. F. O. Schmitt, J. Gross and J. H. Highberger, Proc. Nat'l Acad. Sci. 39, 459 (1953).

16. J. Gross, J. H. Highberger and F. O. Schmitt, ibid, 40, 679 (1954).

17. H. Boedtker and P. Doty, J. Phys. Chem. 58, 968 (1954).

18. C. E. Hall and P. Doty, J. Am. Chem. Soc. 80, 1269 (1958).

19. A. J. Hodge and F. O. Schmitt, Proc. Nat'l. Acad. Sci., U.S. 46, 186 (1960).

20. P. M. Gallop, P. Seifter and E. Meilman, J. Biophys. Bioch. Cytol. 3, 545 (1957).

21. V. Hippel, P. Gallop, P. Seifter and R. Cunningham, J. Am. Chem. Soc. 82, 2774 (1960).

22. M. J. French, J. C. Angus and A. G. Walton, Biochim. Biophys. Acta. 251, 320 (1971).

23. B. Obrink, Eur. J. Biochem. 25, 563 (1972).

24. S. Ananthanarayanan and A. Veis, Biopolymer 11, 1365-1377 (1972).

25. J. Bernengo, B. Roux and D. Herbage, Biopolymer 13, 641-647 (1974).

26. D. Herbage, J. Bouillet and J. Bernengo, Biochem.J. 161, 303-312 (1977).

27. G. Fletcher, Biopolymer 15, 2201 (1976).

28. J. Thomas and G. Fletcher, Biopolymer 18, 1333 (1979).

29. J. Pouradier and A. M. Venet, F. Chim. Phys. 47, 11 (1950).

30. J. Pouradier and A. M. Venet, F. Chim. Phys. 47, 391 (1950).

31. J. W. Williams, W. M. Saunders and J. S. Cicirelli, F. Phys. Chem 58, 774 (1954).

32. H. Boedtker and P. Doty, F. Am. Chem. Soc. 78, 4267 (1956).

33. A. Courts and G. Stainsby, in "Recent Advances in Gelatin and Glue Research," G. Stainsby, Ed., p. 100, Pergamon Press, New York 1958.

34. A. Veis, D. Eggenberger and J. Cohen, F. Am. Chem. Soc. 77, 2368 (1955).

35. A. Veis and J. Cohen, F. Am. Chem. Soc. 78, 6238 (1956).

36. A. Veis and J. Cohen, F. Polymer Sci. 26, 113 (1957).

37. A. Veis, J. Anesey and J. Cohen, in "Recent Advances in Gelatin and Glue Research," G. Stainsby, Ed.,p. 155, Pergamon Press, New York 1958.

38. A. Veis, J. Anesey and J. Cohen, F. Am. Leather Chemists' Assoc. 55, 548 (1960).

39. J. D. Ferry, Advan. Protein. Chem. 4, 1 (1948).

40. J. Eldridge and J. Ferry, F. Phys. Chem. 58, 992 (1954).

41. A. T. Walter, J. Polymer Sci., 13, 207 (1954).

42. T. Y. Chen, P. Ricica and M. Shen, J. Macromol. Sci.-Chem., A7, 889 (1973).

43. E. S. Van de Kraata, J.J.M. Potters, M.A.M. Winketer and W. Prins, Rec, Trav, Chim, T88, 449 (1969).

44. E. M. Cirlin and M. Shen, J. Macromol. Sci. A5, 1311 (1971).

45. T. Tanaka, L. Höcker, G. B. Benedek, J. Chem. Phys. 59, 1515 (1973).

46. A. N. Gent, Macromol. 2, 262 (1969).

47. N. Nagai and T. Ishikawa, Polymer J. 1, 116 (1970).

48. T. Tanaka, G. Swislow, I. Ohmine, Phys. Rev. Lett. 42, 23 (1979).

49. J. E. Eastoe, Biochem. F. 61, 589 (1955).

50. J. E. Eastoe, Biochem. F. 65, 363 (1957).

51. J. E. Eastoe and A. A. Leach in "Recent Advances in Gelatin and Glue Research," G. Stainsby, Ed. p. 173, Pergamon Press, New York 1958.

52. H. Horman, Leder 11, 173 (1960).

53. L. Stryer, "Biochemistry," W. H. Freman and Company, San Fracisco 1976.

54. J. Gross, Sci. Am. Vol. 204, No. 5, 120 (1961).

55. H. Z. Cummins in "Photon Correlation, Light Beating Spectroscopy and Velocimetry," H. Z. Cummins and E. Pike, Ed., Plenum, New York 1974.

56. L. Mandel, "Fluctuations of Light Beams," in "Progress in Optics," Vol. 2, E. Wolf, Ed. North-Holland Pub. Co. Amsterdam 1963 .

57. I. S. Reed, "IRE Transactions on Information Theory," IT-8, 194(1962).

58. E. Jakeman in "Photon Correlation, Light Beating Spectroscopy and Velocimetry," p. 75, H. Cummins and E. Pike, Ed., Plenum, New York 1974.

59. H. Z. Cummins in "Photon Correlation, Light Beating Spectroscopy and Velocimetry," p. 164, H. Cummins and E. Pike, Ed., Plenum, New York 1974.

60. R. Pecora, J. Chem. Phys. 40, 1604 (1964).

61. R. Pecora, J. Chem. Phys. 48, 4126 (1968).

62. H. Z. Cummins, F. Carlson, T. Herbert and G. Woods, Biophys. J. Vol. 9, No. 4, p. 518-546 (1969).

63. S. Broersma, J. Chem. Phys. 32, 1626 (1960).

64. S. Broersma, J. Chem. Phys. 32, 1632 (1960).

65. D. E. Koppel, J. Chem. Phys. 57, 4814 (1972).

66. H. Z. Cummins and P. N. Pusey in "Photon Correlation Spectroscopy and Velocimetry," H. Z. Cummins and E. R. Pike, Ed., p 164-199, Plenum, New York 1976.

67. P. Pusey in "Photon Correlation, Light Beating Spectroscopy and Velocimetry," H. Cummins and E.Pike, Ed.,Plenum, New York 1974.

68. P. G. DeGennes, Macromolecules Vol. 9, No. 4, 587 (1976).

69. P. G. DeGennes, Macromolecules, Vol. 9, No. 4, 594 (1976).

70. M. Daoud, J. P. Cotton, B. Farnox, G. Jannink, H. Benoit, R. Duplessix, C. Picot and P. G. DeGennes, Macromolecules, Vol. 8, No. 6 (1975).

71. M. Adam and M. Delsanti, Macromolecules, No. 10, p. 1229-1237(1977).

72. J. P. Munch, P. Lemarechal, S. Candau, J. Herz, De Journal de Physique, No. 12, Torne 38, 1499 (1977).

73. P. G. DeGennes, J. Chem. Phys., Vol. 55, No. 2, 572 (1971).

74. H. Hervet, L. Leger and F. Rondelez, Phys. Rev. Lett., Vol.42, No. 25, 1681 (1979).

75. T. A. King, A. Knox and J. D. G. McAdam, J. Polymer Sci.: Symposium No. 44, 195-202 (1974).

76. F. D. Carlson and A. B. Fraser, J. Mol. Biol. 89, 273 (1974).

77. K. L. Wun and F. Carlson, Macromolecules, Vol. 8, 190-194 (1975).

78. S. B. Dubin, J. H. Lunacek and G. B. Benedek, Proc. Nat'l. Acad. Sci. U.S.A. 57, 1164 (1967).

79. K. H. Keller, E. R. Canales, S. I. Yum, J. Phys. Chem., Vol. 75 No. 3 (1971).

80. R. Frost and D. Caroline, Macromolecules, No. 3, 616-618 (1977).

81. J. P. Munch, S. Candau, R. Duplessix, C. Picot, J. Herz and H. Benoit, J. Polymer Sci., Vol. 14, 1097-1109 (1976).

82. J. P. Munch, S. Candau and G. Hild, J. Polymer Sci., Vol. 15, 11-26 (1977).

83. T. Tanaka, I. Ishimata and C. Ishimata, Plys. Rev. Lett.Vol 38, No. 14, 771 (1977).

84. T. Tanaka, Phys. Rev. Lett. Vol. 40, No. 12, 820 (1978).

85. K. Yoshioka and C. T. O'Konski, Biopolymer, 4, 499 (1966).

86. J. Newman, Ph.D. Thesis, City College of New York 1975).

87. P. Pusey, D. Koppel, D. Schaefer and R. Camerini-Otero, J. de Phys. 33, Suppl. Cl., 163-168 (1972).

88. P. Pusey, D. Koppel, D. Schaefer, R. Camerini-Otero and S. Koenig, Biochem. 13, 952 (1974).

89. C. Oliver in "Photon Correlation and Light Beating Spectroscopy," H. Cummins and E. Pike, Ed., Plenum, New York 1974.

90. C. D. Thurmond, J. Polymer Sci. Vol. 8, No. 6, 607 (1952).

91. P. Debye and A. M. Bueche, J. Chem. Phys., Vol. 16, No. 6, 573-579 (1948).